INVESTIGATION OF MODES OF THERMAL FRACTURE

OF SOME BRITTLE MATERIALS

by

CHARLES R. NELSON

BS, University of North Dakota
(1962)
MS, Massachusetts Institute of Technology
(1965)
CE, Massachusetts Institute of Technology
(1967)

Submitted in partial fulfillment

of the requirements for the degree of

Doctor of Philosophy

at the

Massachusetts Institute of Technology

September 1969

Signature of Author ....
Department of Civil Engineering

Certified by ....
Thesis Supervisor

Accepted by ....
Chairman,
Departmental Committee on Graduate Students

ABSTRACT

INVESTIGATION OF MODES OF THERMAL FRACTURE

OF SOME BRITTLE MATERIALS

by

CHARLES R. NELSON

Submitted to the Department of Civil Engineering on September 2, 1969, in partial fulfillment of the requirements for the degree of Doctor of Philosophy.

An analysis of the temperatures and the thermal stresses in a detailed and accurate manner with the finite element technique resulted in the following advancements in the understanding of the nature of the thermal spalling problem.

Thermal spalling due to local heating on the surface of brittle materials is the result of the complete propagation to total failure of a fracture induced by tensile stresses acting on a plane parallel to the surface and just under the heated area. If the material at this surface fails in compression before the tensile stress induced fracture occurs, spalling is prevented. There must be sufficient strain energy released by the fracture process to form the fracture surface required for complete failure.

Experiments conducted on granite, marble and porcelain corroborate the theoretical expectations. The granite and porcelain specimens spalled at the heating time which produce calculated tensile stresses equal to the tensile strength. Crushing of the surface was observed on the marble specimens as predicted from the calculated stresses.

Convex surfaces and a high ratio of compressive strength to tensile strength increase the likelihood that spalling will occur in a given situation.

Thesis Supervisor: Fred Moavenzadeh

Title: Associate Professor of Civil Engineering

ACKNOWLEDGMENTS

TABLE OF CONTENTS

TABLE OF CONTENTS
(Continued)

5

TABLE OF CONTENTS
(Continued)

CHAPTER I

INTRODUCTION

1.1 GENERAL

Today an increasing amount of rock is being excavated
for construction and mining projects. New methods are
being introduced to increase the excavation rates, reduce
the cost or both. Some of these methods are modifications
of older methods while others are essentially new or
novel. The design and use of the equipment for these new
methods is at the present difficult because of lack of
knowledge of what the requirements are.

An example of a modification of an older method of
excavation is the boring or tunneling machines for large
tunnels which use rolling cutter wheels in much the same
manner as do the smaller drills that have been used for
sometime. The design and operation of these large machines
can be based, in part, on the large amount of data and
experience which has been slowly and expensively accu-
mulated from the operation of the smaller drills. However,
for many of the new methods being developed the empirical
data and experience are totally inadequate for proper
designing of equipment. Typical of these methods are the
use of shaped explosive charges, electrical heating elements

and combinations of older methods such as simultaneously heating and using convential cutting rollers.

There is a need to develop a rational technique for the design and use of the excavating equipment for these new methods, since the alternative to the development of such a rational technique is the establishment of large amounts of empirical data with extensive and comprehensive full scale tests. This would be costly and time consuming, whereas a rational technique should only require a few full scale experiments to establish its validity and range of applicability. The basis of such rational techniques for the design and use of new equipment would be a quantitative understanding of the mechanisms within the rock which result in the removal of the material. This would allow the engineer to design equipment to most effectively activate those mechanisms. For example, fracture is one class of mechanisms which are important in the removal of rock by spalling due to rapid heating of the surface. A detailed and accurate knowledge of the stress field that causes this fracture would be required before the equipment which generates the stress field could be rationally and correctly designed.

1.1.1 <u>Basic Mechanisms</u>. Most methods of excavation, old and new, are based on one or more of the following

basic mechanisms which degrade the rock to a state
that allows easy removal [1].

       1. Phase Change

       2. Chemical Reaction

       3. Fracture

The most common method based on a phase change is
to employ heat to melt or vaporize the material which
will then flow away. For example, large scale use of
this is being made to mine sulfur. The sulfur is then
pumped to the surface and allowed to solidify before
further processing.

The chemical reactions may be caused by the addi-
tion of chemicals which will react with the rock and
result in products which can be simply and easily removed.
Also in this category are the chemical reactions which
occur due to heating the material. An example of this
is the decomposition of calcium carbonate in marble which
results in a soft crumbly product that is easily removed.

Methods which are based on fracture have the most
wide spread use today and are usually the most efficient
in terms of cost and energy absorbed per unit of rock
removed. This energy is dissipated within the rock during

fracture by plastic deformations, formation of new sur-
faces, heating, shock waves, kinetic energy of chips and
others. For mechanical drilling methods it has been estab-
lished that the energy required is approximately inversely
proportional to the final size of the removed rock [1].
Therefore, the methods which produce the largest chips
requires the least energy input to the rock. However,
since different methods have different energy conversion
efficiencies and may use different sources of energy,
the one which uses the least energy is not necessarily
the least expensive.

The fractures in the rock are induced by the stresses
which exist in the material at the start of fracture.
These stresses are usually induced mechanically by apply-
ing concentrated loads at the surface, or thermally by
heating or cooling the surface. Also, of great importance
are the stresses which exist in the rock due to natural
causes which may make the fracturing process easier or
more difficult depending on their pattern and magnitude.
For example, in very deep wells the high existing stresses
make the rock behave in a plastic manner which makes
fracturing more difficult. The size and shape of rock
pieces removed depends on the type of rock and the method
used.

The use of methods based on fracturing the rock by thermal stresses is gaining wide spread acceptance today in rocks which are exceptionally hard to drill by convential methods [1]. A prime example is the use of flame jets to drill the blast holes during the mining of the iron ore, called taconite. The flame jets are also being used to channel blocks of granite, thus eliminating blasting operations which tended to degrade the material that is used for building and monument use.

The actual mechanisms by which the flame jet removes the rock during spalling is not understood in any detail [2], although it is usually assumed that it is a thermal stress induced fracture. The rock removal rate decreases and in some cases nearly stops in some rocks and in the region of faults and other discontinuities. The addition of an abrasive to the flow of hot gas increases the removal rate in some soft rocks [2]. It is not well understood why hard rocks usually spall best and some rocks do not seem to spall at all.

1.2 OBJECTIVE AND SCOPE

The objective of the thesis is to develop and demonstrate a practical method to study in a quantitative manner the basic failure mechanisms of the brittle fracture

type in rock during excavation. This will help in the rational design of excavation equipment by evaluating the effect of the applied loads or heating in an analytical manner.

The scope of the thesis is:

1. The development of an analysis technique to evaluate the temperatures and stresses induced in the rock with sufficient detail and accuracy that the mechanisms of failure of the brittle fracture type may be investigated. It is capable of handling complicated boundary conditions and nonlinear and nonisotropic material properties.

2. The comparison of results from the analysis with experimental data to validate the analysis technique and the assumptions which went into it.

3. The development of hypotheses about some of the important fracture mechanisms of failure which may occur when rock or other brittle materials are heated rapidly on the surface. These hypotheses are sufficient, for many cases, to predict if spalling results for a given set of conditions. These hypotheses are based on the material's properties and the temperatures and stresses evaluated with the developed analysis technique.

4. The experimentation on specimens of marble, granite and porcelain using a gas laser for a heat source.

The developed hypotheses are applied and comparisons made between predicted and experimental results.

The finite element method was used for the heat transfer and stress analyses so that it was possible to solve problems having irregular boundaries and nonlinear and nonisotropic material properties. The heat transfer analysis computer program evaluates the transient temperatures throughout the body based on the initial conditions, boundary conditions and material properties. The stress analysis computer program evaluates the stresses based on the temperature distribution, boundary conditions and material properties. Both computer programs are limited to two-dimensions in order to minimize time.

The theory of spalling is based on the concepts of modern fracture mechanics: It expresses the spallability of a material, i.e. criteria for crack initiation and crack propagation, in terms of the material properties and the functions evaluated with the analysis technique.

Experiments were conducted on specimens of marble, granite and porcelain in the shapes of disks, cylinders and spheres. The specimen was locally heated using a carbon dioxide gas laser. The experimental data and results were compared with results predicted by the analysis and theory to check and verify both.

13

CHAPTER II

THEORY

2.1 GENERAL

The theoretical development in this thesis is divided into two parts. The first is the development of hypotheses about the fracture mechanisms for thermal spalling The second is the development of analysis techniques to calculate the temperatures and stresses for use in the first part.

2.2 FRACTURE MECHANICS

To date, most of the research into the destruction of rock for mining or construction purposes has not investigated the mechanisms of failure in detail. It has instead been experimental parameter studies using full scale; or nearly full scale equipment, or "theoretical" studies based on assumed stress fields or overly simplified models [3].

The results of this work has been very valuable in reaching local optimums in the design and the operational technique for the existing equipment. However, since detailed accurate knowledge of the mechanism or mechanisms of destruction was not available, it was difficult to apply

the results of this type of research to other materials
or excavating equipment which were different in even
modest ways.

The mechanisms were not investigated in detail because
the stresses induced within the material by the equipment
was not known with sufficient detail or accuracy nor were
the basic principles of rock failure well understood.
There were at least two reasons why the stresses could not
be found with the required detail and accuracy. First, the
boundary conditions that existed between the rock and the
excavating equipment were not known with the detail and
accuracy required for analysis. Second, due to the complex
boundary conditions and the nonlinear material properties,
an analysis was impossible with the classical methods.

2.2.1 Past Work on Rock Destruction. Evens and
Murrell [4] modeled the problem of a wedge penetrating
soft coal in a simple manner. They assumed that the
normal stress between the wedge and the coal was equal to
the unconfined compressive strength of the coal and that
the tangential stress between the wedge and the coal acted
upward on the surface of the wedge and was equal to the
normal stress times the coefficient of friction. This
simple model resulted in predictions which correlated well

with experiments conducted in soft coal but very poorly with experiments conducted in limestone, a more brittle rock in which chipping is important.

Paul and Sikarskie [5] modeled the problem of a wedge penetrating a brittle material in which chipping would take place. Their assumptions were that the Mohr-Coulomb criteria was satisfied along the fracture plane at the time of chip formation, and the fracture extends in a straight line from the tip of the wedge to the surface of the material some distance away from the wedge. This model accurately predicted the shape of the loading curve and the required penetration force if the slope of the load-deformation curve was found experimentally.

Several studies using the technique of photo-elastic analysis to find the stresses have been conducted. One, by Garner [6] found that there existed tensile stresses across the potential fracture plane for the case of in-dexed penetrations by a single bit-tooth. However, since the materials used for the photo-elastic analysis have different properties than real rock and the interaction with the bit is hard to simulate, little quantitative work has been done.

2.2.2 <u>Related Past Work</u>. Research conducted by non-mining orientented groups has investigated the destruction mechanisms in some detail. One reason they have been able to do this is that the loading, material properties and geometry were often more favorable to a simple, but accurate and detailed analysis. An example of the experiments which they conducted was to submerge spheres of homogeneous material into hot fluids and observe the resulting fracture phenomena.

In particular, people in the ceramics industry have been interested in the phenomenon called thermal spalling because of the many products that must be designed to withstand rapid heating or cooling. They have been interested in finding the actual mechanisms of failure so that products of ceramic materials could be rationally designed to withstand conditions for which it was not practical, or economical to run experiments on prototypes. At first their efforts were not successful because a good analysis was not possible due to the complex specimen shape used to study the problem. This lead to erroneous conclusions as to the mechanisms responsible for the spalling. An example of this was the work by Norton [7] in which he incorrectly hypothesized the cause of spalling to be a fracture induced by shear stresses which he thought

17

existed along the isothermal lines. He even derived
equations for these imaginary shear stresses, but they
were not valid. His experiments consisted of rapidly
heating one end of oven liner bricks and noticing loss
of material at the heated end due to spalling. (See
Figure 1). Initially for analysis, Norton modeled the
problem with a half-space which was subjected to an in-
crease in surface temperature. It was the lack of tensile
stresses for this model that lead him to misinterpret the
mechanism to be a shear stress induced fracture. Later
[8] he conducted a photo-elastic study of heating of
brick shaped models. However, he again erroneously
interpreted the results to justify his shear stress
mechanism.

Norton [9] continued to put forth his shear stress
induced mechanism theory in one form or another. Norton's
theory was rebutted by Preston [10], who suggested that
thermal spalling is always caused by tensile stresses with-
in the material. However, he was not certain of the
location of the tensile stresses that started the spalling
but indicated that the stress may be such that the crack
would start at the surface and travel into the body.

Preston also stated that the strain energy released
by the propagating crack must exceed the energy required

19

FRACTURE SURFACE

THIS END HEATED

¢

z

x

σ_x
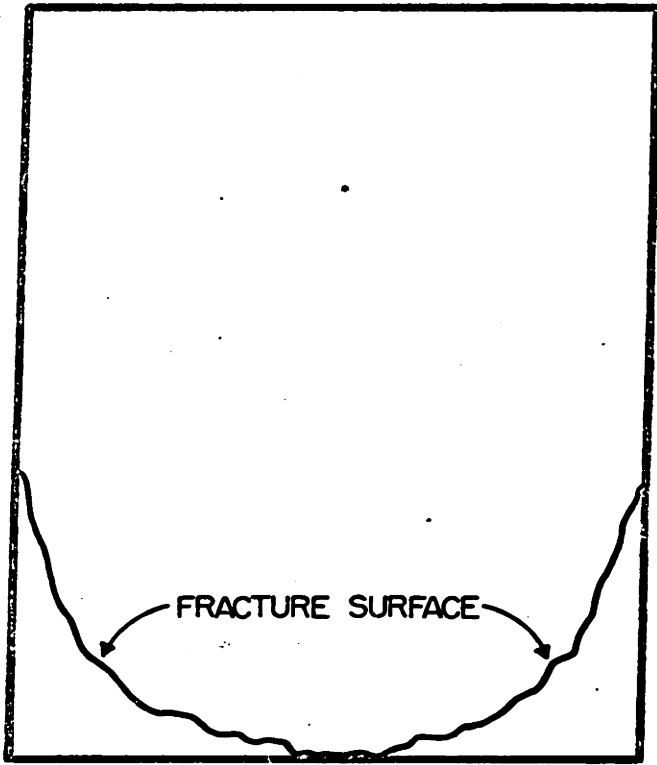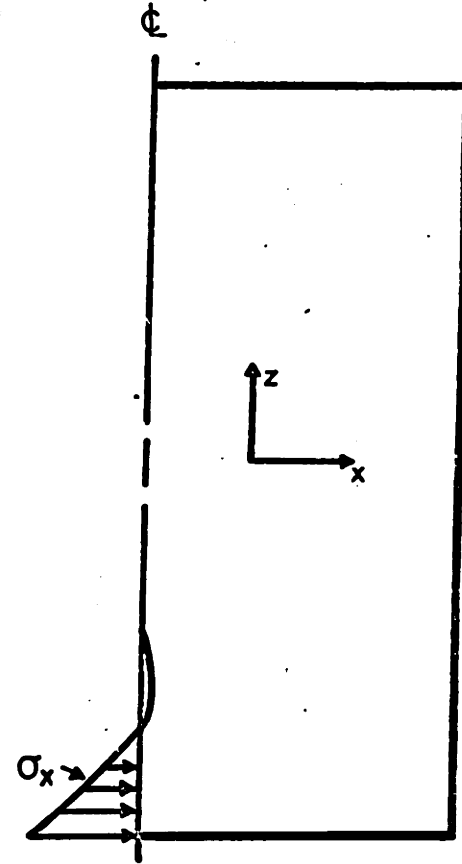
STRESSES NORMAL
TO THE CENTER

FIGURE I: SPALL SHAPE AND ASSOCIATED STRESSES   [7]

to form the new surface area. In this respect he seems to have been the first to apply both the concept of crack initiation and crack propagation to the spalling problem. Preston did not conduct any analysis or experiments to back up this theory about the mechanisms of spalling.

In 1955 Kingery [11] concluded, based on the investigations to that date, that the mechanism responsible for thermal fracture was a stress induced fracture. Based on this idea, it was possible to establish the effect that the values of the material properties have upon the spallability of a material.

Since a stress initiated fracture was the mechanism which causes spalling, it was shown that materials with high strength and a low modulus of elasticity would be the most spall resistant. Also, for the case of spalling caused by sudden surface heating, materials with a high thermal conductivity and diffusivity, and a low coefficient of thermal expansion and emissivity were the most spall resistant.

In 1963 Hasselman [12] again brought up the hypothesis (first pointed out by Preston [10]) that the strain energy released by the crack's formation must exceed the energy required to create the new surface area or else the crack will be halted and spalling will not occur.

Hasselman conducted experiments with specimens of a very brittle material, a less brittle material and a tough material. These materials were rapidly heated to observe their spalling behavior. The brittle material shattered when heated, the second and third did not break completely apart. However, they may have had spall fractures within since it was calculated that the tensile stress of each material was exceeded in the interior region of the spheres. His calculations show that for the two tougher materials there was not sufficient energy available for release, during fracture, in order to create the new surface area required to completely separate a "chip" from the parent material.

The conclusion to be drawn from this work is that there exist two conditions that are necessary and sufficient to incur a spalling type of failure: 1) The fracture strength of the material must be exceeded at some point in the specimen. 2) The releasable strain energy associated with the projected crack formation must exceed the energy required to form the new surface area created by this crack.

To minimize this available energy for a spall resistant material, the strength should be low and the modulus of elasticity and effective surface energy should be high.

The effective surface energy referred to is the energy required to create a unit area of new surface by the fracture process.

Before this work by Hasselman, other efforts to find what a material's properties should be to prevent spalling had considered only the initiation of the crack. Their observations had never included a situation in which a crack was observed to form, but did not propagate a sufficient distance to form a spall. The reasons for this oversight were as follows: 1) The crack usually starts in the interior of the specimen and is difficult to find if it has not propagated to the surface. 2) Most materials which the other people tested have properties such that if a crack starts there is sufficient energy available to completely propagate the crack and thus cause spalling.

2.2.3 The Problem of Spalling. The phenomenon, commonly known as spalling, occurs in many different materials and situations. Often it is desirable to control the phenomenon for the advantage of man. Some of these situations will be considered to gain insight into the problem and to demonstrate that there is a marked similarity between the stress fields for the various cases.

22

First, the term spalling will be defined as the loss

of material from a body by a fracturing process which is

induced by the stresses existing in the body. These

stresses may be due to mechanical loadings, temperature

changes, phase changes, changes in moisture content, etc.

While in most cases the final stresses are the result of

some combination of these, often only one will predominate.

The spalling of fire bricks has long been a problem

in large industrial ovens. It was this problem that lead

Norton [7] to conduct his research in the field of

spalling. The end of the brick which formed the inside

surface of the oven was the location at which the spalling

occurred. This end would be exposed to rapid heating

when the oven was started inducing stresses as shown in

Figure 1.

Spalling in concrete is a problem in sidewalks, roads,

buildings and most other structures made from that material.

There are two locations at which the spalling usually occurs.

The first is at joints which are not separated an adequate

distance or do not have an appropriate soft filler in place:

When a joint with either of these shortcomings tends to

close due to loading, temperature change or others, large

stresses will be locally transmitted across the joint as

shown in Figure 2 causing a spall to form at the edges.

The second place that spalling commonly takes place in concrete is at the surface, around a piece of porous aggregate: If the aggregate is filled with water when subjected to freezing temperatures, stresses are developed as shown in Figure 2 causing the spalling of material around the porous aggregate.

When some types of rocks and other materials are rapidly heated at the surface, spalling occurs. This has been observed in detail by the author while heating materials with a gas laser. The associated temperature and stress distributions are shown in Figure 3.

Spalling is also observed to occur in some materials during compressive tests. This spalling usually occurs at a compressive stress which is approaching the compressive strength of the materials. A hard inhomogeneity in the material being tested would cause a local stress distribution as shown in Figure 4.

In each of the cases cited above there is great similarity among the various stress fields associated with each of the spalling regions. In all cases, there exist high compressive stresses near the surface and parallel to it. Also, in each case there were tensile stresses acting on a plane parallel to and at a small distance below the surface.

HARD FILL

EXPANDING AGGREGATE

POTENTIAL
SPALLING
CONDITIONS

ACTING
STRESSES

σ

σ

JOINT IN CONCRETE

EXPANDING AGGREGATE
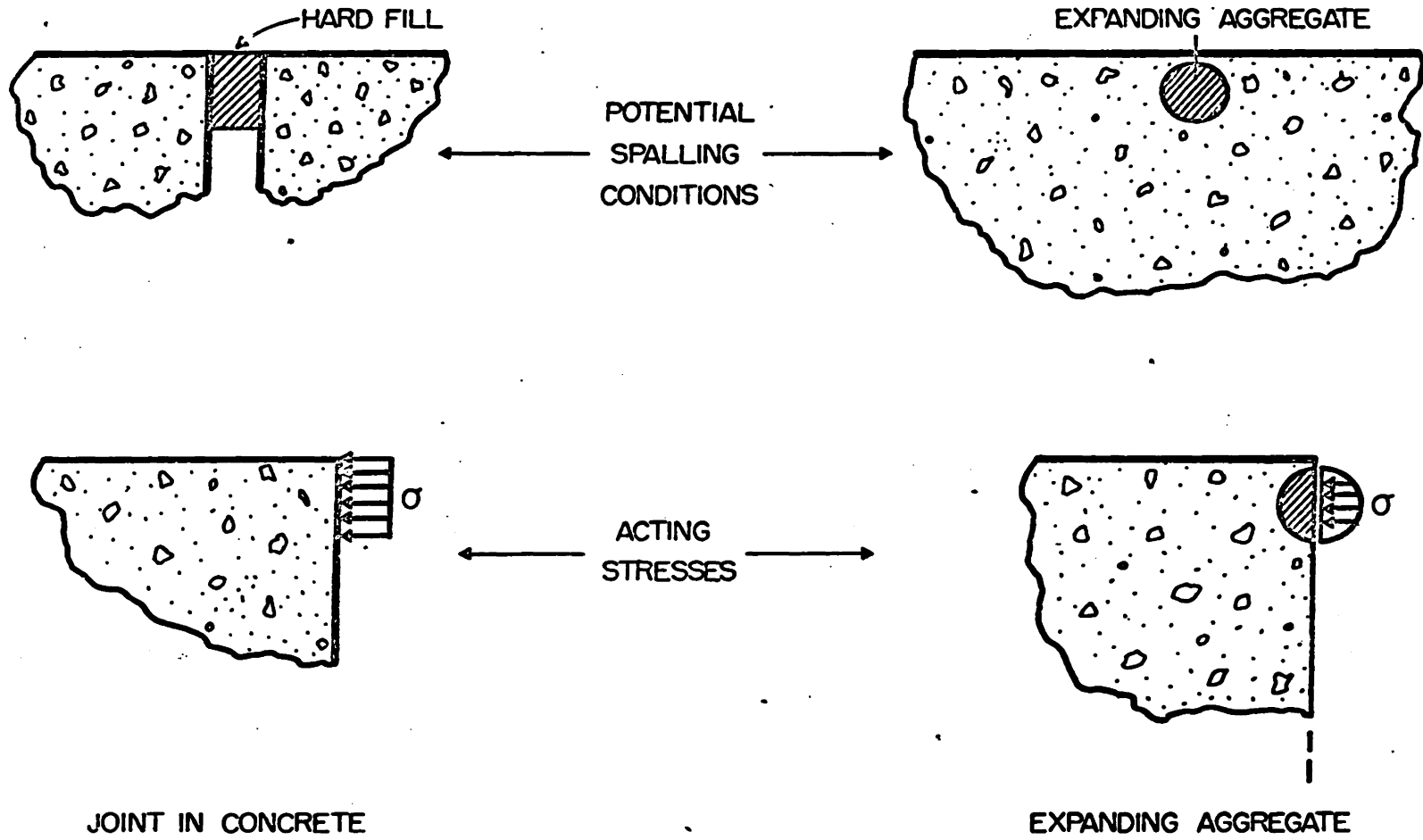
FIGURE 2: POTENTIAL SPALLING CONDITIONS IN CONCRETE

LASER RADIATION

(COMPRESSION)

ENLARGED
SECTION
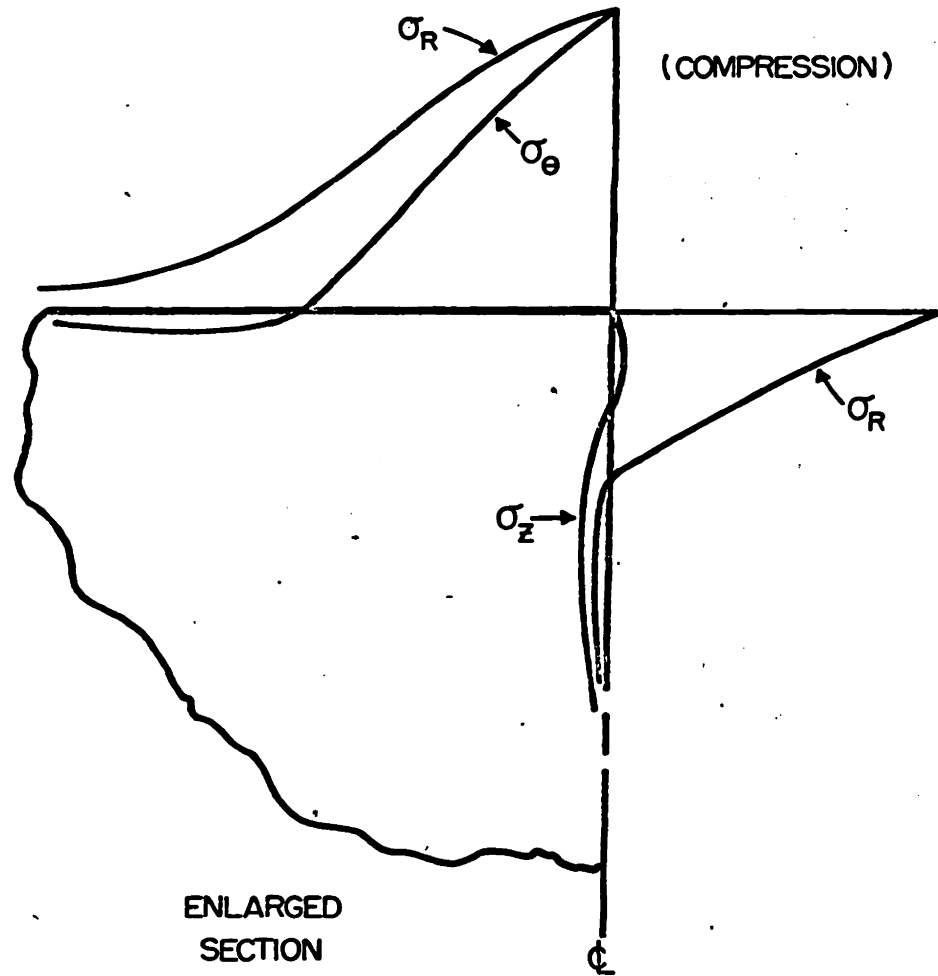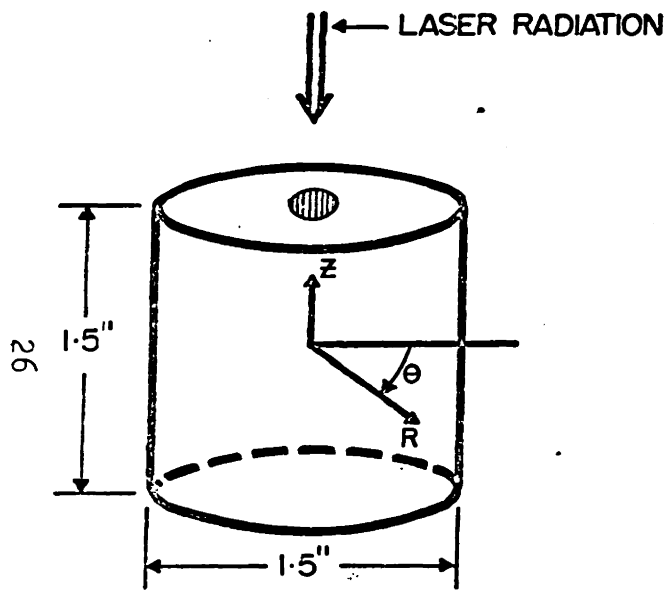
FIGURE 3: THERMAL STRESS DISTRIBUTION FROM LASER RADIATION

HARD INCLUSION →
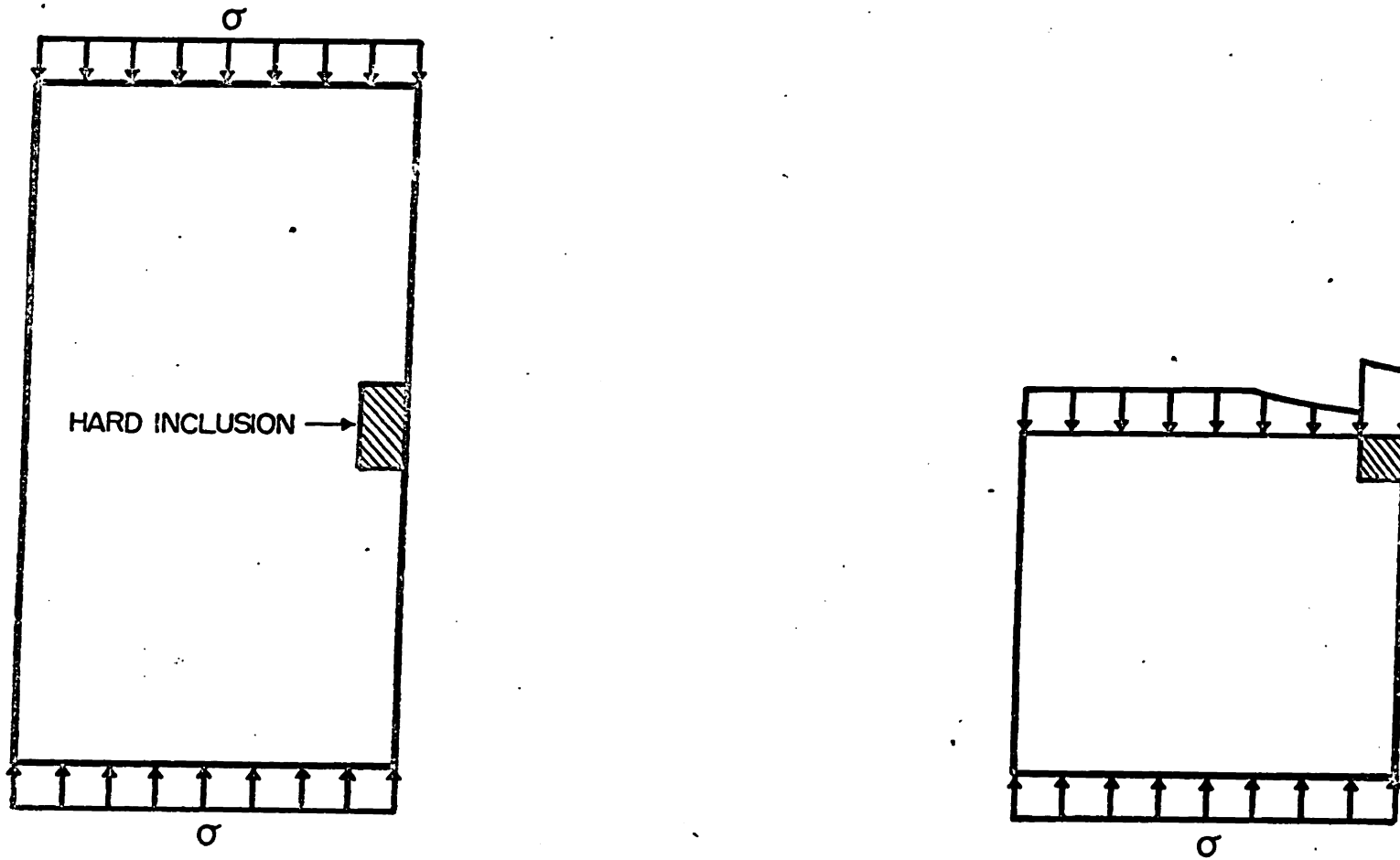
FIGURE 4:　NOMINAL UNIFORM COMPRESSIVE TEST

The material for each case was brittle in nature from which little or no yielding could be expected.

2.2.4 Initiation and Propagation of Fractures. The study of the failure modes of brittle materials with consideration given to initial flaws was first considered by Griffith [13]. He was considering the problem of the tensile strength of glass being much lower than theoretically expected. He postulated that there were initially very small natural cracks existing in the glass which produced stress concentrations at their tips, thus causing the critical crack to propagate. This resulted in total failure at a nominal tensile stress, much lower than theoretically expected.

When the crack propagated, energy was absorbed by the process which formed the new fracture surfaces. Griffith attributed this surface energy to the rupturing of the bonds between the atoms on each side of the fracture. For most materials, other than the most brittle, such as glass, it has since been found [14] that a significant amount of the apparent effective surface energy is absorbed in plastic flow and formation of branch cracks. In addition, if the fracture propagates at high speed, energy is lost in the production of sonic waves [14].

The energy required to create the fracture surface is found experimentally in simple experiments in which the propagation rate can be controlled and the total energy input measured. This total energy is divided by the total new surface area formed to arrive at a figure called the effective specific surface energy, γ.

The source of the energy for the propagation is conveniently divided into the strain energy released by fracture and the energy added during propagation from sources outside the body. Griffith initially considered only the released strain energy.

Based on the assumption that the crack was penny-shaped, Griffith derived the following equation of the nominal uniaxial strength of a brittle material in terms of the crack width and the effective surface energy. It neglects outside sources of energy.

$$\sigma_f = \pi \, \gamma \, E \, / \, 2 \, c \, (1-\mu^2)$$

σ_f — The nominal uniaxial tensile strength normal to the crack.

c — The radius of the penny shaped crack.

E, μ — Modulus and Possion's ratio.

γ — Effective surface enery per unit of area.

This equation was derived using energy considerations in the following manner: First, the strain energy associated with the crack was added to the energy consumed by crack growth, and the sum was differentiated with respect to the crack length c, and set equal to zero. Physically, this is saying that when the strain energy released by crack growth equals that absorbed in formation of new fracture surfaces, the crack will be unstable and propagate.

For the simple case of uniaxial tension normal to the crack, the resulting fracture is referred to as an extension fracture. Another, called shear fracture, occurs when there exist stresses which slide the two surfaces parallel to each other during propagation.

For fractures caused by more complex two-dimensional stress disturbances, the following failure criterion has been derived [3]. For shear fracture it is:

$$(\sigma_1 - \sigma_2)^2 - 8\sigma_f (\sigma_1 + \sigma_2) = 0 \quad \text{if} \quad \sigma_1 + 3\sigma_2 > 0$$

Extension fracture:

$$\sigma_1 + \sigma_f = 0 \qquad \text{if} \quad \sigma_1 + 3\sigma_2 < 0$$

σ_1 and σ_2 are the principal stresses (compression positive) and σ_f is the uniaxial tensile strength. They are shown graphically in Figure 5.

σ₁, σ₂ — PRINCIPLE STRESSES

T — UNIAXIAL TENSILE STRENGTH

FRICTION ACROSS CLOSED
CRACKS CONSIDERED

RANGE OF
EXTENSION
FAILURES

RANGE OF
SHEAR
FAILURES

T   3 T   8 T   σ₁

T
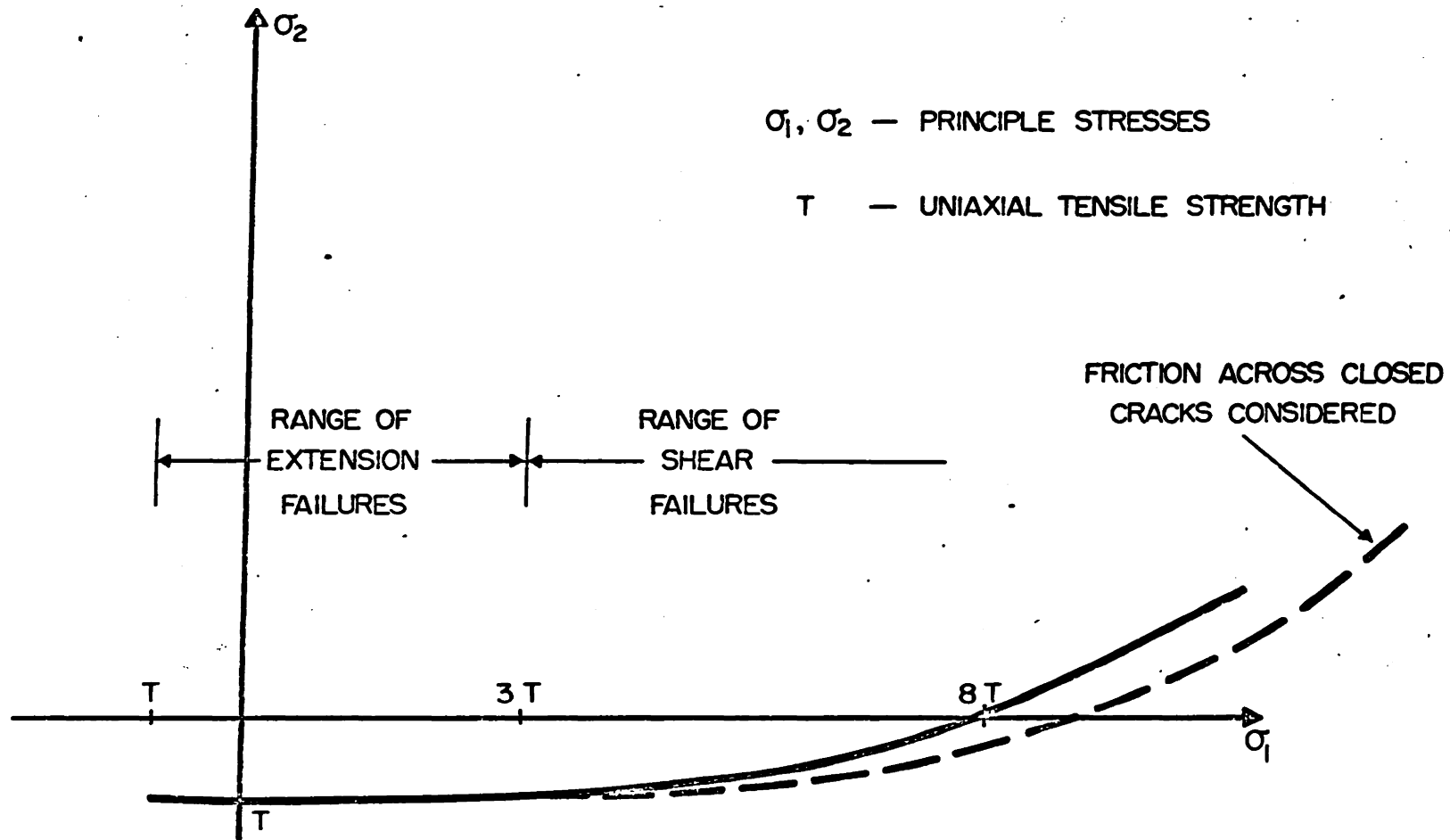
FIGURE 5:   BRITTLE FRACTURE CRITERION IN TWO DIMENSIONS [3]

Also shown is the envelope for the theory which
considers cracks closing in compressive loadings with
the resulting friction reducing the stress concentrations
of the crack. This theory was developed to explain the
fact that most materials were stronger in compression
than the simple Griffith theory predicted. It has no
effect in the range of extension fractures because the
cracks open, not close for this case.

Besides the friction across the closed cracks, it
has been shown that the cracks propagate in compressive
loadings in a manner and direction in which they tend
to become stable [15]. They do this by effecting a
running together of the initial cracks or flaws, thus
forming long fractures aligned in the same direction as
the compressive stress. The columns of intact materials
between the fractures continue to carry load until they
fail by buckling. (See Figure 6).

The failure criterion in three dimensions has not
been firmly established, but it is believed that there
will be a strong similarity to the two-dimensional case.
It is expected that for an extensional fracture to be
initiated in a three dimensional case, the minimum
principal stress must exceed the uniaxial tensile strength.
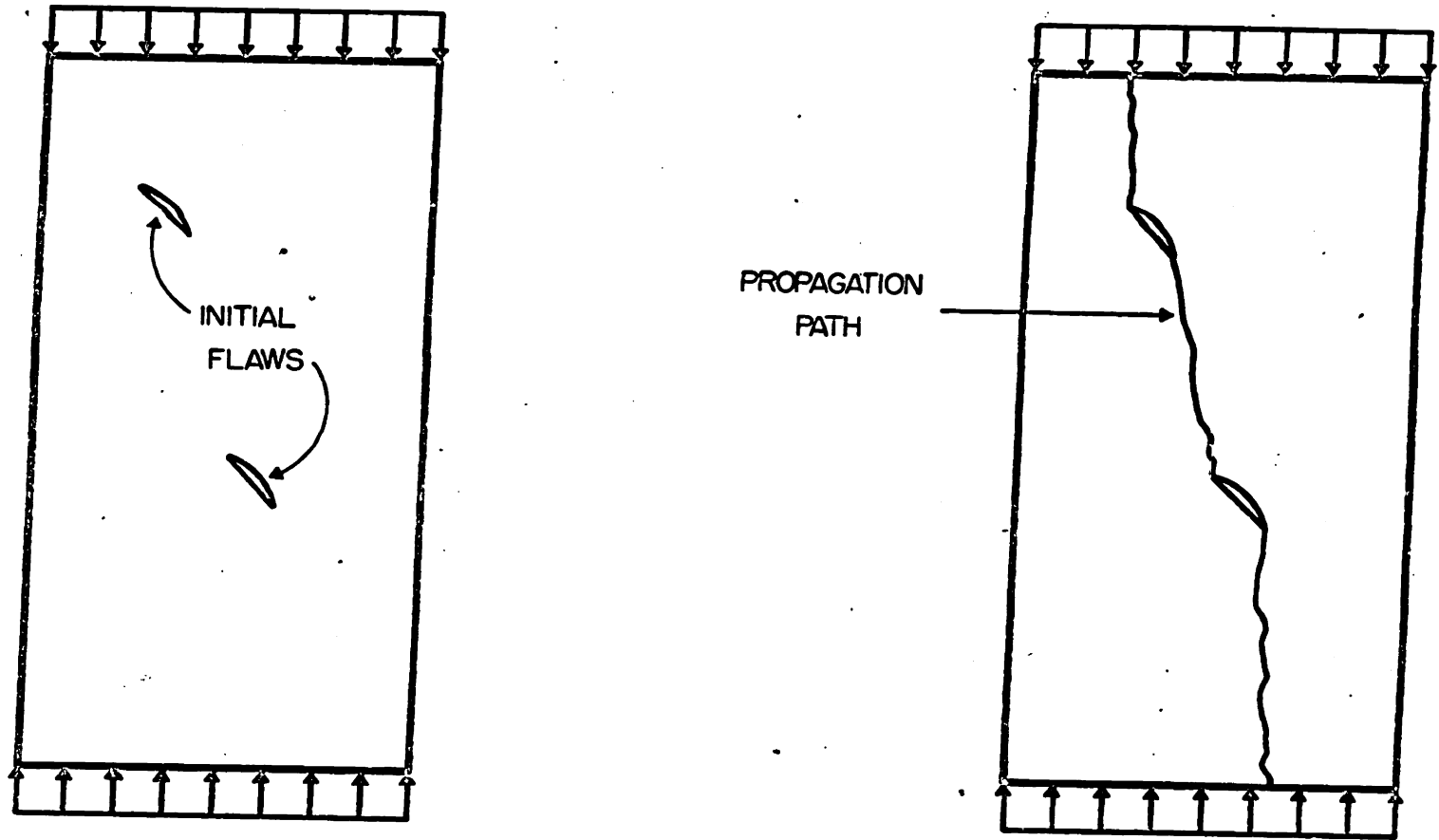
FIGURE 6:   FRACTURE IN SIMPLE COMPRESSION   [15]

This is the same as the condition for the two-dimensional case.

$$\sigma_3 + \sigma_f = 0$$

$$\sigma_3 = \text{minimum principal stress (maximum tension)}$$

$$\sigma_f = \text{uniaxial tensile strength}$$

To date, consideration of the fracture process has been confined to the case of homogeneous stress fields. Since most problems encountered in reality have non-homogeneous stress fields, they must be considered in the study of fracture failures. The influence of the nonhomogeneous stress on the initiation of the fracture would be negligible for many cases because the initial flaws are usually very small and the stresses would change very slowly with respect to the flaw length. Thus, the initiation would occur under conditions similar to the case of a homogeneous stress distribution. However, the fracture may propagate over a distance in which the stresses vary in a substantial manner. The direction and distance the fracture travels must be known in order to accurately predict such types of complete failure as spalling.

The direction that the fracture takes will be dependent

on the instantaneous stresses at the moving tip. These
will be a function of the initial stresses, additional
loading since crack initiation and the changes in stresses
brought about by the fracture. The fracture will
propagate in the direction of the line on which the maximum
tensile stress acts at the tip. For many cases, the
knowledge of the prefracture (initial) stresses and the
initial fracture path will allow a very good qualitative
estimate of the direction of further propagation. If
this is not possible, a detailed analysis must be used
to evaluate the new stress distribution with due regard
given the new boundary conditions. Experimental observa-
tions of the exact path of fracture should be done
wherever possible.

Once the expected direction of the fracture is known,
it must be established if there is sufficient energy to
drive the crack the full distance causing the failure
anticipated. This evaluation must be quantitative in
nature and ideally would be made in the following manner:
The rate that at which energy is made available as a
function of fracture propagation would be calculated and
compared with that energy required for creation of the
new fracture area. If the available energy exceeded that
required, the propagation would continue. The energy

available for further propagation would be that released by such propagation, and any energy left over from earlier propagation which was not used in creating new fracture area or lost by wave motion to distant parts of the body. This excess energy would be stored locally in the form of kinetic energy and would be lost if the speed of propagation was not continuous and rapid.

To state the problem more formally, consider G as the energy made available by a unit area increase in fracture surface. Much of this energy G is made available by the release of strain energy from the reduction in stresses due to the fracture. If it is an extension type fracture which penetrates into a zone where compressive stresses are acting across the fracture then G will be negative. Following this, consider additional notation for other relevant parameters: γ is the energy consumed to create a unit of fracture area; TG is the total energy made available if the fracture propagates to completion; $T\gamma$ is the total energy required to form the new fracture surface; LG is energy lost during the creation of a unit of fracture area and TLG is the total lost during the creation of the whole fracture. A_o is the total new fracture area formed during propagation to complete

failure. The relations between these quanities are:

$$TG = \int_{A_0} G\,da$$

$$T\gamma = \int_{A_0} \gamma\,dA$$

$$TLG = \int_{A_0} LG\,dA$$

The NG net energy at a given time when the fracture area
is A is:

$$NG = \int_A (G - \gamma - LG)\,dA$$

$$NG = \int_A G\,dA - \int_A \gamma\,dA - \int_A LG\,dA$$

If NG is positive for all values of A it can be
expected that the fracture will propagate to completion.

If NG > 0 for all A from 0 to A_0 complete
propagation occurs.

37

The previous relation implies an excess of energy available at all times. It is also true that propagation would continue if the available energy was zero at discrete points. Expressed mathematically, this is to say that

if NG = 0 and G - γ - LG > 0 for any point

and NG > 0 for all other points

then complete crack propagation will occur.

The evaluation of these energy relations for the entire fracture area for most practical problems would be beyond the scope of present analysis techniques. For most cases there would only be two relations known in a quantitative manner. The first is at initiation where the rate of available energy equals or exceeds that required to form the new area:

$$G - \gamma - LG \geqslant 0 \qquad \text{at initiation}$$

The second relation which can be established is the total energy absorbed in fracture work and the total made available. The total energy absorbed in creating new fracture area is:

$$T\gamma = \int_{A_o} \gamma \, dA$$

The total energy made available is found by evaluating

the initial potential energy, subtracting the final
potential energy and then adding any energy input to the
system during propagation:

$$TG = PE_{initial} - PE_{final} + IE$$

where PE is the potential energy and IE is the energy input
during the fracture propagation process.

A necessary, but not sufficient, condition for complete
fracture may then be established between the final energy
terms. The total energy made available must equal or
exceed that which is lost plus that which is used to form
the new fracture surface for complete failure.

$TG > T\gamma + TLG$ necessary (not sufficient) to
complete fracture

$TG < T\gamma + TLG$ complete fracture is impossible
where TG is the total energy made available, $T\gamma$ is the
total energy used in creating new fracture surface area
and TLG is the total energy lost outside the system during
propagation to complete failure.

2.2.5 <u>Failure Mechanisms for Spalling</u>. For most
practical problems with nonhomogeneous stress distributions,
only two quantitative relations can be established. These
are the last two equations in Section 2.2.4. One is the

39

energy balance at fracture initiation and the other is the overall energy balance. These, together with the qualitative information about fracture direction, must be used in hypotheses about overall failure mechanisms.

There are several possible types of fracture which may initiate potential spalling situations. Of these, only one leads directly to the formation of a spall. The requirements of spalling are that the fracture completely separate materials from the main body. To do this the completed fracture must run under and up to the surface. Considering the thermal stresses in Figure 3 , which were due to local heating with a laser, the tensile stresses acting in the zone behind the hot spot will initiate an extension type of fracture in the material if they exceed the uniaxial tensile strength of that material. If the fracture is initiated in a plane approximately parallel to the surface, the stress distribution will change in the manner shown in Figure 7. This stress distribution will cause further propagation in the same general direction, with a slight preference to approach the surface on account of the bending stresses being tensile on the bottom of the chip. (See Figure 8)

The energy required to drive the fracture would come

RADIANT HEAT

FRACTURE

ENLARGED
SECTION

₵
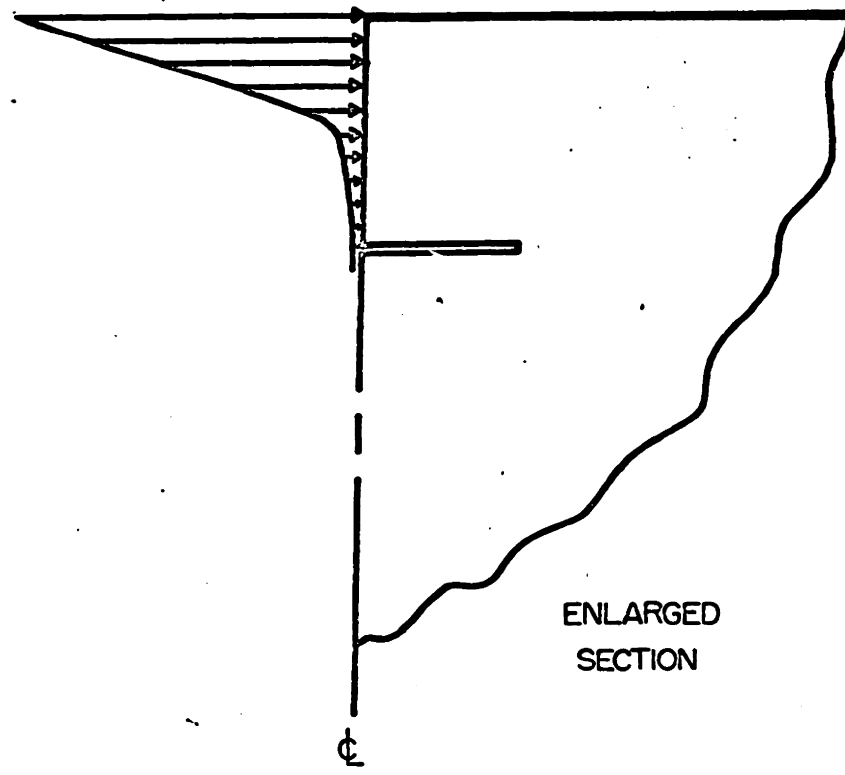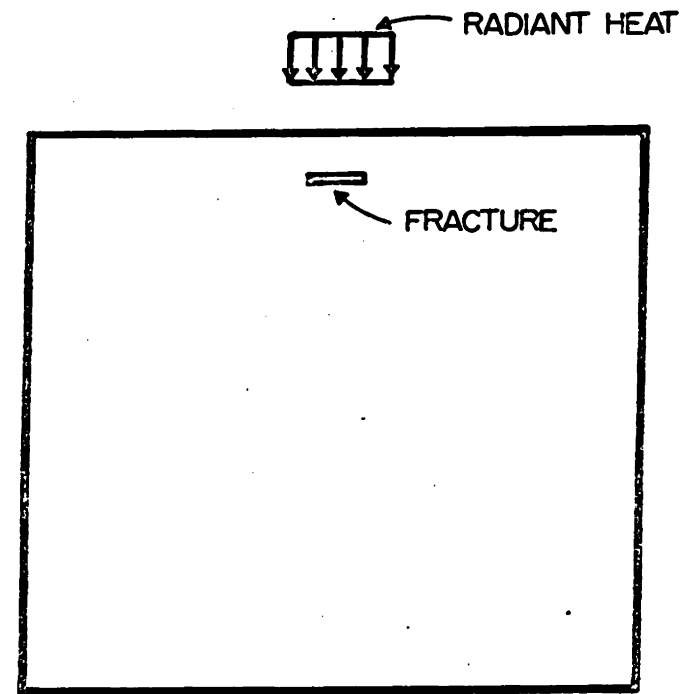
FIGURE 7:   STRESSES AFTER FRACTURE INITIATION

DURING THERMAL SPALLING

THE STRESS DISTRIBUTION SHOWN IN
THIS FIGURE IS NOMINAL.
THE ACTUAL TENSION AT THE TIP
OF THE FRACTURE WILL BE MUCH
GREATER THAN SHOWN DUE TO THE
CONCENTRATION FACTOR.

COMPRESSION

TIP OF FRACTURE

TENSION
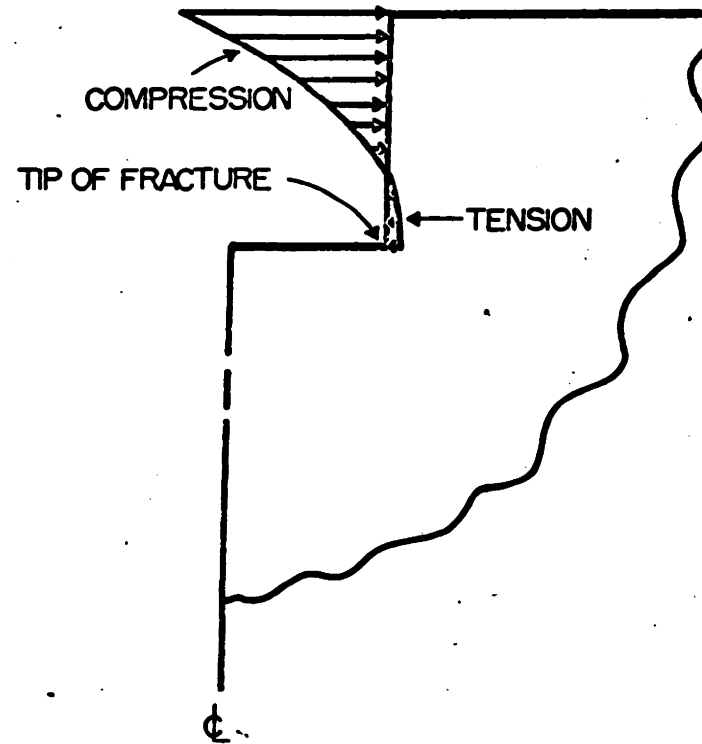
FIGURE 8:   NOMINAL STRESS DISTRIBUTION

NEAR TIP OF FRACTURE

from the release of stored elastic strain energy and
further heating during the fracture process. If the
releasable elastic strain energy is initially sufficient
for complete formation of the spall, the propagation
will be at such speed that the energy contributed by
further heating would be negligible.*

If the fracture had initiated in a vertical direction,
propagation would cease upon entering the compressive zone
above or the large very slightly stressed zone below. (See
Figure 9). Such vertical fracture does not significantly
reduce the tensile stresses acting on the planes parallel
to the surface.

Fracture may also be initiated at the surface where
the compressive stresses are the greatest. (See Figure10).
A failure of this type would tend to reduce the tensile
stresses underlying the compressed zone. It is thus
possible and probable that there would never be a tensile
failure and hence spalling would never occur.

For the thermal stress problem, a compressive failure
at the surface would increase the porosity of the surface

* The released strain energy, greatly in excess of that
required, is converted into kinetic energy which results
in faster propagation.

RADIANT HEAT

POSSIBLE
FRACTURE

RADIAL STRESS SHOWN

COMPRESSION

TENSION

ENLARGED
SECTION
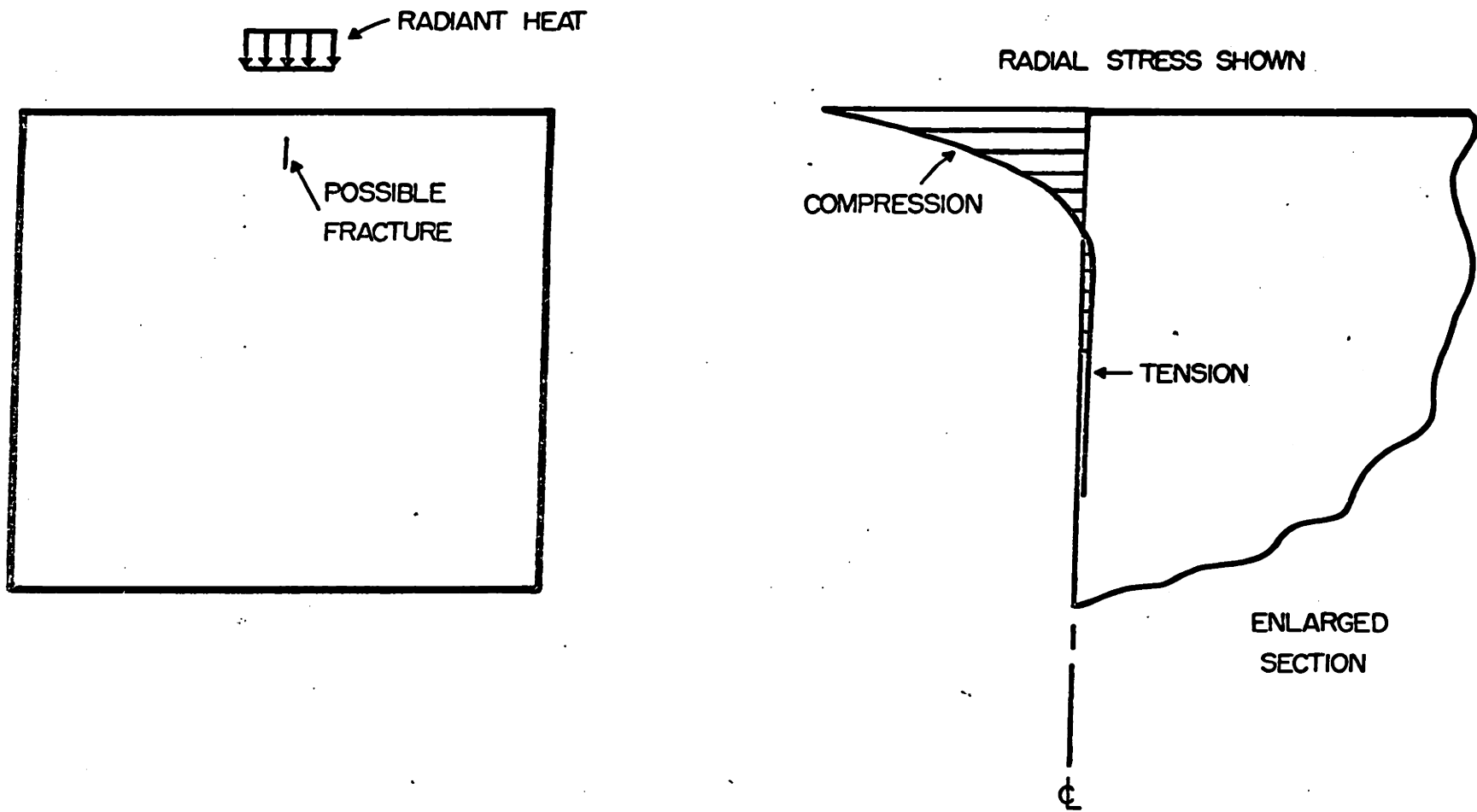
FIGURE 9:   VERTICAL CRACK IN THERMAL SPALLING

RADIANT HEAT

CRUSHED ZONE

RADIAL STRESS SHOWN

COMPRESSION

TENSION

ENLARGED
SECTION

45
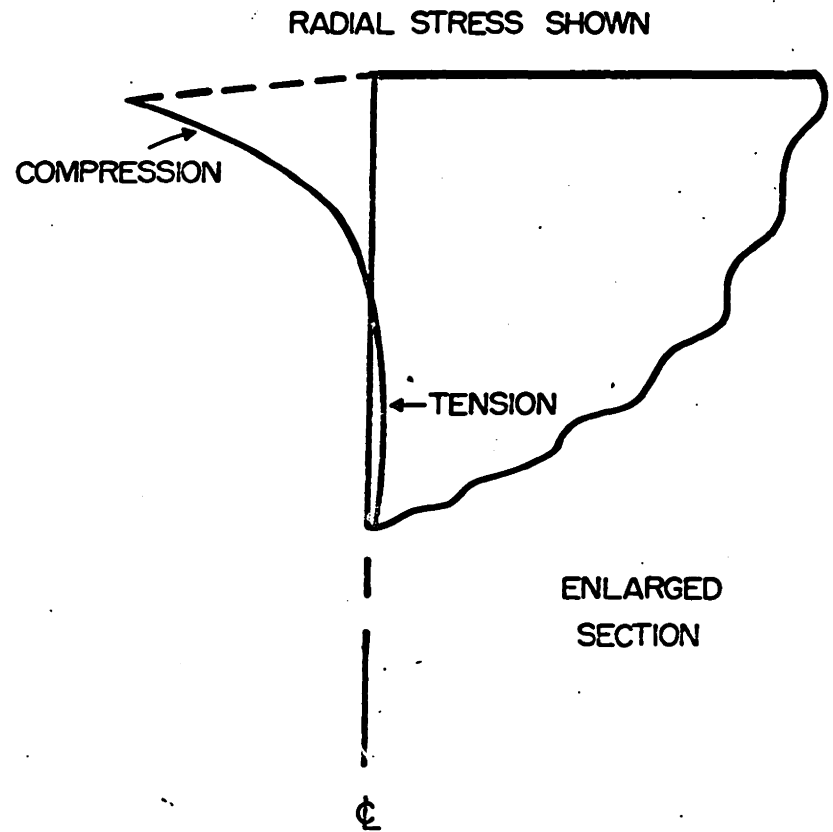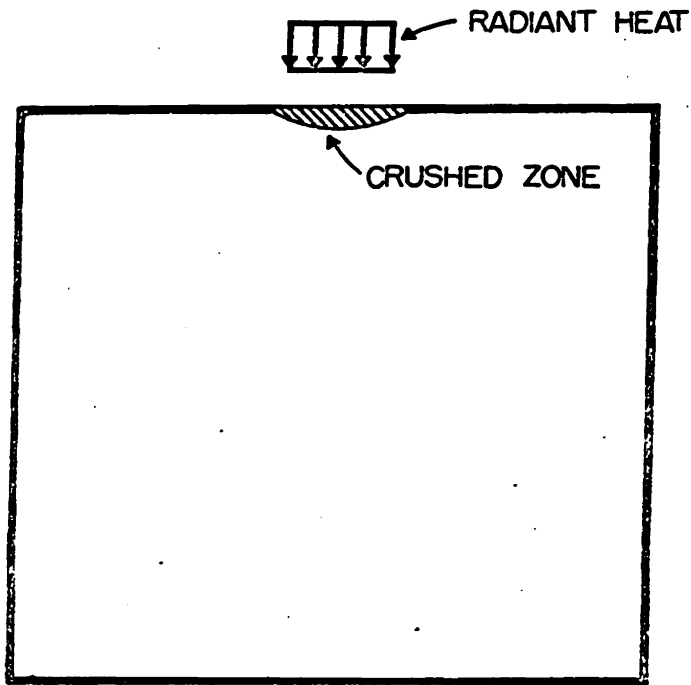
FIGURE 10:   FAILURE OF SURFACE

material, which would decrease the thermal conductivity, resulting in less heat penetrating into the intact zone. This would reduce the existing stresses, preventing spalling from ever occuring. Accompanying the crushing would be possible melting at the surface by the large amount of heat being retained there. This melting would result in loss of the heat energy in fusion, and in radiation, conduction and convection to the surrounding medium.

The circumferential tensile stresses surrounding the hot spot could initiate a fracture which then might propagate down into the body and sideways into slightly stressed zones next to the hot spot, and finally into the hot spot which is in compression. Thus this crack would not cause spalling.

The initial lack of energy to completely propagate a fracture may be overcome by additional loading or heating. There is at least one important potential application of this concept of increased loading to cause complete propagation, i.e. failure. This is in heat assisted mechanical destruction, where the material is heated before being subjected to mechanical loads. If the heating initiates the fracture, the mechanical loading may complete the propagation, or if the sharp bit of the

mechanical tool initiates the fracture, the heating with its large areas of highly stressed material may supply the energy needed to propagate the fracture.

Materials which are not completely brittle, but undergo some plastic deformation before fracture occurs, will require complex analysis for the stress state at time of fracture initiation. The evaluation of the available energy will also require careful consideration due to the nonlinear nature of the problem.

Detailed consideration of the stress that causes the fracture initiation and the energy for the propagation will be given to specific problems of thermal spalling in Chapter III.

2.3 THE ANALYSIS TECHNIQUE

2.3.1 <u>General</u>. The analysis technique was developed
to evaluate with sufficient accuracy and detail the func-
tions necessary for predictions of the spalling behavior
of rock and other brittle materials. It has a large degree
of flexibility and generality so that solutions can be
found for complex problems having both thermal and mechan-
ical loads, irregular boundary shapes and conditions and
nonlinear material properties.

Spalling is caused by stress induced brittle fracture
in the material. Under the conditions and range of
stresses which spalling takes place the material properties
are not stress dependent. The materials in which spalling
is a problem are ceramics, the harder rocks and concrete.
The spalling occurs at a surface which is subjected to
low (usually one atmosphere) pressure with high local
stresses due to mechanical or thermal surface loads causing
the initial failure by tensile fracture. Up to the point
of tensile fracture, the behavior of these materials is
known to be nearly linear and elastic [3].

These same materials if loaded to failure in simple
compression or in triaxial loading can, and usually do,
have large nonlinearities in the stress-strain relation-
ships. However, when the stresses in the body are such

that crushing or flow takes place before a tensile fracture, the tensile stresses are relieved and spalling does not occur. For these reasons linear stress analysis will suffice for the prediction of spalling behavior.

The material properties will change with the temperatures which accompany thermal spalling. The non-linearity of the coefficient of thermal conductivity affects the analysis of thermal stresses more than any of the other properties. In general, the conductivity of oxides, such as most rocks, decreases substantially with increases in temperature to the level needed to cause thermal spalling. The material which becomes the hottest is at the surface where the heat is applied and a great decrease in the conductivity at the surface prevents the heat from penetrating into the body. This heat retained at the surface further raises the temperature of this thin layer and causes additional decreases in the conductivity. This problem is further compounded if the surface material fails in compression increasing the porosity which further decreases the conductivity at the surface.

It is recognized that while it is possible to predict the thermal spalling behavior for simple cases based on linear behavior for most properties, there exist a large

class of problems in which it is necessary to consider more nonlinear behavior. Practical problems of this nature are combined heating and mechanical disintegration of rock, slow fatigue type fracture in a heat cycling environment and others. Since the investigation of these and similar problems is envisioned in the future, it was desirable to develop the analysis technique as general as possible. This required that the method have room for growth to the more complex cases while taking advantage of past developments which have been proven accurate by comparisons with experimental data. To meet these requirements, numerical methods of analyses for both the temperatures and stresses were used.

The method of analysis developed for this thesis is not in itself unique (although the heat transfer program was developed independently before it was available in the literature) but the solution of thermal stress problems with the complex boundary conditions has not been confirmed with laboratory experiments as is done in this work.

The thermo-elastic coupling is assumed to be of importance only as the temperatures affect the stresses and not the reverse. The stress levels encountered in rocks near a free surface are sufficiently low for convential sources of heating and mechanical loads that the

assumption is reasonable. This may not be the case if

blasting with convential or nuclear explosives is used

in disintegrating rock or for fracturing materials with

very intense sources of heat such as a laser in the

pulsed mode.

The inertia forces were neglected in the analysis.

Again this is reasonable in light of the conventional heat

sources and for a large category of the mechanical equip-

ment used in rock disintegration. However, there is a

significant number of rock disintegration methods in

which the inertia forces play an important role.

Examples of these are blasting, percussion drilling,

some erosion methods and others. The basic numerical

technique used could be modified in the future to eval-

uate dynamic problems with a useful carry-over of know-

ledge generated herein on the static problem.

2.3.2 Characteristics of the Material Properties.

The characteristics of the material properties include the

usual stress related nonlinearities caused by yielding and

crushing and in addition, those due to temperature var-

iations. Also, many rocks of sedimentary origin display

a great deal of anisotropy in their materials. Some of

the changes in the properties are brought about by the

temperature. However, those brought about by phase changes

are abrupt in nature and multivalued functions of the temperature.

The developed analysis technique has the capability to handle these nonlinear and anisotropic properties, but only the nonlinear thermal conductivity was considered for the examples analyzed.

2.3.3 <u>Unusual Boundary Conditions</u>. There are two unusual boundary conditions which will have to be considered for practical thermal spalling conditions and the numerical analyses developed can simply be extended to each. One is radiation away from a boundary with a changing temperature and the other is moving boundaries.

The radiation problem is of importance for evaluation of the net heat transfer to the heated object when radiant heat sources are used. The relative heat transfer by radiation between two bodies is not linear with respect to temperature, but is proportional to the difference of their surface temperatures to the fourth power. It was not needed for the examples in this thesis where heating was done with a gas laser becuase the radiant heat away from the specimen was negligible compared to the laser's input of heat.

The moving heat source or surface must be given consideration, respectively, in evaluating the use of

equipment for continuous spalling where the surface will recede in discrete jumps a distance equal to the thickness of the spall, or for equipment which moves the heat sources over the working surface.

2.3.4 Sequence of Operations. The analysis technique consists of a series of separate calculations of the different functions which control the process under consideration. The appropriate sequence of the calculations to determine the thermal spalling behavior is as follows:
1) Calculation of the temperature distribution based on the initial conditions and the proper boundary conditions.
2) Calculation of the stress distribution based on the proper boundary conditions and temperature distribution calculated in the first part. 3) These calculated temperatures and stresses are compared with the values required for failure of the material to see if failure has occurred, and if so, what type it is. 4) If part three indicates that an extension fracture is initiated in the proper location and headed in the proper direction, a calculation is made of the strain energy available to drive the fracture and a prediction is made of whether or not the fracture will propagate to form a spall.

2.3.5 Heating Time. In thermal spalling environments the temperature distribution is continuously changing with

time due to the application of heat at the surface and its transfer to the more remote regions of the body which results in continuous variation of the magnitude and distribution of the thermal stresses. It is necessary to find the magnitude and distribution of the stresses at the time they initiate the failure. To do so requires that the stresses be computed for time intervals sufficiently small such that the first failure mode is correctly evaluated.

2.3.6 Numerical Methods. To achieve the required flexibility and generality, a numerical approach called the finite element method [18] was used for both the heat transfer analysis and the stress analysis. With this numerical method, the body is modeled as an aggregate of many small, but finite size regions within which assumptions are made about the behavior of the function. Based on these assumptions, equations are formed which relate the function at discrete points throughout the body. The solution of these equations together with the assumptions within each element define the value of the function at all points in the body.

2.3.7 Heat Transfer Analysis. For the heat transfer analysis, the temperature is assumed to undergo a linear variation with respect to the space coordinates within each element. The temperature of the nodes (corners) of the

54

elements are related to each other by equations based on the conservation of energy. These equations are solved for the nodal temperatures. The element size must be chosen small enough such that the assumed linear variation of temperature within each element is a good approximation to the true temperature distribution.

There are two methods of solution to obtain the transient temperature distribution. One is to use modal analysis [19] in which the solution is found by super-imposing the contribution of each of the modes which significantly contributes to a particular solution. The other method is to march the solution forward by small time increments based on known values of the temperatures.

The second method was used because it is more flexible with regard to nonlinear material properties and changing boundary shape. The complete formulation of the heat transfer analysis technique and a listing of the computer program is given in Appendix A and Appendix B.

As developed, the method can solve problems which have the following characteristics for the transient temperature distributions.

1) No more than two-dimensional (plane or axi-symmetric).

2) The material properties may change only at the boundary between elements.

3) The conductivity may be different in the two directions (x, ẏ).

4) The boundary conditions may be

    A) Adiabatic

    B) Given Heat Flux

    C) Radiation

    D) Given Temperature

    E) Conduction to a Fluid of Given Temperature

5) The boundaries must be at a finite distance.

2.3.8 <u>Stress Analysis</u>. To evaluate the stresses, a finite element program was used which was developed by others [20]. This program would analyze the stresses for problems which have the following characteristics:

1) Plane strain, plane stress or axi-symmetric.

2) The modulus of elasticity may be a function of the stresses all other properties are constant.

3) The material properties may be different in directions parallel to the three axis.

4) Both the temperature distribution for initial stress free condition and the final conditions are known.

5) The boundaries must be finite.

6) The condition allowed at the boundaries are:

A) Free or fixed in any of the directions
parallel to the axis.

B) Applied Stresses

2.3.9 Energy Calculations. As stated in Section 2.2.4
the energy which is available to drive the fracture is the
result of the release of stored strain energy and that
added by further loading or heating. For thermal spalling
it is observed experimentally that the fracture process
occurs at such a rapid rate that the additional heating is
negligible compared to the heating which precedes the
initiation of fracture. To obtain the total energy made
available for fracture, it is necessary to calculate the
total strain energy before and after spalling and subtract
to get the strain energy released.

However, for spalling which is caused by sudden heating
of the surface, it is possible to make approximations which
are sufficiently accurate for the purposes intended. This
is done in Appendix B.

CHAPTER III

EXAMPLES

3.1 PURPOSE

Specific examples were studied both experimentally and analytically in order to achieve the following:

1) Demonstrate the validity and accuracy of the analysis technique used to predict the thermo-elastic response of brittle materials, and evaluate the estimates of material properties and boundary conditions. This was achieved by lasing thin disks in an axi-symmetric fashion, observing the temperatures and strains, and then comparing these with the analytical results.

2) Investigate and study the spalling phenomenon in brittle materials subjected to rapid local heating on the surface. This was similarly achieved by axi-symmetrically lasing cylinders of natural rock (such as granite and marble) and spheres of man-made brittle materials (such as porcelain).

3) Test the validity of the theory developed which explains and predicts spalling in brittle materials. This was done by obtaining the calculated stresses as a function of lasing time from the analysis technique, and by knowing the strength characteristics of the material involved, one

could find the time and location at which the predicted stress condition overcomes the strength of that material.* Several experiments would then be performed which involved lasing three-dimensional specimens. The time and location of failure initiation was observed and compared to the theoretical predictions.

3.2 MATERIAL PROPERTIES

The material properties required for the analysis technique and prediction of the spalling behavior were:

1) Thermal Conductivity

2) Specific Heat

3) Density

4) Modulus of Elasticity

5) Poisson's Ratio

6) Coefficient of Thermal Expansion

7) Tensile and Compressive Strengths

8) Specific Surface Energy

The experimental evaluation of some of these properties was beyond the scope of this work and estimates were made based on published data for the same or similar material. To establish confidence in the results of analyses based

* In addition to this the energy available for the propagation of the fracture was evaluated, and taken into consideration.

on some estimated data, comparisons were made between analytical and experimental results in certain experiments. Since the results compared well, the analysis program was used with confidence to solve other problems having the same materials and heat source for ranges of temperatures and stresses that were similar to the control experiment.*

The following material properties were evaluated for the granite and marble used in the experiments:

1) Modulus of Elasticity

2) Tensile and Compressive Strengths

3) Coefficient of Thermal Expansion

For the porcelain, only the tensile strength was evaluated. The specific surface energy has already been experimentally evaluated for the granite and marble [16]. These rocks were from the same quarries as those used in the experiments conducted herein.

All other material properties were taken from handbooks and other published data. Table 1 lists the value of each property and the source of information.

* If the analytical and experimental results had not compared well, a more detailed evaluation of the individual properties and boundary conditions would have been required.

MATERIAL PROPERTIES

SYMBOL	DEFINITION	MARBLE	GRANITE	PORCELAIN
	Specific heat capacity (BTU/lb $^{\circ}$F)	0.42	.21	.21
K	Thermal conductivity (BTU/in. sec. $^{\circ}$F)	$\dfrac{1}{24000.+30T}$	$\dfrac{1}{31500+21.6T}$	2.35×10^{-5}
P	Density (lbs/in^3)	$.097 \dfrac{lbs}{in^3}$	$.094 \dfrac{lbs}{in^3}$	$.094 \dfrac{lbs}{in^3}$
	Linear coefficient of expansion (/$^{\circ}$C)	1.22×10^{-5} *	0.72×10^{-5} *	$.50 \times 10^{-5}$
E	Modulus of elasticity (psi)	8.3×10^{6} *	2.4×10^{6} *	6.0×10^{6}
	Poisson's ratio	0.3	0.1	0.3
S_T	Breaking tensile stress (psi)	1960 *	1560 *	8,500 *
S_C	Breaking compressive stress (psi)	9100 *	34000 *	70,000
γ	Specific surface energy (ergs/cm^2)	50,000	50,000	2,000

* Denotes those properties found by experiment. The source of the other data was the literature [17], [11] for the natural rock and porcelain, respectively.

TABLE 1

3.3 EXPERIMENTAL EVALUATION OF SOME MATERIAL PROPERTIES

The modulus of elasticity was experimentally evaluated for granite and marble by placing electric strain gages on the top and bottom of beams one inch wide by one inch deep by twelve inches long. The beams were loaded at their quarter points and the strain gage readings recorded. From this information and simple beam theory for the stresses, the modulus of elasticity was calculated. To evaluate this property at much higher compressive stresses, the beams were loaded in axial compression and the strain was recorded. The average values of the two tests was used in the analyses.

The tensile strength was experimentally evaluated by center point loading of beams one inch wide by one inch deep by five inches long. The value of tensile strength given by such bending tests is usually about twice that for a uniaxial test [3] and this must be taken into consideration in using the data.

The compressive strength was experimentally evaluated by axially loading to failure four inch long prisms with one inch by one inch square cross-sections.

The coefficient of thermal expansion was found by measuring the change in length of a 12 inch beam of the material when it was heated from the freezing point to the

boiling point of water. The coefficient calculated from this range of temperatures was used for a much broader range of temperatures in analyzing the experiments done with the laser heat source. This extrapolation is reasonable since the material does not undergo a phase change in the higher temperature of the laser experiments.

The tensile strength of the porcelain balls was found by applying a compressive load to the ball through steel platens.* This loading condition was then analyzed for the maximum tensile stress in the ball at the time of failure using the finite element stress analysis program. The maximum tensile stress is in the interior of the body as it is for the thermal spalling tests. The size and shape of the tensile zone is also much the same as for the thermal spalling condition. For these reasons, the tensile strength found by this method seems particularly valid to use in the prediction of the spalling response of the porcelain.

3.4 SPECIFIC EXAMPLES WITH THIN DISKS

    3.4.1 General. The analysis technique and the assumptions or estimates about the material properties

_____

* This is similar to the Brazilian test for splitting cylinders.

and boundary conditions were evaluated for accuracy by comparing the results of lasing experiments conducted on thin disks with the predicted results of analysis. The thin disk shape was suitable for the following reasons: 1) It would result in axi-symmetric problems which can be analyzed with the computer programs. 2) The shape was well suited to available test apparatus for experimentally measuring the temperatures. 3) It was possible to arrange strain gages in such a manner that the effects of a change in gage temperature would be compensated for and the resulting measurement could be directly compared with the analysis. 4) This shape was easy to prepare to close tolerances by slicing cores cut from larger blocks of rock.

The material properties used in the analysis of the temperatures were:

1) Thermal Conductivity

2) Specific Heat

3) Density

The boundary conditions used in the analysis of the temperatures were:

1) Net Heat Input by the Laser

2) Thermal boundary conditions elsewhere on the surface.

Each of the properties were taken from published data on material which was similar to that used in these experiments. The boundary conditions were approximations based on the known total output of the laser and judgment of the amount of heat lost from the rock. The amount of heat lost was considered to be negligible since the tests are of short duration and the rock remains relatively cool over most of its surface. The cool surface would not lose much heat by either convection to the air or by radiation. The fraction of radiation energy (of 10.6 micron wavelength) from the carbon dioxide laser, which the surface would receive, was assumed to be unity. In all cases, the surface of the rock where the laser was focused was covered with temperature sensitive paint.*

The analysis of the thermal strains required the use of the coefficient of thermal expansion and Poisson's ratio in addition to those required for the temperature analysis. The coefficient of thermal expansion was experimentally evaluated over the zero to one hundred degrees

* The paint used was "Detectotemp" brand made by Hardman Inc., Belleville, New Jersey. The painted area at which the laser radiation struck the surface would almost immediately turn black. (This was the color corresponding to the highest temperature indicating capability of the paint.)

centigrade temperature range for samples of rock from the same source as the rock used in the other experiments. The value obtained in this manner was used for the laser heating experiments in which the temperatures are, in general, in excess of one hundred degrees centigrade. Poisson's ratio was experimentally found for the rock used in the experiments. The range of stresses used in the evaluation experiments was about the same as that encountered in the laser heating experiments.

The application of the analysis technique in the prediction of failure modes involves finding the stresses. To do this only the modulus of elasticity is needed in addition to those factors which are included in the analysis of the strains. Since the modulus of elasticity was found experimentally for the rocks over the same range of stresses as exist in the thermal spalling experiments, the accuracy of the analytically predicted stresses can be expected to be as good as that of the strains.

The modulus of elasticity of the porcelain was taken from published data and thus may not have the accuracy that is expected in the case of the natural rocks. However, the porcelain is a man-made material in which the quality control may render the estimate based on published data quite good.

The temperature variation with time on the surface of thin disks were predicted theoretically by using the finite element heat flow analysis, in conjunction with the material properties shown in Table 1.   In addition, the following assumptions were made: 1) The entire energy output of the laser was absorbed by the rock. 2) There were adiabatic boundary conditions elsewhere on the surface. This record was then compared with the temperatures observed using a radiometric microscope. In calibrating this instrument, it was found that the emissivity was about 94 per cent (a black body is 100 per cent) in an experiment where the surface temperature was a few hundred degrees centigrade. Details of the experimental equipment and more data are available [17].

A typical result for these experiments is shown in Figure 11. The difference between the analytical and experimental results is usually about ten to twenty per cent with no pattern of consistency of one being lower than the other.

The strains caused by heating the center of marble disks with a laser were compared with strains calculated analytically. The strains near the edge of the disk were measured using electric resistance strain gages and recorded with an oscilloscope. Multiple gages were used
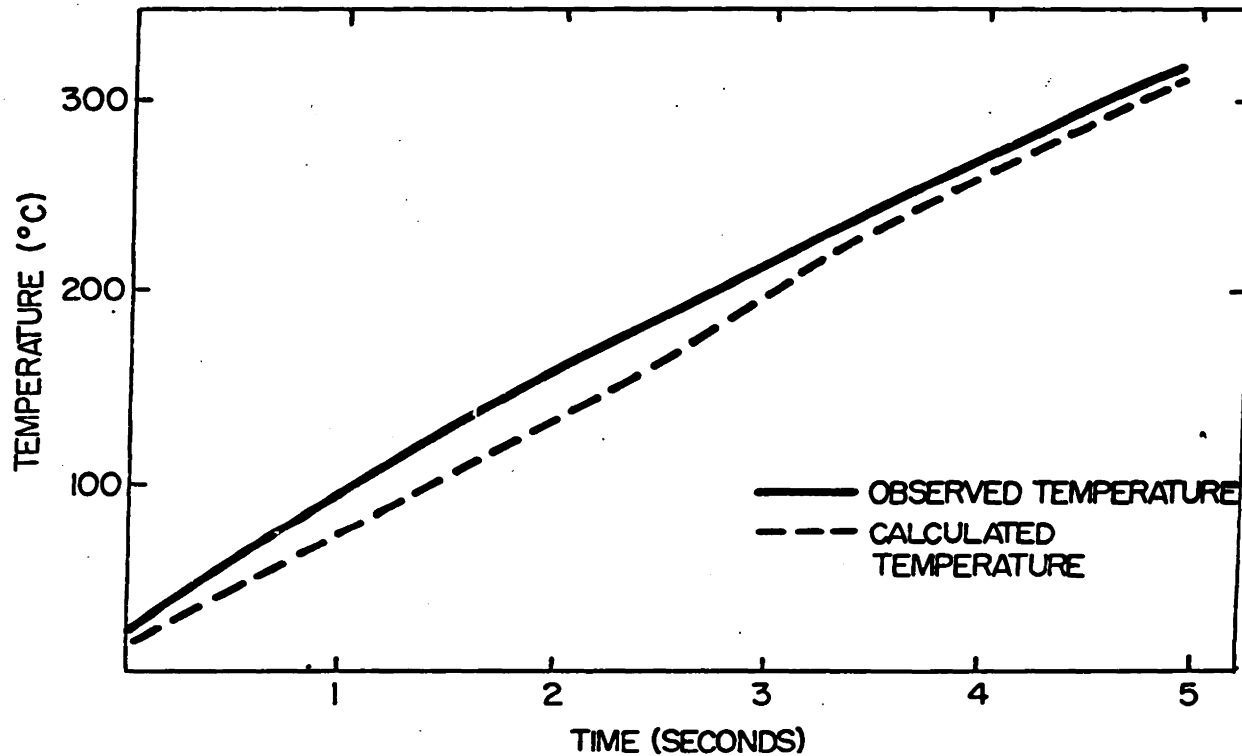
FIGURE II⁝ OBSERVED AND CALCULATED TEMPERATURES AT BACK-

SIDE CENTERSPOT OF DISC. THIS CONSISTED OF LASING A 0.05" THICK

MARBLE DISC AT A POWER LEVEL OF 10 WATTS [17]

so that the effects of temperature changes of the gage would be compensated for. Figure 12 shows both the analytical and experimental strain as a function of heating time. The error is about ten per cent with the analytical value lower then the experimental.

3.5 SPECIFIC EXAMPLES WITH CYLINDERS

3.5.1 <u>General</u>. The responses of rock cylinders to local heating was studied both experimentally and analytically in order to understand the nature of the thermal spalling mechanisms. The approach taken was to conduct experiments in which the time required to spall at a given power level was measured and then using the analysis technique to find the temperatures, the stresses and the releasable strain energy at the time of fracture initiation. This information allowed a prediction of spalling response to be made with the developed theory. This would then be compared to the experimental behavior for marble and granite at different power levels, thus illustrating different modes of failure.

The specimen shape used to investigate and study the spalling phenomenon was designed to have responses which would be similar to that which occurs in the field. The field condition is usually a relatively large mass of rock heated over a small portion of its surface. For the

LASER BEAM OF 5
WATTS, TOTAL POWER
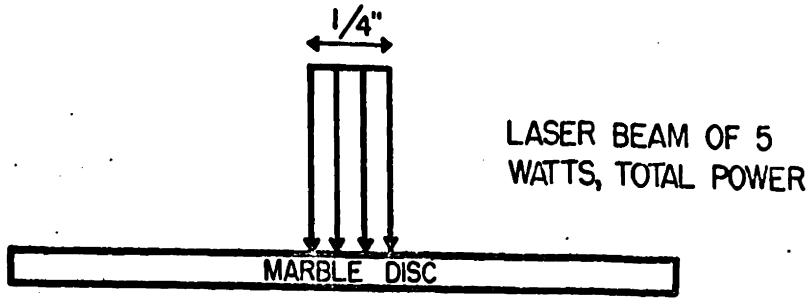
THE DISC IS INSTRUMENTED TO MEASURE RADIAL AND TANGENTIAL
STRAINS AT A DISTANCE OF 0·60" FROM THE CENTER, ON BOTH SIDES.
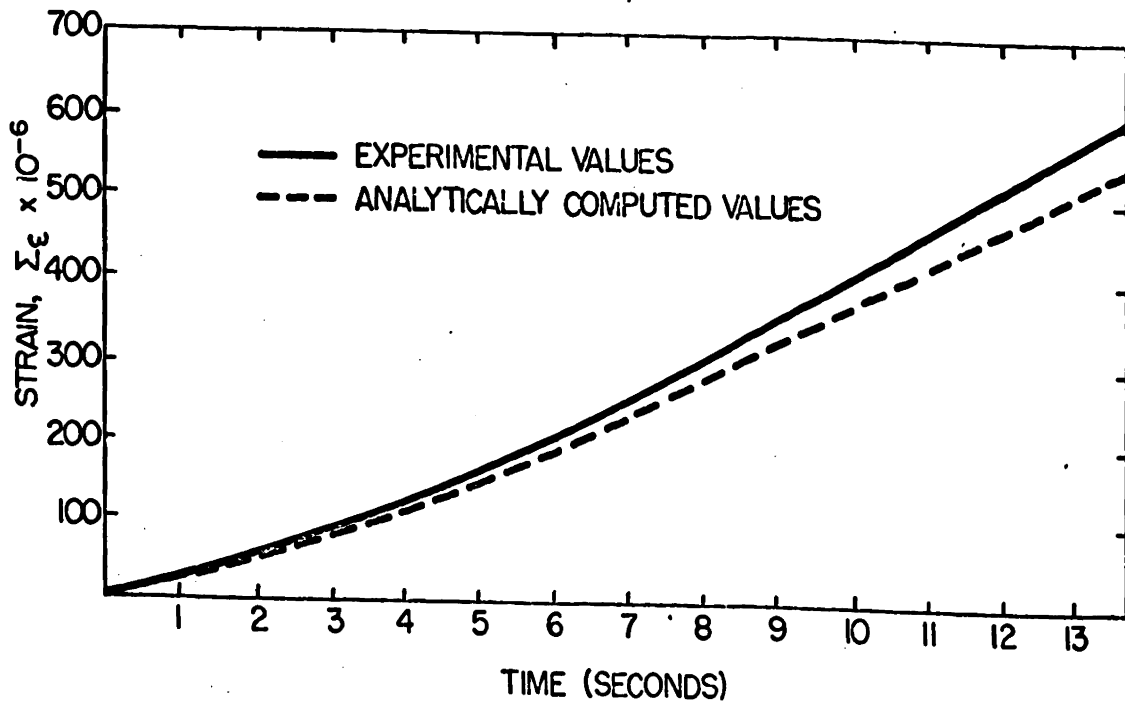
FIGURE 12: COMPARISON OF EXPERIMENTAL
AND ANALYTICAL VALUES OF MEMBRANE STRAINS

[17]

experiments, it was desirable to keep the specimens as small as possible for ease and economy of preparation and handling, and it was also necessary that the specimens have an axis of symmetry to render the two-dimensional analysis program applicable. The cylindrical shape satisfied these requirements and was used for the natural rock (marble and granite) specimens. These specimens were prepared by drilling cores out of large blocks which were then cut to the proper length.

Spalling experiments were conducted on the granite and marble cylindrical shaped specimens by heating at the center of one end. A microphone was placed near the heated end to pick up the sound of the spalling which was a snapping noise audible to the human ear a few feet away from the specimen. The sound of the window of the laser being opened was also picked up by the microphone and when displayed together on an oscilloscope screen gave a record of the heating time to cause spalling. The size of the heated spot was controlled by reflecting the beam from a focusing mirror and adjusting the distance between the mirror and specimen.

Most specimens were $1\frac{1}{2}$ inches long and $1\frac{1}{2}$ inches inches in diameter. Initially tests were conducted on shorter cylinders and it was concluded that $1\frac{1}{2}$ inches of

length was sufficient to cause spalling of granite specimens
for the range of heating rates that were used in the exper-
iments. This length was also easy to handle and position
in the test equipment.

3.5.2 Variation in Length (Granite). To establish
the minimum length of specimen that could successfully
be used to study spalling, experiments were conducted on
granite specimens of different lengths. Specimens $1\frac{1}{2}$
inches in diameter with lengths of $\frac{1}{2}$, 1, $1\frac{1}{2}$, and 2 inches
long were heated on one end with the laser set at low
power and focused. By using a power in the low end of
the operational range for that laser, the conclusions
reached about the minimum length for spalling also held
true for higher ranges of power rates. This was because
at higher powers the spalling condition was reached in
shorter times, i.e. a smaller region of the material would
be heated thus requiring a smaller amount of cooler
surrounding material to sufficiently restrain it. The
focusing apparatus was required in order to heat only a
small portion of the surface.

Spalling was not observed in the $\frac{1}{2}$ long specimen; the
1 inch long specimens underwent some spalling, and the
longer specimens exhibited very good spalling. On the
basis of these tests, it was decided that specimens $1\frac{1}{2}$

inches long would be used for all other tests.

The chips formed by the spalling were about 3/10 inch in diameter. The front side of the chip, which was the surface of the specimen, remained the same in appearance with no signs of crushing or melting.

For those specimens in which spalling occured, the temperatures and stresses were calculated with the analysis technique for the time at which spalling was experimentally observed to start. These temperatures and stresses are shown in Figure 13 and Table 2.

The tensile stresses acting under the heated area on a plane parallel to the surface were the largest tensile stresses in the longer specimen and for the specimens shorter than about $\frac{1}{2}$ inch, the largest tensile stress is the tangential one around the heated spot. Thus, the first fracture to be initiated in the short specimens would tend to split the specimen. However, the combination of the large fracture area required to completely split the specimen and the low releasable strain energy associated with this mode would lend to a stable crack as was observed in the experiments. After the experiment, the outward appearance of the specimen was that it was intact and sound to the touch. The extent of the splitting fracture could only be estimated because the analysis of the stresses

SUMMARY OF EXPERIMENTS AND STRESSES FOR VARIATION IN SPECIMEN LENGTHS

Material = Granite
Diameter = 1.5 inches
Power   = 50 watts
Laser   = 0.3 inches
Time   = 2.0 seconds

No. of Tests	Conditions	Maximum Tension ksi	Maximum Compression ksi	Strength** St ksi	Sc ksi	Energy* Ratio	Observed Behavior	Correct Prediction
3	0.5" long	1.42	14.8	0.78	34	.5	no spall	Yes, but see below
2	0.0" long	1.15	15.3	to		15	some spall	Yes
3	1.5" long	1.15	15.3	1.56		15	good spall	Yes
2	2.0" long	1.15	15.3			15	good spall	Yes

* ratio of releasable strain energy to energy required to form fracture surface for complete spalling.

NOTE: For the $\frac{1}{2}$ inch long specimens the maximum tensile stress was not the stress required to initiate a spalling type fracture but a splitting of the specimen. Estimates show that there is insufficient energy for this fracture to propogate through the specimen.

** for tensile strength a range of $\frac{1}{2}$ to full value of tensile strength from beam bending tests is given.

TABLE 2

LASER POWER := 50 WATTS

LASER BEAM DIAMETER = 0·3 INCH

HEATING TIME = 2·0 SECONDS

—————— THE MAXIMUM TENSILE STRESS IN THE VERTICAL DIRECTION
UNDER THE SURFACE HOT SPOT (INDUCES A SPALLING FRACTURE)

— — — THE MAXIMUM TENSILE STRESS IN THE TANGENTIAL DIRECTION
IN ANULAR ZONE ABOUT THE SURFACE HOT SPOT (INDUCES
A SPLITTING FRACTURE)
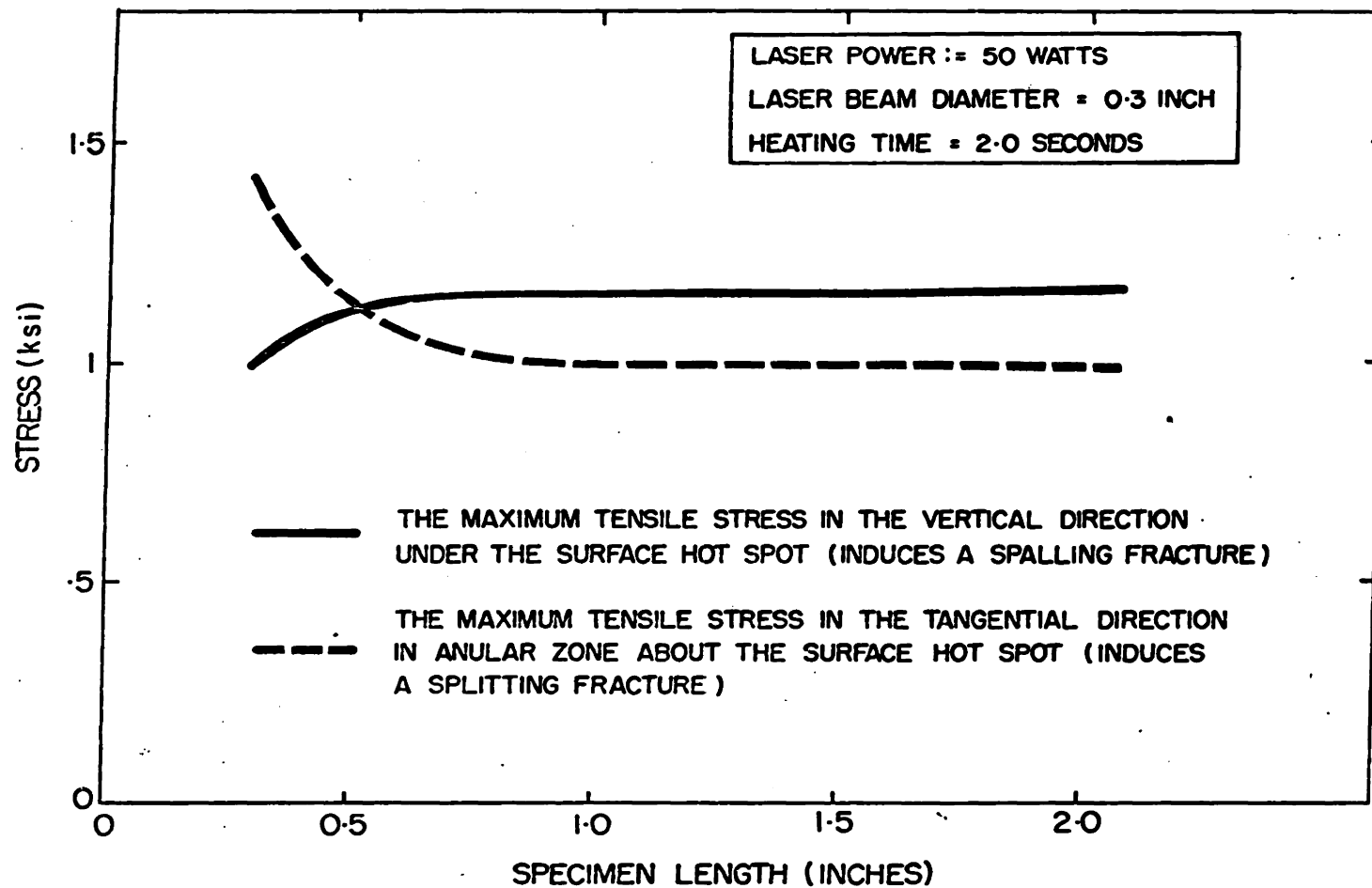
FIGURE 13:   STRESSES IN GRANITE CYLINDERS AS
A FUNCTION OF SPECIMEN LENGTH

after splitting was not a two-dimensional symmetric problem.

By comparing the maximum calculated tensile stresses at the time spalling started for the longer specimens, it is seen that these stresses are about equal to the tensile strength of the granite.

Investigation of the calculated stress distribution for the cylinders that underwent spalling at the time of failure initiation shows that the maximum compressive stress at the surface (and parallel to it), where the heat was applied, was less than the compressive strength of the granite. This corresponds to the experimental observations that the outer surface of the chip showed no signs of crushing or melting.

The amount of energy released by the spalling greatly exceeded that required to form the new fracture area. The area of the fracture used for the energy calculation was based on the experimentally observed chip size.

3.5.3 <u>Variation in Power (Granite)</u>. Experiments were conducted on granite cylinders $1\frac{1}{2}$ inches by $1\frac{1}{2}$ inches at three different power levels using the same diameter laser beam. The heating time to cause spalling was recorded for each experiment using a microphone and oscilloscope. The

data for the tests are shown in Table 3 and in Figures 14 through 18.

Figure 14 shows the distribution of the temperatures and the stresses for a given heating time. The general shape of these functions remains the same throughout the typically short heating time required to cause the spalling and for the various power levels. With longer heating times the temperatures increase in magnitude, penetrate deeper into the specimen and spread out further over the surface. The tensile stress which initiates the spall fracture is the Z stress shown along the centerline.

Figure 15 shows the increase in calculated maximum temperature (on the specimen's centerline at the surface) with respect to heating time for the three power levels. These temperatures are calculated on the basis of low temperature material properties and may not be accurate for the higher ranges of temperature. Therefore, the very high temperatures should be considered only for illustrative purposes.

Figure 16 shows the variation of the maximum compressive stress and the maximum tensile stress which causes spalling in the specimen with respect to the heating time. It can be seen that for each power level the maximum tensile stress exceeds the modulus of rupture before the maximum compressive stress exceeds the

compressive strength.

It is to be expected that the material will fail in tension at a level lower than the modulus of rupture (which is typically from 1.5 to 2.0 times the uniaxial strength of brittle materials). This is confirmed by the experimentally observed mean heating time (shown on the figure) which indicate that the calculated stress was about $\frac{3}{4}$ of the modulus of rupture.

The ratio of the compressive strength to the modulus of rupture and the ratio of the maximum compressive stress to the maximum tensile stress which causes spalling, are shown in Figure 17 as a function of heating time for three different power levels. If the ratio of the stresses is less than the ratio of the strengths the tensile strength will be exceeded before the compressive strength is. If this is the case, then a fracture will be initiated which will cause spalling if there is sufficient energy available for complete propagation. If not, the surface will crush, and since this will subsequently reduce the tensile stresses, a spall producing fracture will probably not occur. It is seen from Figure 17 that the ratio of stresses is less than the ratio of the strengths, and therefore spalling can be expected. This prediction was confirmed by

experimental observation.

Figure 18 shows the required thermal energy to cause spalling as a function of power. For the granite cylinders there was a slight decrease observed when increasing the power from 50 to 200 watts.

In Table 3 the term "Energy Ratio" is the ratio of the strain energy that would be released by complete propagation to the energy that would be consumed by the fracture process. Since this term is greater than unity for all three power levels, it was expected that complete propagation would occur. Experimental observations corroborated this hypothesis.

3.5.4 <u>Variation in Power (Marble)</u>. Experiments were conducted on marble cylinders $1\frac{1}{2}$ inches by $1\frac{1}{2}$ inches at power levels of 50, 100 and 200 watts. Table 4 gives the details of the experiments and parameters. For each of these cases (and for a few trial ones at even higher and lower power levels) there was no sound of spalling recorded with the microphone and oscilloscope·nor was there any other evidence that spalling had occured. If the heating was stopped before melting of the surface began, the heated material showed signs of crushing. It could be easily removed with a knife blade.

Figure 19 shows the distribution of temperatures and

Granite Cylinders ($1\frac{1}{2}$" by $1\frac{1}{2}$") Heated with a Laser Beam 0.2 inches in Diameter

No. of Tests	Power Watts	Mean[1] Heating Time Sec.	Maximum[2] Tension ksi	Maximum Compression ksi	Strength[3] St ksi	Sc ksi	Energy[4] Ratio	Prediction	Agree with Exp.
4	50	0.83	1.25	13.3			2.9	Tensile fracture and spall	Yes
5	100	0.38	1.34	14.0	.78 to 1.56	34.	2.1	Tensile fracture and spall	Yes
5	200	0.18	1.35	15.0			1.5	Tensile fracture and spall	Yes

(1)   Mean of experimentally observed heating time required to cause first spall.
(2)   The calculated stresses for the mean heating time.
(3)   The range for the tensile strength is 1/2 to the full value of the modulus of rupture.
(4)   Ratio of the calculated releasable strain energy to the energy required to form the fracture area for complete failure.

TABLE   3

RADIANT HEAT

−7·6 ksi

695°C

0·1"

σ_R

σ_θ

−7·6 ksi   695°C

σ_R

σ_Z

——— STRESS
− − − TEMPERATURE
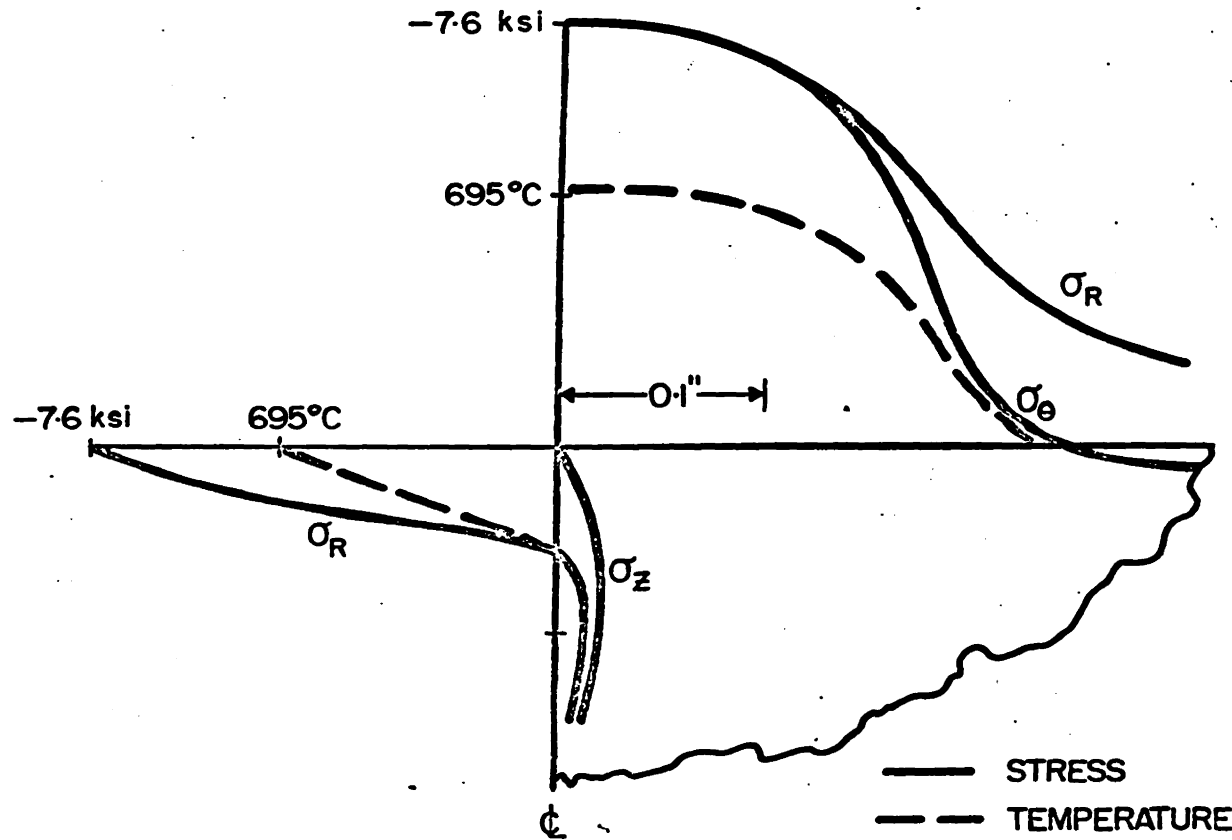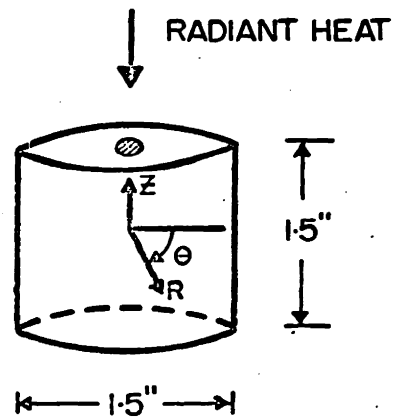
FIGURE 14: TEMPERATURE AND STRESS DISTRIBUTION FOR A
GRANITE CYLINDER (50 WATTS, 0·4 SECONDS HEATING)
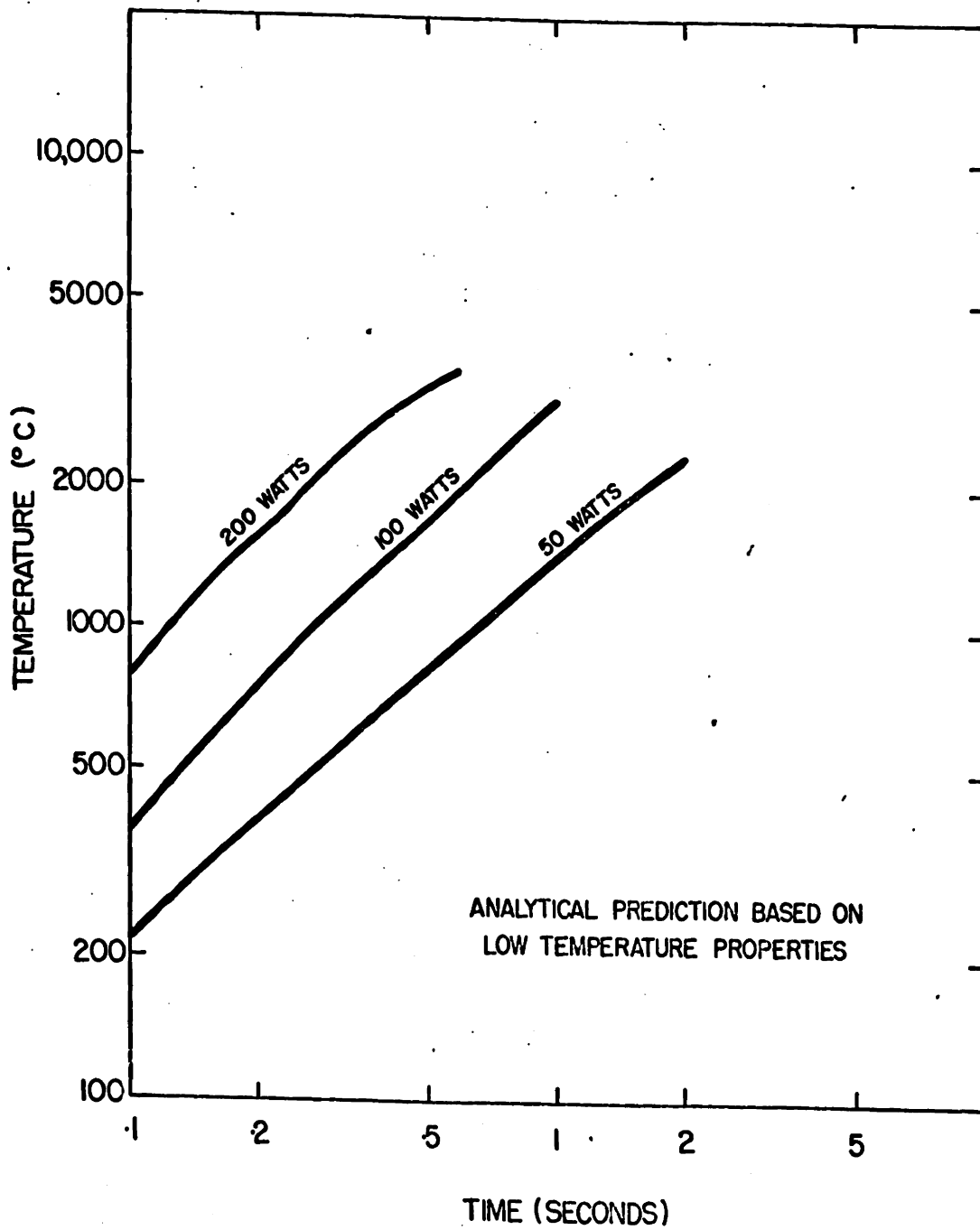
FIGURE 15: MAXIMUM SURFACE TEMPERATURE
VS. HEATING TIME FOR GRANITE CYLINDERS
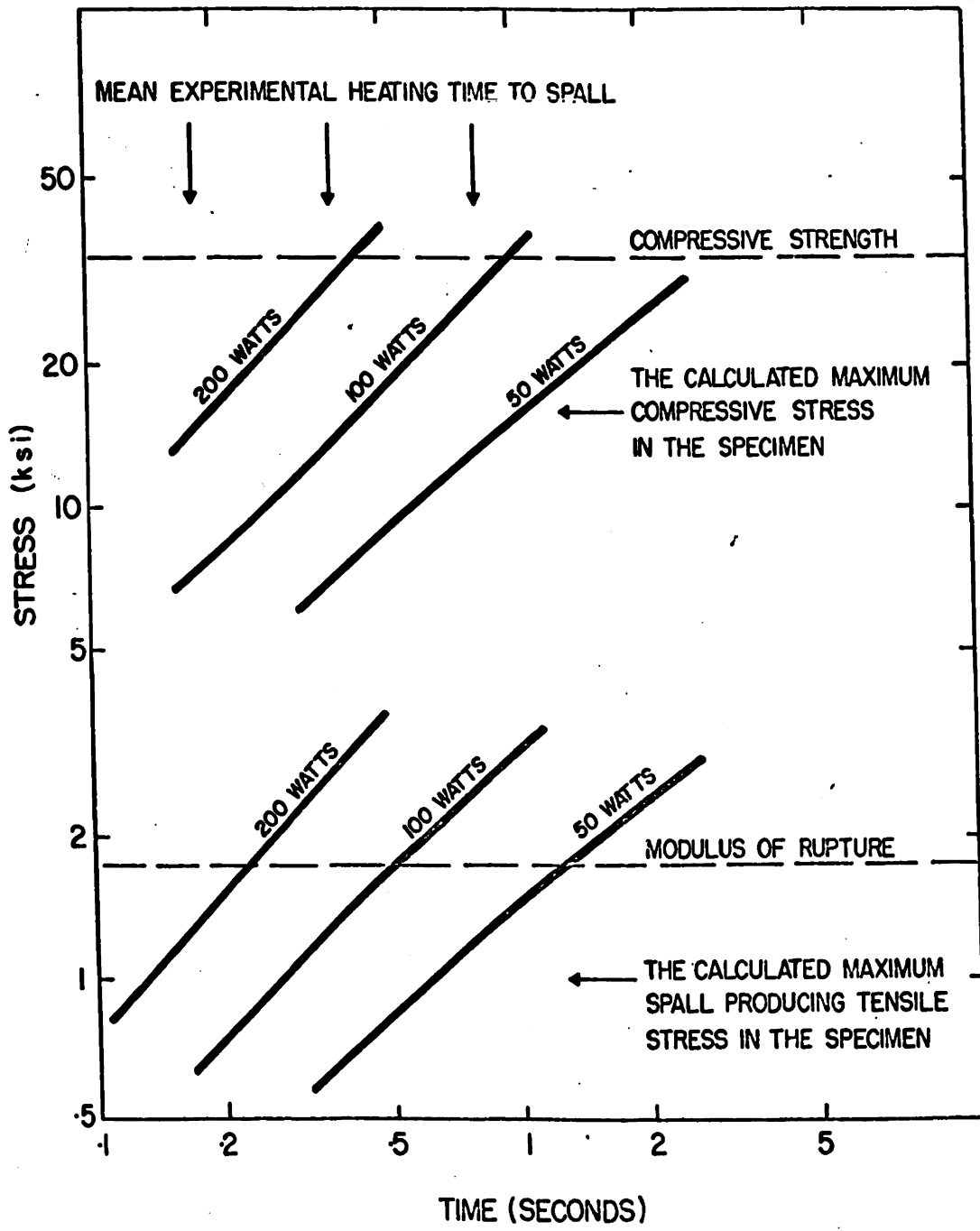
FIGURE 16: STRESS VS. HEATING TIME

FOR GRANITE CYLINDERS
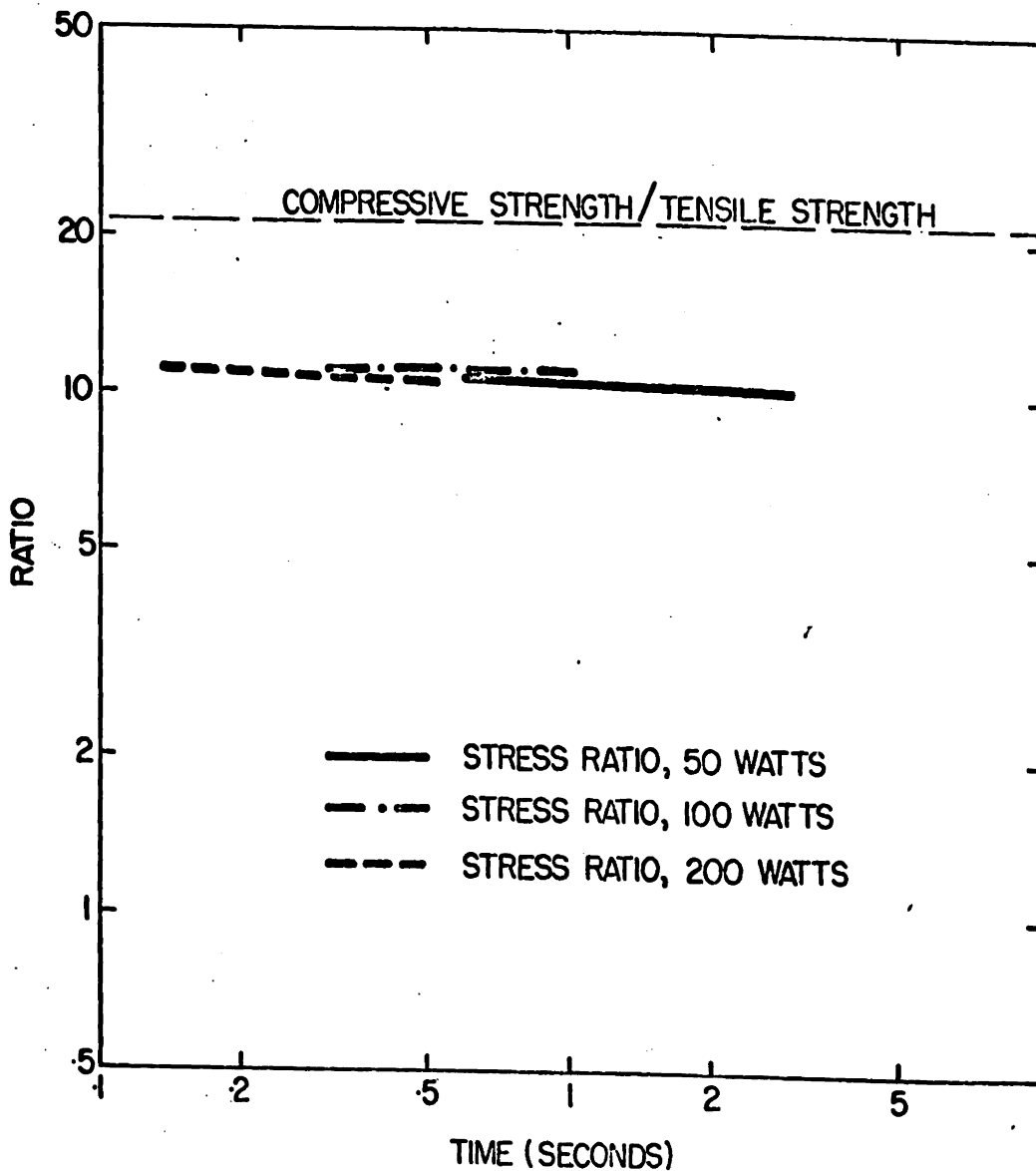
FIGURE 17: VARIATION WITH RESPECT TO
HEATING TIME OF THE RATIO OF
MAXIMUM COMPRESSIVE STRESS OVER THE
MAXIMUM SPALL PRODUCING TENSILE STRESS
IN GRANITE CYLINDERS

84
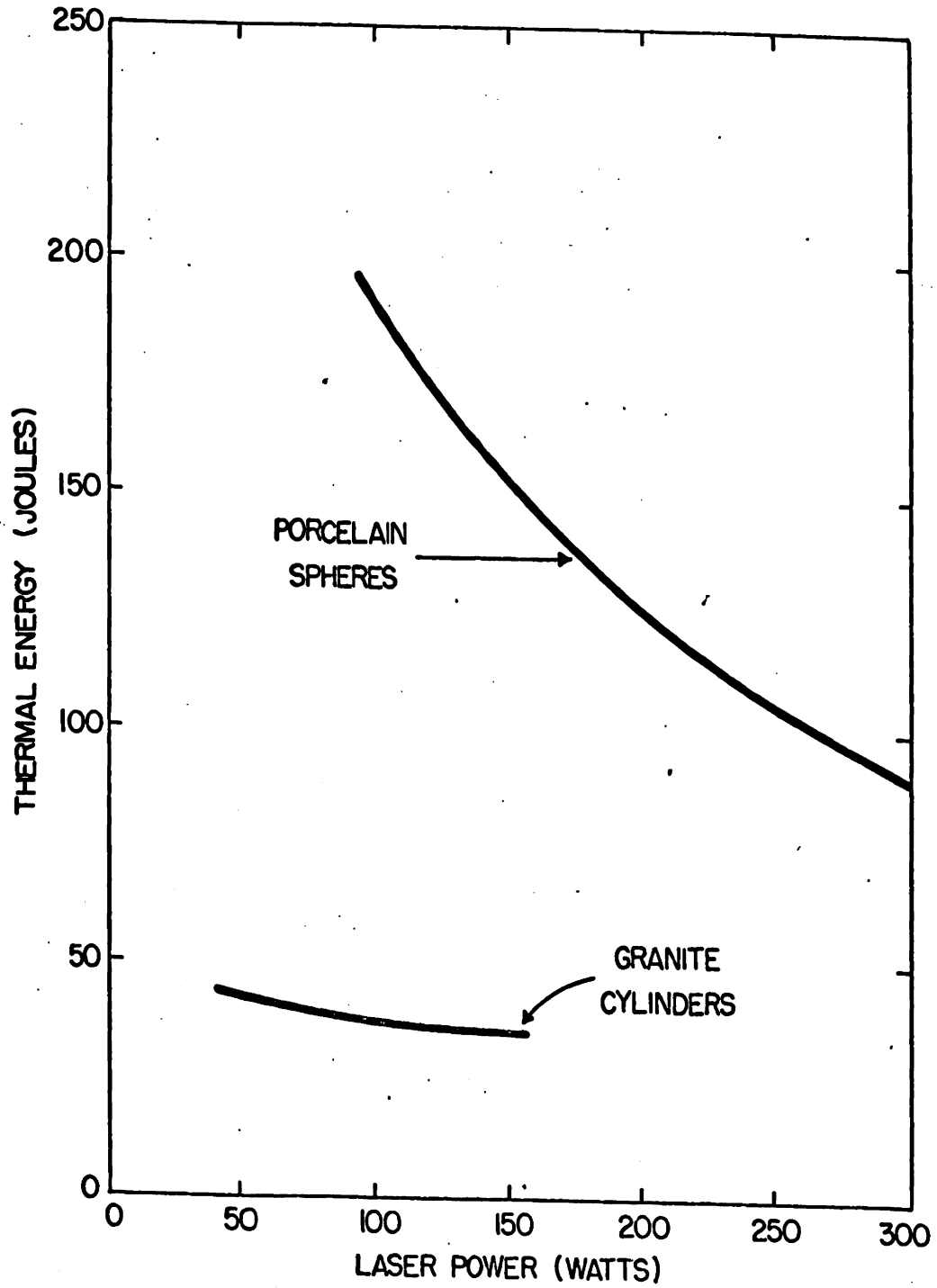
FIGURE 18: THERMAL ENERGY REQUIRED TO CAUSE SPALLING VS. POWER LEVEL

stresses in the specimen. This distribution is very nearly like that for the granite cylinders and will change only in relative size and magnitude with changes in heating time or variation of power levels.

The increase in the calculated maximum temperature (on the specimen's centerline at the surface) is shown in Figure 20. The analyses were performed based on the low temperature properties of the marble and may not be accurate for the higher temperature ranges with the accompanying phase changes. Therefore, the highest temperatures should be considered only for illustrative purposes.

Figure 21 shows the variation with heating time of the maximum compressive stress and the maximum tensile stress (which would tend to cause spalling in the specimen). For each power level the maximum compressive stress exceeds the compressive strength before the maximum tensile stress exceeds the modulus of rupture. Thus, it is expected that the surface would fail in compression before a spall producing fracture could be initiated. Even if a tensile failure could occur at one half the modulus of rupture, the compressive failure at the surface would still be the first mode of failure. This crushing type of failure was the type that was

observed in the experiments.

A crushing of the surface under the laser radiation has two effects which prevent spalling. First, the local crushing relieves the spall producing tensile stresses. Second, the crushing increases the porosity of the material, which decreases the thermal conductivity. Thus, a crushed layer will act as an insulator, retaining the heat at the surface where it would cause melting and heat loss by reradiation. The reduced heat flux into the intact material underneath would tend to reduce the thermal gradients and the thermal stresses.

The ratio of the compressive strength to the modulus of rupture and the ratio of the maximum compressive stress to the maximum tensile stress are shown in Figure 22 as a function of heating time for three different power levels. For all heating times and power levels, the ratio of the stresses exceeds the ratio of the strengths which means that a compressive failure will occur first.

3.5.5 <u>Variation in Power (Porcelain)</u>. Porcelain spheres $1\frac{1}{2}$ inches in diameter were heated at three different power levels and the heating time required to cause spalling was recorded using a microphone and oscilloscope. Table 5 gives details of the experiments and the parameters.

Marble Cylinders ($1\frac{1}{2}$ " by $1\frac{1}{2}$") Heated With a Laser Beam 0.2 Inches Wide

No. of Tests	Power Watts	Average[1] Stress Ratio	Strength[2] Ratio	Prediction	Agree with Experiment
3	50	10.25	4.6	Compressive Failure no Spalling	Yes
4	100	11	4.6	Compressive Failure no Spalling	Yes
5	200	9.5	4.6	Compressive Failure no Spalling	Yes

(1) Ratio of maximum compressive stress to the maximum tensile stress which tends to induce spalling averaged over the heating time

(2) Ratio of the compressive strength to the modulus of rupture

TABLE 4
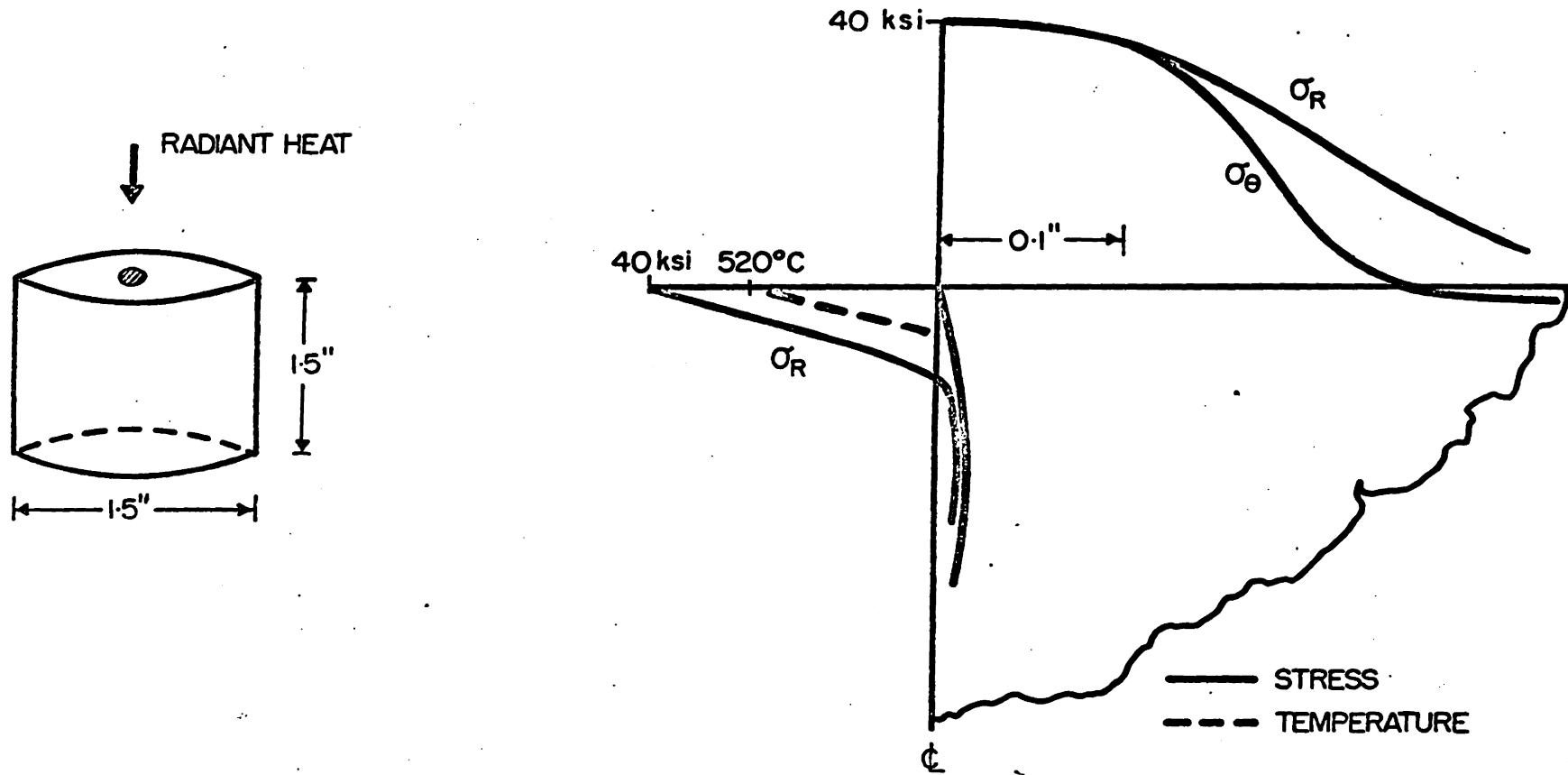
FIGURE 19: TEMPERATURE AND STRESS DISTRIBUTION FOR A
MARBLE CYLINDER (50 WATTS, 0·6 SECONDS HEATING)
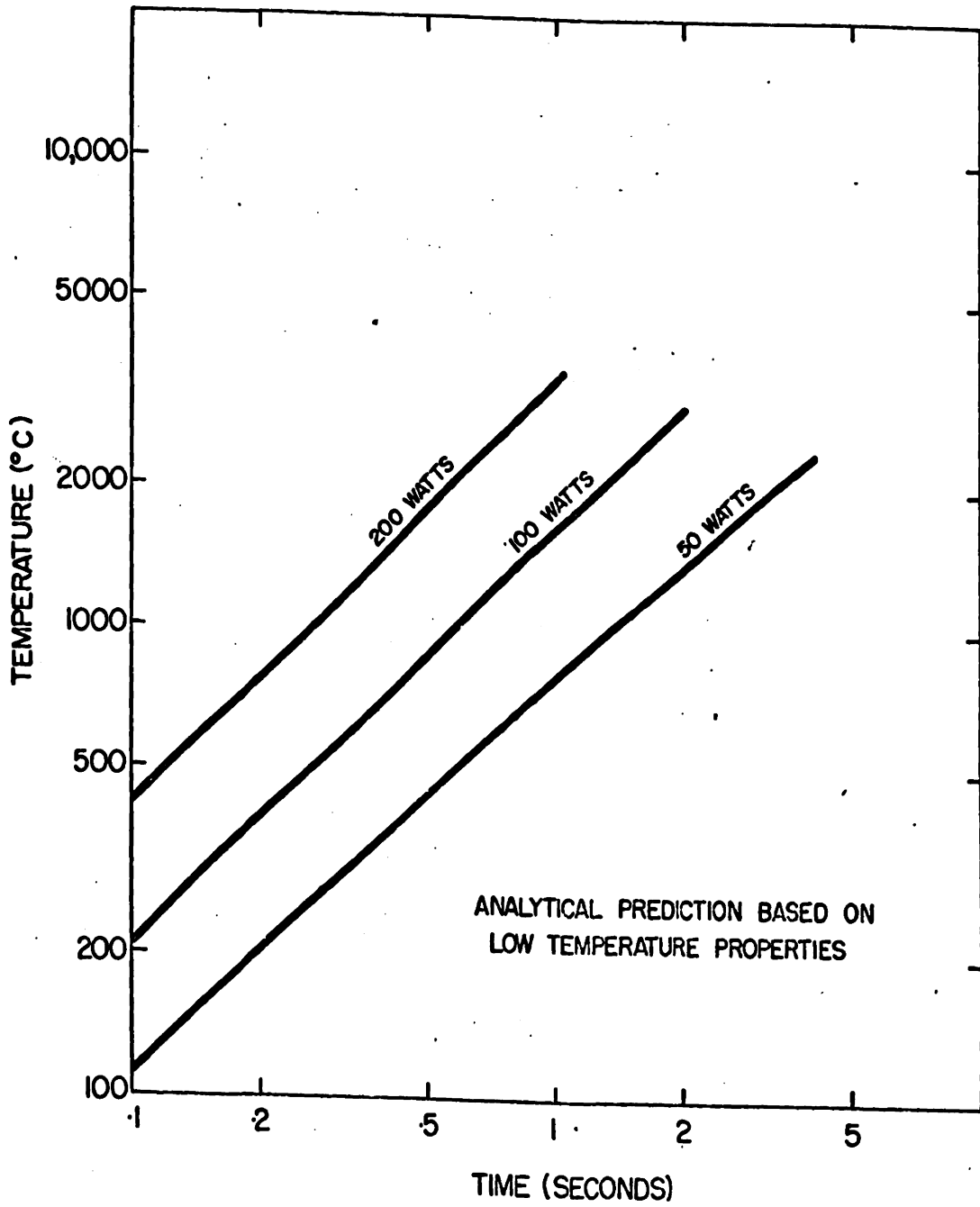
FIGURE 20: MAXIMUM SURFACE TEMPERATURE
VS. HEATING TIME FOR MARBLE CYLINDERS
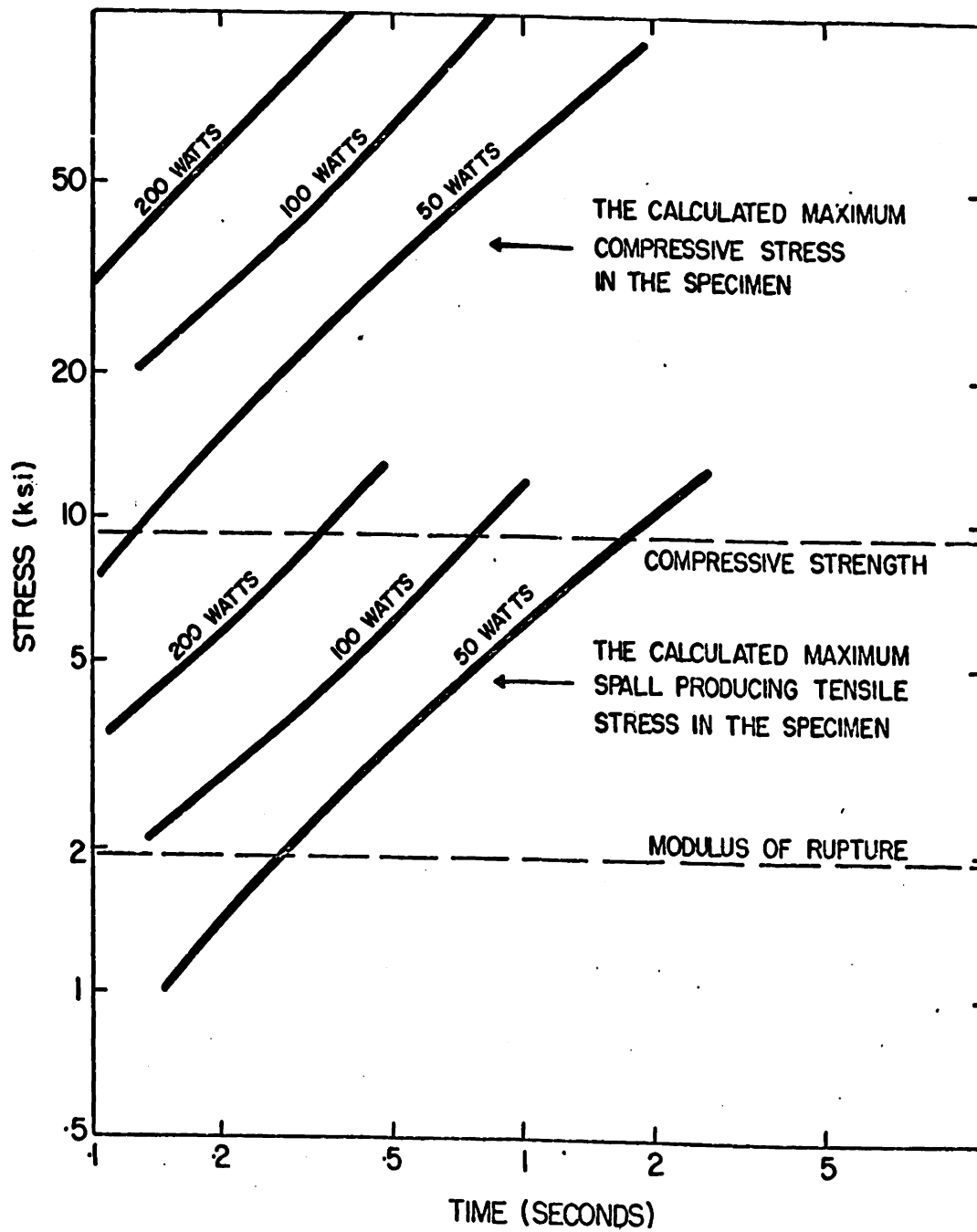
FIGURE 21: STRESS VS. HEATING TIME
FOR MARBLE CYLINDERS
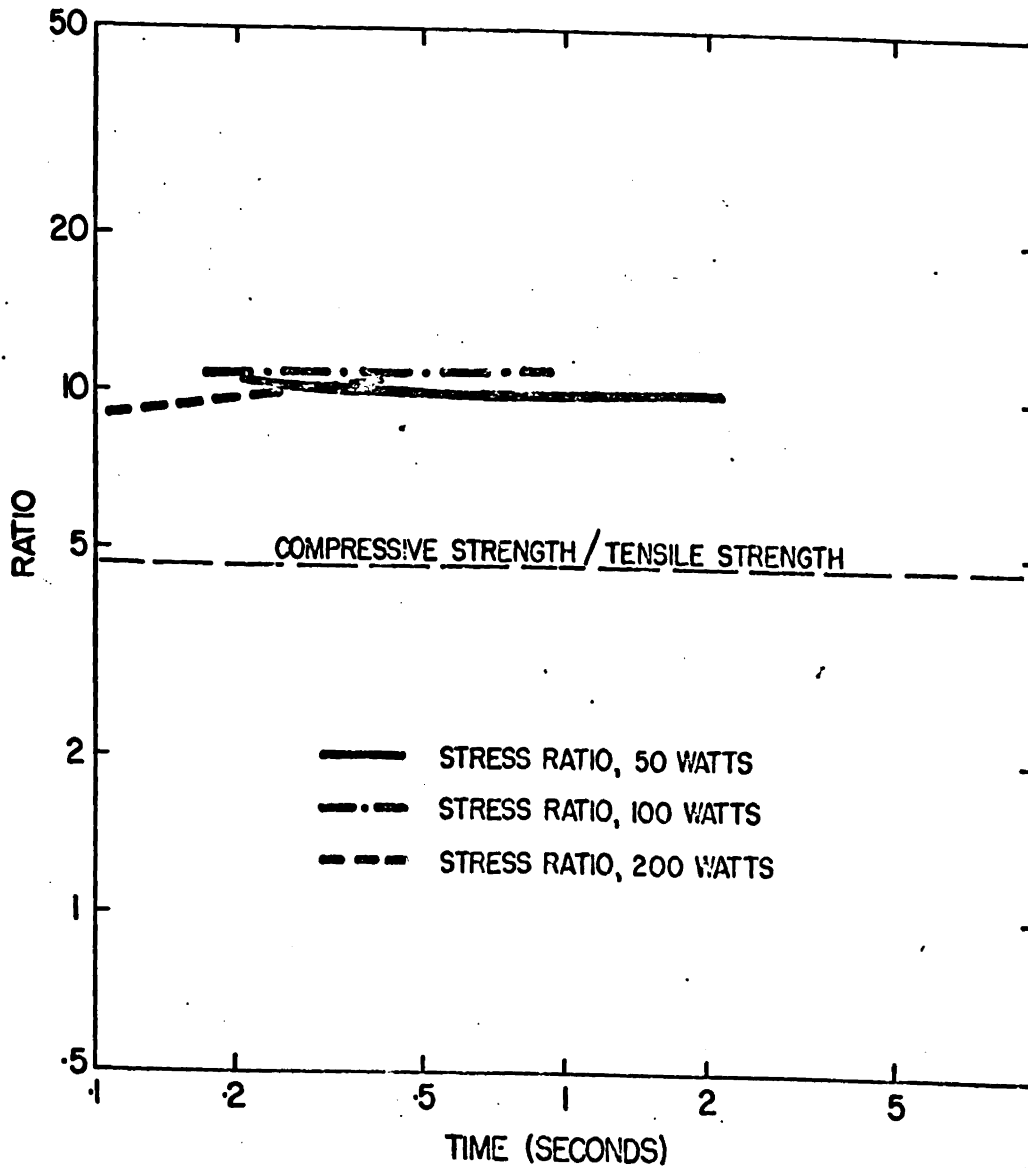
FIGURE 22: VARIATION WITH RESPECT TO
HEATING TIME OF THE RATIO OF
MAXIMUM COMPRESSIVE STRESS OVER THE
MAXIMUM SPALL PRODUCING TENSILE STRESS
IN MARBLE CYLINDERS

The distribution of the temperatures and stresses for a given heating time and power are shown in Figure 23 These are similar in pattern to those for the cylinders and change in the same manner with respect to changes in power level or heating time.

The variations in calculated temperatures as a function of time for different power levels are shown in Figure The analyses were based on the material's low temperature properties and may not be accurate for the higher temperature ranges. Therefore, the highest temperatures should be considered for illustrative purposes only.

The variation of the maximum compressive stress and the maximum tensile stress (that causes spalling) with respect to heating time are shown in Figure 24 for the three power levels. Observations of the values shows that the maximum tensile stresses will exceed the tensile strength well before the maximum compressive strength for all power levels. The mean experimentally observed heating times are also depicted in the figure. The calculated maximum tensile stresses at these times corresponds well with the tensile strength as found experimentally by static loads on the spheres.

The ratio of compressive strength to the tensile strength and the ratio of the maximum compressive stress

to maximum tensile stress that causes spalling as a
function of the heating time for the three power levels
are shown in Figure 25. The ratio of the stresses is
larger than the ratio of the strengths for all values
of power level and heating time. Thus, the tensile
strength will be exceeded before the compressive strength
is. This will initiate a fracture and cause a spalling
type of failure if there is enough releasable strain
energy for complete propagation.

Note that the ratio of the stresses was more than
twice that for granite and marble cylinders. This is
because the spherical shape used for the porcelain
specimens insured a sharp curvature in the compressive
stresses parallel to the surface which cause the
spalling inducing tensile stresses in the vertical
direction to increase. Thus convex surfaces result in
more favorable stress patterns for thermal spalling.

Figure 18 shows the required thermal energy to cause
spalling as a function of power. For the porcelain
spheres there was a substantial decrease in the required
thermal energy with an increase in power from 100 to 300
watts. This was not the case with the granite cylinders.
The reason for the difference was the shape of the surface
at the point of heating. For higher powers and the

shorter heating times required the large compressive
stresses parallel to the surface were much closer to the
surface and constrained to follow it with its relatively
sharp radius.

In general, the porcelain required more thermal
energy to cause spalling because the tensile stress required
for fracture initiation in the porcelain was much higher
than in the granite.

In Table 5 the term "Energy Ratio" is the ratio
of the strain energy that would be released by a complete
spall at the time of fracture initiation to the energy
that would be absorbed by the fracture process. This
term was greatly in excess of unity for all power levels,
which resulted in very high chip velocity during spalling
for all experiments.

Porcelain Spheres ($1\frac{1}{2}$" diameter) Heated with a Laser Beam 0.2 Inches Wide

No. of Tests	Power Watts	Mean Heating Time Sec. [1]	Maximum Tension ksi [2]	Maximum Compression ksi	Strength [3]		Energy Ratio [4]	Pre-diction	Agree with Exp.
					St ksi	Sc ksi			
5	100	1.90	7.8	43.5			17.6	Tensile fracture and spall	Yes
5	200	0.63	9.0	52.0	8.5	70.	14.3	Tensile fracture and spall	Yes
5	300	0.30	9.3	54.0			12.7	Tensile fracture and spall	Yes

(1)   Mean of experimentally observed heating time required to cause first spall.
(2)   The calculated stresses for the mean heating time.
(3)   The range for the tensile strength is 1/2 to the full value of the modulus of rupture.
(4)   Ratio of the calculated releasable strain energy to the energy required to form the fracture area for complete failure.

TABLE 5

RADIANT HEAT

37 ksi

σ_R

σ_θ

1800°C

0·1"

37 ksi

1800°C

σ_R

O_Z

—— STRESS
‐ ‐ ‐ TEMPERATURE
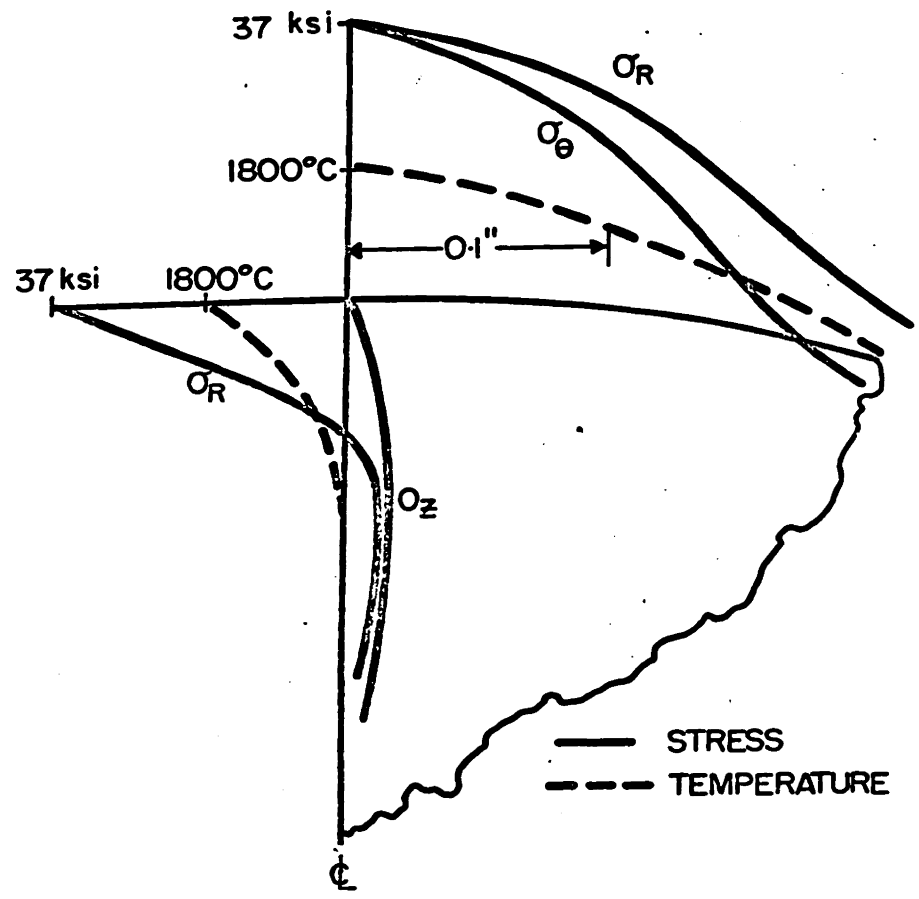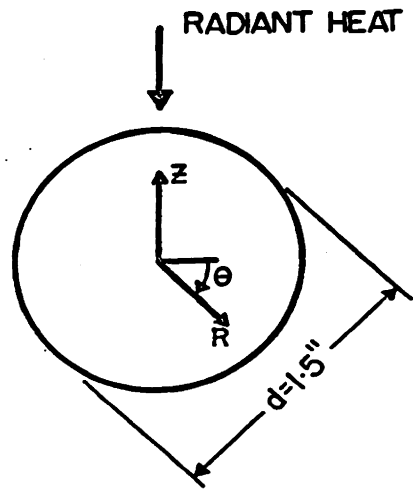
FIGURE 23: TEMPERATURE AND STRESS DISTRIBUTION FOR A PORCELAIN SPHERE (100 WATTS, 1·25 SECONDS HEATING)
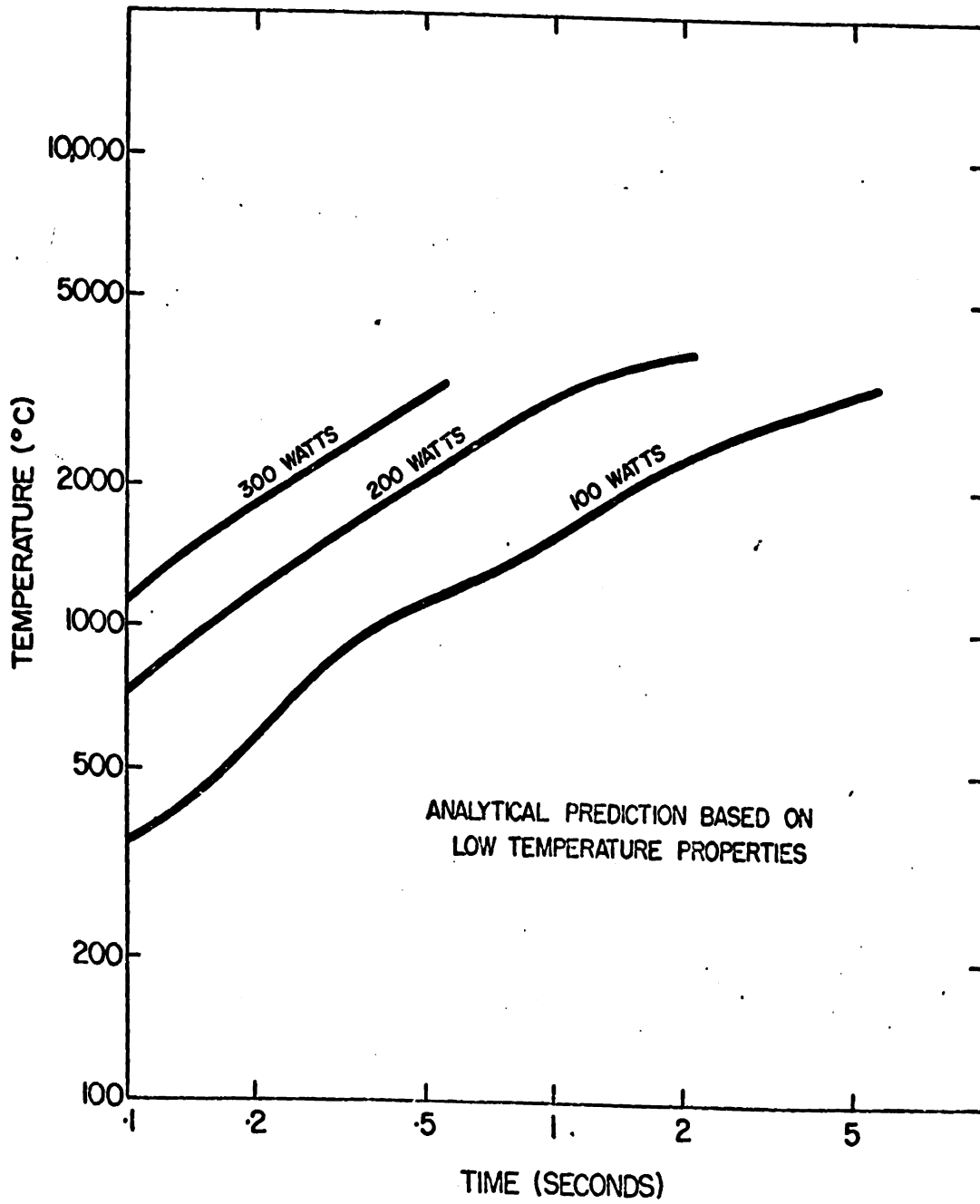
FIGURE 24: MAXIMUM SURFACE TEMPERATURE
VS. HEATING TIME FOR PORCELAIN SPHERES
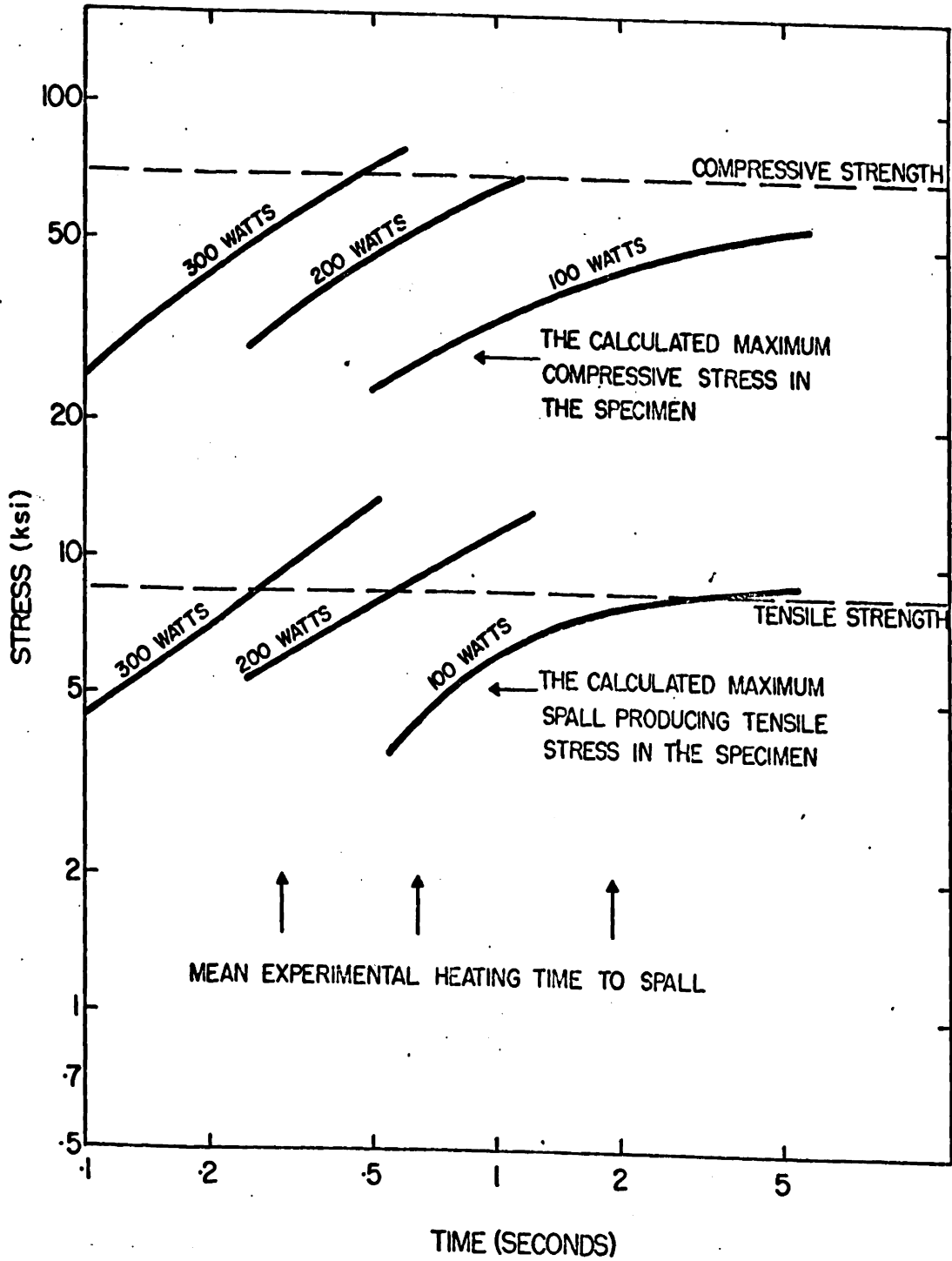
FIGURE 25: STRESS VS. HEATING TIME
FOR PORCELAIN SPHERES
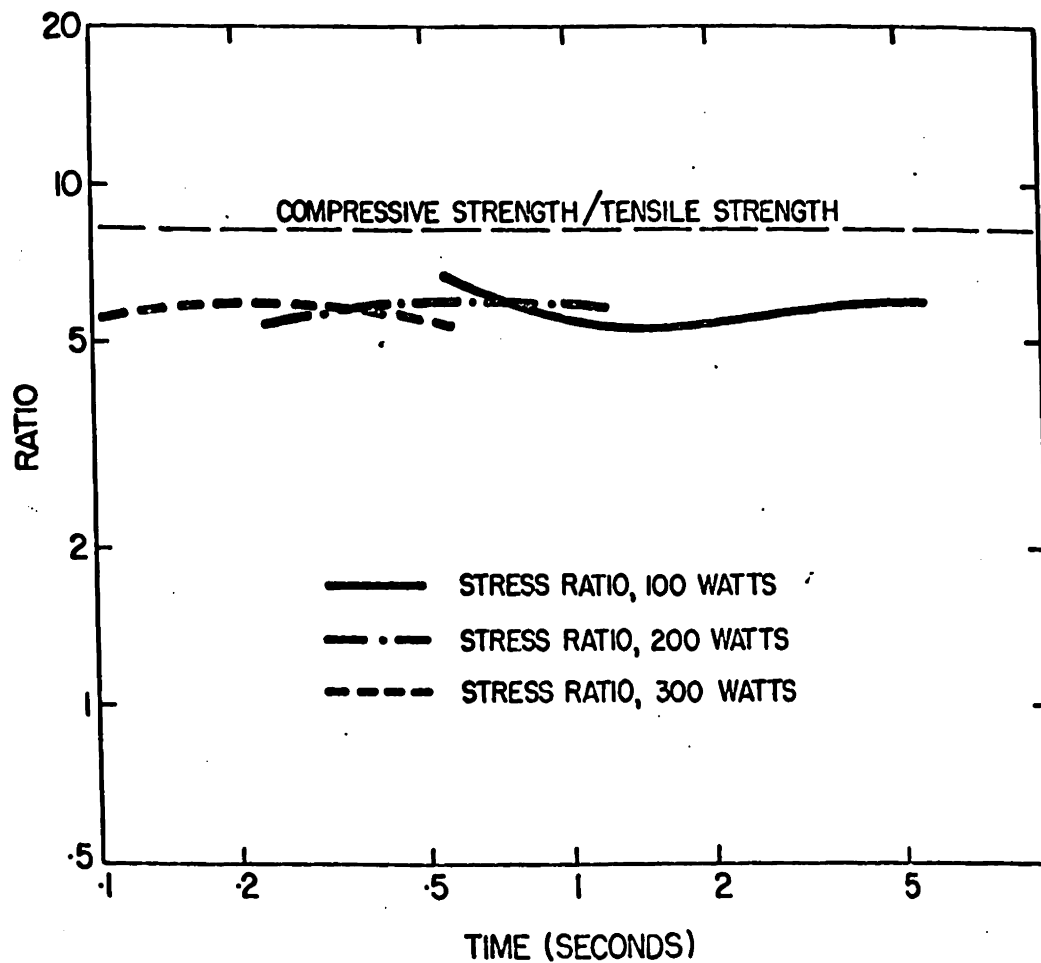
FIGURE 26: VARIATION WITH RESPECT TO
HEATING TIME OF THE RATIO OF
MAXIMUM COMPRESSIVE STRESS OVER THE
MAXIMUM SPALL PRODUCING TENSILE STRESS
IN PORCELAIN SPHERES

CHAPTER IV

CONCLUSIONS AND FUTURE WORK

4.1 CONCLUSIONS

There are several conclusions that can be made based
upon the results of the analytical and experimental work.
They fall into two main categories: first, the con-
firmation of the analysis technique and second, the under-
standing of the nature of spalling in brittle materials.
The conclusions are:

1) It is possible to analyze the temperatures and
the resultant thermal stresses with sufficient detail
and accuracy to predict and understand the thermal spalling
response of some brittle materials when locally heated.

2) The analysis technique does not require excessive
computation or precise evaluation of the material prop-
erties and boundary conditions. This is because the
results of the analysis may be checked for accuracy by
comparison with results from simple experiments which
validate the assumptions made about the material properties
and boundary conditions as a group.

3) Thermal spalling by local heating on the surface
is due to complete propagation of a fracture initiated by

tensile stresses acting below and normal to the heated surface.

4) The compressive strength of the material must be sufficiently large compared to the tensile strength to prevent a compressive failure at the surface before the spall producing fracture can be initiated by a tensile failure below the surface.

5) There must be sufficient energy available to form the new surface area or there will be incomplete fracture and no spalling. This was not a problem in the limited range in which experiments were conducted.

In regard to the above conclusions, the following points may be noted with respect to experiments involving granite, marble and porcelain: The granite and porcelain specimens spalled at the time the maximum tensile stress was about equal to the tensile strength. The marble specimens failed to spall because the surface material failed in compression before a tensile failure could initiate a spalling fracture.

4.2 FUTURE WORK

The research conducted for this thesis can be considered as part of a larger research program at the Massachusetts Institute of Technology to provide new

knowledge which will lead to improved rock excavation methods. In this thesis, a rational analysis technique has been developed to evaluate the thermal stresses which were hypothesized as the basic mechanisms of thermal spalling. Comparisons have been made, with good correlation, to data from experiments which covered a limited range of boundary conditions for a few different materials.

For this work to be of greatest possible use in the development of significant improvements in rock excavation methods, the analysis techniques and theory should be applied to experimental results from tests which have boundary conditions and heat sources similar to those encountered in the field. Extensions and improvements could then be made, if required, to the technique and hypotheses for this larger class of problems in the following areas.

1) Automation of the analysis programs to handle the moving boundary problem.

2) Analysis of the case of surface crushing in more detail.

3) The slow growth case where the propagation is dependent on additional heating due to the initial lack of energy.

Based upon the experience gained during this thesis, it is anticipated that extensions into the following related areas will lead to most valuable results in the understanding and improvement of excavation techniques.

1) The application of the analysis technique to field type conditions with prototype heat sources, and the comparison of these results to experimentally recorded strains: The results of this would indicate the improvements required, if any, in the assumptions made about the boundary conditions and material properties. Then the analysis technique can be used to study the spalling in simulated field conditions and improvements in equipment and/or operating procedure could be done in a rational manner based on the concept of furnishing the maximum tensile stress and minimum compressive stress in the most efficient manner.

2) It is possible to apply the developed analysis technique to the problem of how mechanical bits cause fracture in brittle materials. The most difficult aspect of this problem is to establish the proper shape and conditions at the boundary between the bit and the rock. At this interface, there is crushed material which is controlling both the magnitude and direction of the stresses. An experimental study of the properties and

flow of this crushed material would be used to estimate the proper boundary shape and conditions. Based on these estimated boundary conditions, analyses could be made of the stresses and strains. These strains would then be compared to experimental strains obtained by placing strain gages on the rock very close to the bit. If necessary, the estimates of the boundary shape and conditions could be modified in order to achieve the desired close correlation between the analysis and experiments. When this is satisfactorily done, the analysis technique could be used to study the initiation and propagation of brittle fracture caused by mechanical bit action.

3) It has been observed in this work that often heating alone cannot create a tensile failure in the proper location before the material fails in compression on the surface. Also, there are cases in which the available energy for spalling is sufficient to cause propagation even though the tensile stresses are insufficient to initiate the fracture.

For materials in which this type of behavior hinders the spalling rate, a means of initiating the fracture should be investigated. The most likely means of achieving this seems to be with mechanical cutters. Depending on the type of operation, this could be thought of as a heat

assisted mechanical method or a mechanical assisted thermal spalling method. The study of this thermal-mechanical problem accurately and in detail, would require that the stress problem concerning the interaction of the mechanical bit and the rock surface be done first. Then the method of solution would be to rationally combine heating and mechanical methods in the manner which would best initiate the fracture and propagate it to form chips.

REFERENCES

1. Maurer, W., Novel Drilling Techniques, Pergamon Press
    Ltd., London, 1968.

2. Rolseth, H. C. and Konler R. H., The Use of Rocket-
    Jet Burners, Soc. of Min. Eng. of AIME, Preprint
    68-H-325, September 1969.

3. Fairhurst, C., Failure and Breakage of Rock, Eight
    Symposium on Rock Mechanics Port City Press, Inc.,
    Baltimore, Md. P. 335, 1967.

4. Evans, I. and Murrell, S. A. F., Wedge Penetration
    into Coal, Colliery Engineer, 1962, Vol. 39, No. 455.

5. Paul, B. and Sikarskie, D. L., A Preliminary Theory
    on Static Penetration by a Rigid Wedge into a
    Brittle Material, AIME, Transactions, 1965, Vol. 232.

6. Garner, N. E., The Photoelastic Determination of the
    Stress Distribution Caused by a Bit Tooth on an
    Indexed Surface, M. S. Thesis, Univ. of Texas,
    January 1961.

7. Norton, F. H., A General Theory of Spalling
    J. Am. Ceram. Soc. V. 8, 1925, PP 29-39.

8. Norton, F. H., The Mechanism of Spalling
    J. Am. Ceram. Soc., V.9, 1926, PP 446-461.

9. Norton, F. H., Discussion on Theory of Spalling
    J. Am. Ceram. Soc., V. 16, 1933, PP 423-424.

10. Preston, F. W., Theory of Spalling, J. Am. Ceram.
    Soc., V. 16, 1933, PP 131-133.

11. Kingery, W. D., Factors Affecting Thermal Stress
    Resistance of Ceramic Materials, J. Am. Ceram.
    Soc., V. 38, No. 1, January 1, 1955.

12. Hasselman, D. P. H., Elastic Energy at Fracture
    and Surface Energy as Design Criteria for Thermal
    Shock, J. Am. Ceram. Soc., V. 46, No.11, November 1963.

REFERENCES
(Continued)

13. Griffith, A. A., The Phenomena of Rupture and
Flow in Solids, Phil. Trans. Rog. Soc., 1921,
Vol. A 221, PP 163-198.

14. Tetelman, A. S. and McEvily, A. J., Fracture of
Structural Materials, John Wiley and Sons Inc.,
New York, 1967.

15. Paulding, B. W., Crack Growth During Brittle
Fracture in Compression, Ph. D. Thesis, June
1965, Massachusetts Institute of Technology.

16. Rad, P. F., Personal Communication, Department
of Civil Engineering, Materials Division,
Massachusetts Institute of Technology.

17. Farra, G., Nelson, C. R., Moavenzadeh, F.,
Experimental Observations of Rock Failure
due to Laser Radiation, Massachusetts
Institute of Technology Research Report R69-16,
December 1968.

18. Zienkiewicz, O. C., and Cheuney, Y. K., The Finite
Element Method in Structural and Contenum Mechanics,
McGraw-Hill Publishing Co., London 1967.

19. Fujino, T., Ohsaka, K., The Heat Conduction and
Thermal Stress Analysis by the Finite Element Method,
Technical Headquarter, Mitsubishi Heavy Industries,
Ltd., Tokyo, Japan.

20. Wilson, E.L., A Digital Computer Program for the Finite
Element Analysis of Solids with Nonlinear Material
Properties, Technical Memorandum No. 23, Aerojet-
General Corporation, July 1965.

21. Carslaw, H. S., and J. C. Jaeger, Conduction of Heat
in Solids, Oxford University Press, New York, 2nd
ed., 1959.

BIOGRAPHY OF THE AUTHOR

Name: Charles R. Nelson

Born: September 23, 1940, in Grafton, North Dakota

Education:

   Secondary Schools in Grafton, North Dakota

   Sept. 1958 to June 1962: University of North Dakota

   Sept. 1962 to present: Massachusetts Institute of
                             Technology

   Received the degree of Bachelor of Science from the
   University of North Dakota in 1962, the degree of
   Master of Science from the Massachusetts Institute
   of Technology in 1965 and the degree of Civil
   Engineer in 1967.

Professional Experience:

   June 1967 - Jan. 1969: Staff Engineer for Simpson,
      Gumpertz & Heger Inc., Consulting Engineers.
      Cambridge, Massachusetts.

   Sept. 1966 - June 1967: Instructor in the Civil
      Engineering Department at the Massachusetts
      Institute of Technology. Cambridge, Mass.

   June 1964 - Sept. 1964: Engineer for Lincoln
      Laboratory, Lexington, Massachusetts.

   Sept. 1962 - June 1964: Full-time Research Assistant
      in the Civil Engineering Department at the
      Massachusetts Institute of Technology. Cambridge,
      Massachusetts.

Honors:

   The author graduated Cum Laude from the University of
   North Dakota and received the Outstanding Civil
   Engineer Award of 1962. He was a National Science
   Fellow from 1964 to 1966.

BIOGRAPHY OF THE AUTHOR
(Continued)

Publications:

   Massachusetts Institute of Technology Report
   R64-37 "The Dynamic Response of Reinforced
   Concrete Circular Arches".

   Massachusetts Institute of Technology Report
   R69-16 "Experimental Observations of Rock
   Failure due to Laser Radiation".

   The author was married to Marlys Brown in 1959
   and is the father of two children, Kimberlee
   and Brent.

   The author is joining the School of Minerals and
   Metallurgical Engineering at the University of
   Minnesota as an Assistant Professor of Geo-
   Engineering.

APPENDIX A

HEAT TRANSFER BY THE FINITE ELEMENT METHOD

In this method the body is considered divided into small finite sized elements which are kept compatible with each other and also satisfy overall thermal equilibrium. The problem is thus transformed from solving a differential equation with boundary conditions to one of solving ordinary simultaneous equations.

The finite element method of heat analysis developed here will handle most types and shapes of linear boundary conditions. Nonhomogeneous and nonisotropic rocks can also be handled, but the inhomogeneity must vary slowly when compared to the finite element size. The nonlinear aspects of the problem may be handled by using the incremental loading approach. Using this approach the load is applied in small increments such that linear boundary conditions and material properties may be used during that increment of load. At the end of each load increment, new boundary conditions and material properties are calculated for the next increment of load.

For the finite element method the size and the complexity of the problem that can be handled is limited by

the amount of computation time available. There are two

classes of problems which require a much reduced number

of calculations and still provide solutions useful in

many types of real problems. The first class is that of

plane strain. This condition is approximated in thin

slabs. The other class is the axi-symmetric one in which

all boundary conditions, loadings, and material properties

are symmetric to a single axis. It is the type of problem

that exists in discs and cylinders. By virtue of the

symmetry in such a case, only one pie-shaped wedge need be

considered. This effectively reduces the three-dimensional

problem to a two-dimensional one.

A method to evaluate heat transfer by the finite

element technique for rock specimens subjected to laser

radiation has been developed in the following manner:

In general the element shape in this work is tri-

angular and the temperature within the element is assumed

to be a linear function of the x and y coordinates:

$$T = A + Bx + Cy$$

The values of A, B, and C must be expressed in terms

of the temperatures at the three corners of the element

called T_1, T_2, and T_3.

$$\begin{Bmatrix} T_1 \\ T_2 \\ T_3 \end{Bmatrix} = \begin{bmatrix} 1 & x_1 & y_1 \\ 1 & x_2 & y_2 \\ 1 & x_3 & y_3 \end{bmatrix} \begin{Bmatrix} A \\ B \\ C \end{Bmatrix}$$

$$\begin{Bmatrix} A \\ B \\ C \end{Bmatrix} = \begin{bmatrix} 1 & x_1 & y_1 \\ 1 & x_2 & y_2 \\ 1 & x_3 & y_3 \end{bmatrix}^{-1} \begin{Bmatrix} T_1 \\ T_2 \\ T_3 \end{Bmatrix}$$

For a given element, the heat flow intensity in the x direction is:

$$q_x = - \frac{\partial}{\partial x} (TK_x)$$

and in the y direction:

$$q_y = - \frac{\partial}{\partial y} (TK_y)$$

where K_x and K_y are the conductivities of the material in the x and y direction respectively.

The heat flow of the edge of an element between points i and j is:

$$\int_{x_1}^{x_j} - \frac{\partial}{\partial y} (TK_y)t \ dx + \int_{y_1}^{y_j} - \frac{\partial}{\partial x} (TK_x)t \ dy$$

113
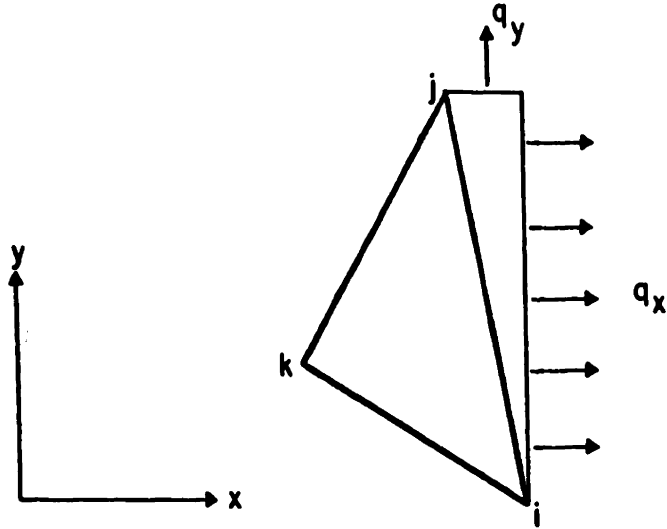
If the value of conductivity does not vary within an element, the intensities become:

$$q_x = - K_x \frac{\partial T}{\partial x}$$

$$q_y = - K_y \frac{\partial T}{\partial y}$$

on substituting for T in terms of A, B, C, X and Y, one finds:

$$q_x = - K_x B$$

$$q_y = - K_y C$$

The values of B and C in terms of $T_1, T_2,$ and T_3 are:

$$B = [(y_k - y_j)T_i + (y_i - y_k)T_j + (y_j - y_i)T_k] \div 2A$$

$$C = [(x_k - x_j)T_i + (x_i - x_k)T_j + (x_j - x_i)T_k] \div 2A$$

where x_i, y_i, x_j, x_k, y_k are the coordinates of the nodes of the element and A is the area of the element which is

$$A = \frac{1}{2} \begin{vmatrix} 1 & x_i & y_i \\ 1 & x_j & y_j \\ 1 & x_k & y_k \end{vmatrix}$$

It should be noted that, if the element were of constant thickness, an integration around all three sides of an element of either q_x or q_y would be equal to zero. That is

$$\int_{x_i}^{x_j} q_y dx + \int_{x_j}^{x_k} q_y dx + \int_{x_k}^{x_i} q_y dx = 0$$

$$\int_{y_k}^{y_j} q_x dy + \int_{y_j}^{y_k} q_x dy + \int_{y_k}^{y_i} q_x dy = 0$$

Therefore the element, by itself, is in thermal equilibrium. However, along a boundary between two elements there will be, in general, a discontinuity in the heat flow intensity. This discontinuity will be assumed to cause the temperature along this boundary to change. This is expressed analytically in the following way. The heat flow out of an element is assumed concentrated at the nearest node. Thus the heat into node i is:

$$Q_i = \frac{1}{2} \int_{x_k}^{x_i} tq_y \, dx + \frac{1}{2} \int_{y_k}^{y_i} tq_x \, dy + \frac{1}{2} \int_{x_i}^{x_j} tq_y \, dx + \frac{1}{2} \int_{y_i}^{y_j} tq_x \, dy$$

The total heat flow into node i would be found by summing over all the elements containing node i :

$$Q_{total} = \Sigma \, Q_i$$

If node i changes in temperature, all elements containing node i must change their internal temperature distributions in a linear fashion. This follows from the initial assumption that the temperature is at all times a linear function of the space coordinates.

It is now possible to find the heat required to change the temperature of only one node of an element. This term

is analogous to a structural stiffness. The temperature change is as shown:
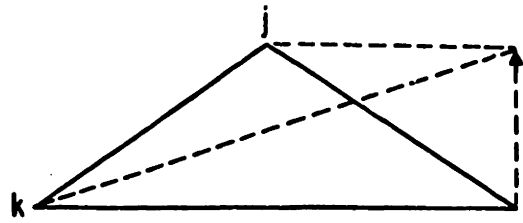
------ temperature function

_____ element

Assuming that the thickness (t), density (p), and specific heat (SpH) are constants within the element, the heat required to change the temperature of node i by T is:

$$CP = tp(SpH) \iint_A T[(x_k y_j - x_j y_k) + (y_k - y_j)x + (x_j - x_k)y]dxdy = \frac{1}{3} tp(SpH)TA$$

Thus the heat required to raise only one node to a given temperature, with a linear distribution within the element, is $\frac{1}{3}$ that required to raise the entire element to that temperature. Since there is, in general, more than

one element at a node, the effect must be summed over
all adjacent elements giving a total heat capacity (CPT)
at a node of:

$$CPT = \Sigma\ CP$$

If there is any heat being generated within the element,
it would uniformly raise the temperature of that element.
This will be accounted for by having this heat divided
equally to each node of the element in the same way as the
heat capacity of each element was divided equally among
the nodes.

$$HGN = \frac{1}{3}\ tA\ (HG)$$

HG = Heat Generated per Unit Volume

Summing over the several elements at a node:

$$HGN_{total} = \Sigma HGN$$

Boundary conditions at any point may be specified
in one or more of the following ways: given temperature
(e.g., water bath), given heat flux (e.g., laser), ra-

diation, or a conductive zone to some given temperature. The case in which the boundary conditions are specified as a set of given temperatures is easy to analyze since the boundary nodal temperatures are held fixed at those given temperatures.

$$T_{boundary} = T_{given}$$

The radiation and flux conditions are assumed concentrated at the nearest boundary nodes.

$$Q_{boundary} = \iint q_{boundary}$$

The conductive zone is handled by adding an extra layer of elements to account for the conductivity of the boundary layer and thus converting it to a fixed temperature boundary condition.

The heat equilibrium equation at each node can now be written as :

$$Q_{total} + Q_{boundary} + HGN_{total} - \frac{\partial T}{\partial t} CPT = 0$$

$\frac{\partial}{\partial t}$ means differentiation with respect to time.

An equation of this nature can be written for each node in the system. The number of unknown temperatures in the system would be equal to the total number of nodes minus the number of boundary nodes at which the temperature was given. The number of independent equations would be the same as the number of unknown temperatures since the equations for the boundary nodes where the temperature was given would be null.

Thus, at this point, there are N equations, N unknown temperatures, and N unknown $\frac{\partial T}{\partial t}$, that is, a total of $2N$ unknowns. If the steady state solution is wanted, the N unknown $\frac{\partial T}{\partial t}$'s are zero. The system now has N unknowns and N equations which can be solved.

$$\frac{\partial T}{\partial t} CPT = Q_{total} + Q_{boundary} + HGN_{total}$$

If we let:

$$\frac{\partial T}{\partial t} = \frac{T_f - T_p}{\Delta t}$$

We get:

$$T_f = \left(\frac{Q_{total} + Q_{boundary} + HGN_{total}}{CPT} \right) \Delta t + T_p$$

The temperature in the future, T_f, is predicted in terms of the present temperature, T_p, and the time increment, Δt, into the future. The Q_{total}, $Q_{boundary}$, and HGN_{total} are functions of the present temperatures and known boundary conditions. The temperature for all future time can now be found by marching the solution out from some known initial boundary conditions.

The maximum rate at which the solution can be marched forward in time is controlled by the stability of the solution. To find the maximum rate, the following logic is used:

Assume there is an error introduced into the solution at some point due to round off or other causes. If this does not diminish with time, the solution will become unstable. If the system had zero values throughout except for an error (E) at one node, then this error should diminish with time. Initially, T_i = E, all other T = 0 and the heat flow into node i is $Q_{total} + Q_{boundary}$. After one time increment Δt the temperature at node i is:

$$T_i\ (\Delta t) = (\frac{Q_{total} + Q_{boundary}}{CPT})\Delta t\ + E$$

121

Now if:

$$|T_1(\Delta t)| > |T_1(0)|$$

there is instability since the error may grow with time. For the limiting case:

$$|T_1(\Delta t)| = |T_1(0)|$$

which gives:

$$\frac{Q_{total} + Q_{boundary}}{CPT} \Delta t = 0, \quad -2E$$

For the first case a lower limit on Δt is zero, that is, in a heat transfer problem one can not predict back in time. The second case will give the maximum rate at which the solution can be marched forward. Neglecting the Q (boundary) term:

$$\frac{Q_{total}}{CPT} \Delta t = -2E$$

CPT is a function of the element size, shape, thickness, arrangement and material properties, and varies from one node to another. The Q_{total} is a function of these as well as the temperature of the node in question and the ones adjacent to it. Since, initially, the adjacent nodes have zero temperature and the problem is linear, E can be factored out of Q_{total}. After cancellation of E there is for the limiting case:

$$\frac{Q_{total}(1)}{CPT} \Delta t = -2$$

$$0 < \Delta t < \frac{2CPT}{Q_{total}(1)}$$

where $Q_{total}(1)$ is the Q of that node which has a unit temperature and all other nodes have zero temperature. In one dimension the condition is:
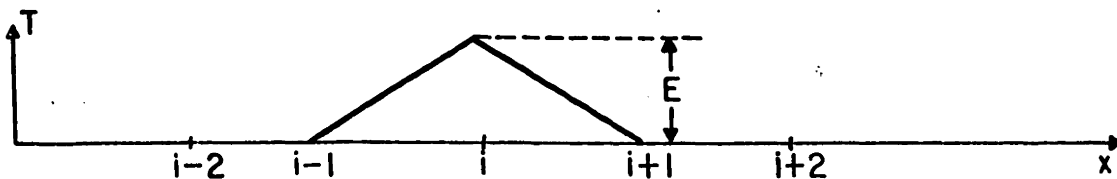
If the initial conditions are as shown, the time in-
crement (Δt) must be limited such that after (Δt),
T_i is less than E but greater than −E.

Note that the minimum value of Δt must be used
after checking all nodes and also that CPT grows with
element size, and Q_{total} (1) diminishes with element
size. Thus smaller elements require smaller time
increments.

The computer program to do the heat transfer was
checked by considering a problem which was solved in
closed form [21]. The problem consisted of a wall at
constant temperature which, at time zero, had its out-
side surface temperature changed to zero. For the
computer solution the wall was split (about its axis of
symmetry) and one half of it was represented by twenty
elements such as:
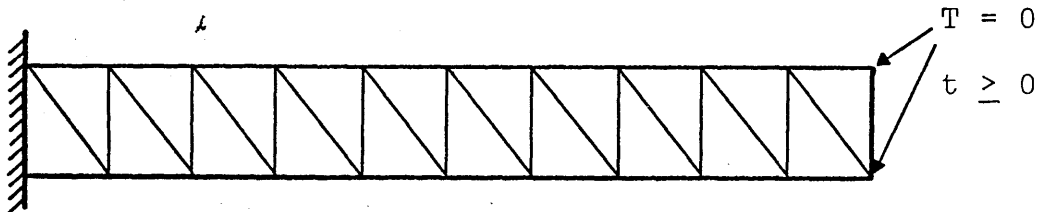
The computer solution was within 0.1 per cent of the plots

for the closed form solution given by Carslaw and Jaeger [21].

In varying the time increment in this problem, the derived

limit for stability was established.

APPENDIX B

STRAIN ENERGY CALCULATION

It was necessary to calculate the strain energy in the specimens before and after the formation of a spall. This was done by summing the strain energy in each finite element over all of the elements. The strain energy in element i is [ ]:

$$= \frac{1}{2}E\ (\sigma_x{}^2 + \sigma_y{}^2 + \sigma_z{}^2) - \frac{\mu}{E}\ (\sigma_x\sigma_y + \sigma_y\sigma_z + \sigma_z\sigma_x)$$

$$+ \frac{1}{2}G\ (\tau_{xy}{}^2 + \tau_{yz}{}^2 + \tau_{zx})\ V_i$$

Where V_i is the volume of the element. The total energy is then

$$PE = \sum_{i=1}^{N} PE_i$$

where N is the total number of elements.

An approximation of the strain energy in the body can be obtained by assuming that for the case of suddent heating at the surface the strain is limited to one dimension (in the direction normal to the surface). The strain energy per unit volume is then:

$$PE = (1 + \mu)\ E\ \alpha^2\ (\Delta T)^2 \quad \text{(Approximate)}$$

126

where ΔT is the change in temperature applied to a single element is:

$$PE_i = (1 + \mu)\ E\ \alpha^2\ (\Delta T_i)^2$$

where ΔT_i is the change in temperature of the element.

The total energy is:

$$PE = \sum_{i=1}^{N} PE_i$$

The comparison of this approximation with the exact value shows that for the cases investigated in this work the approximation is about four times the exact value. This means that displacement parallel to the surface reduces the stresses by about a factor of two from the stresses that would exist if the problem were truly one-dimensional. The more precise method requires that the stresses be evaluated while the second method only required knowledge of the temperatures.

APPENDIX C

DETAILED INSTRUCTION FOR THE ANALYSIS TECHNIQUE

The required modeling and data preparation for the analysis technique will be shown for a thermal stress problem.

First, to evaluate the temperature distribution, the appropriate boundary conditions and material properties must be known or estimated. For granite the following estimates of the properties are based on published data [   ]

$$
\begin{aligned}
\text{Conductivity} &= \quad 1./(31500 + 21.6T) \\
& \qquad \text{BTU in sec } {}^{\circ}F \\
\\
\text{Specific Heat} &= \quad .21 \text{ BTU/lb } {}^{\circ}F \\
\\
\text{Density} &= \quad .094 \text{ lbs/in}^3
\end{aligned}
$$

The boundary conditions are the estimated heat flow into and out of the material. For this example the heat flow into or out of the boundary of the specimen at all places other than that area heated by the laser are assumed to be zero. This assumption has been proven valid for short heating times with the laser in which the surface does not become incandescent.

It is estimated that the total energy of the laser
(as recorded by absorption in the power measuring
calorimeter) is absorbed by the rock. This estimate
appears to be valid because the surface has several
impurities, such as water and dust, and has irregularities,
such as micro-cracks and adhesions all of which tend to
increase the surface absorptivity. The estimated shape
of the beam is that of an axi-symmetric gaussian curve.
These estimates are accurate if the laser is operating in
a single mode, which is normally sought in operation for
accurate targeting of the beam.

The specimen to be analyzed must be modeled by a
finite number of triangular elements. Since the
temperature can only vary in a linear manner in any element,
each element must be sufficiently small such that the true
shape of the temperature function can be well estimated
by the small straight segments.

For the example under consideration the shape is a
cylinder, $1\frac{1}{2}$ inches long and $1\frac{1}{2}$ inches in diameter. Of
this, only the top center zone which will experience an
increase in temperature need be modeled by the finite
elements. That part of the body which remains at a
constant temperature does not affect the solution or its
accuracy.

The model used for this example is shown in Figure 27.
Note that due consideration has been given to the axi-
symmetry of the problem.

The input for the computer program is shown in the
listing.   The first line of data input has the
following meanings.

TERM	VALUE	PHYSICAL MEANING
KTMAX	200	The total number of time steps the program will take.
KTPRT	10	The number of time steps the program takes between printing of the temperatures.
NODES	53	The exact number of nodes (joints) there are in the model.
NOEL	79	The exact number of elements there are in the model.

TERM	VALUE	PHYSICAL MEANING
DENS	.094	The density of the material ($lbs./in^3$).
SPHET	.21	The specific heat of the material (B.T.U./lb.)
DTIME	.02	The step size in time the program takes in finding new temperatures.
COND	1./(31500+21.6T)	The thermal conductivity of the material (B.T.U./ in. °F sec.) (this input is overridden by the non-linear function for the conductivity in the program.)
BTEMP	0.	The temperature any boundary may be fixed at. (not needed for the example)(°F)
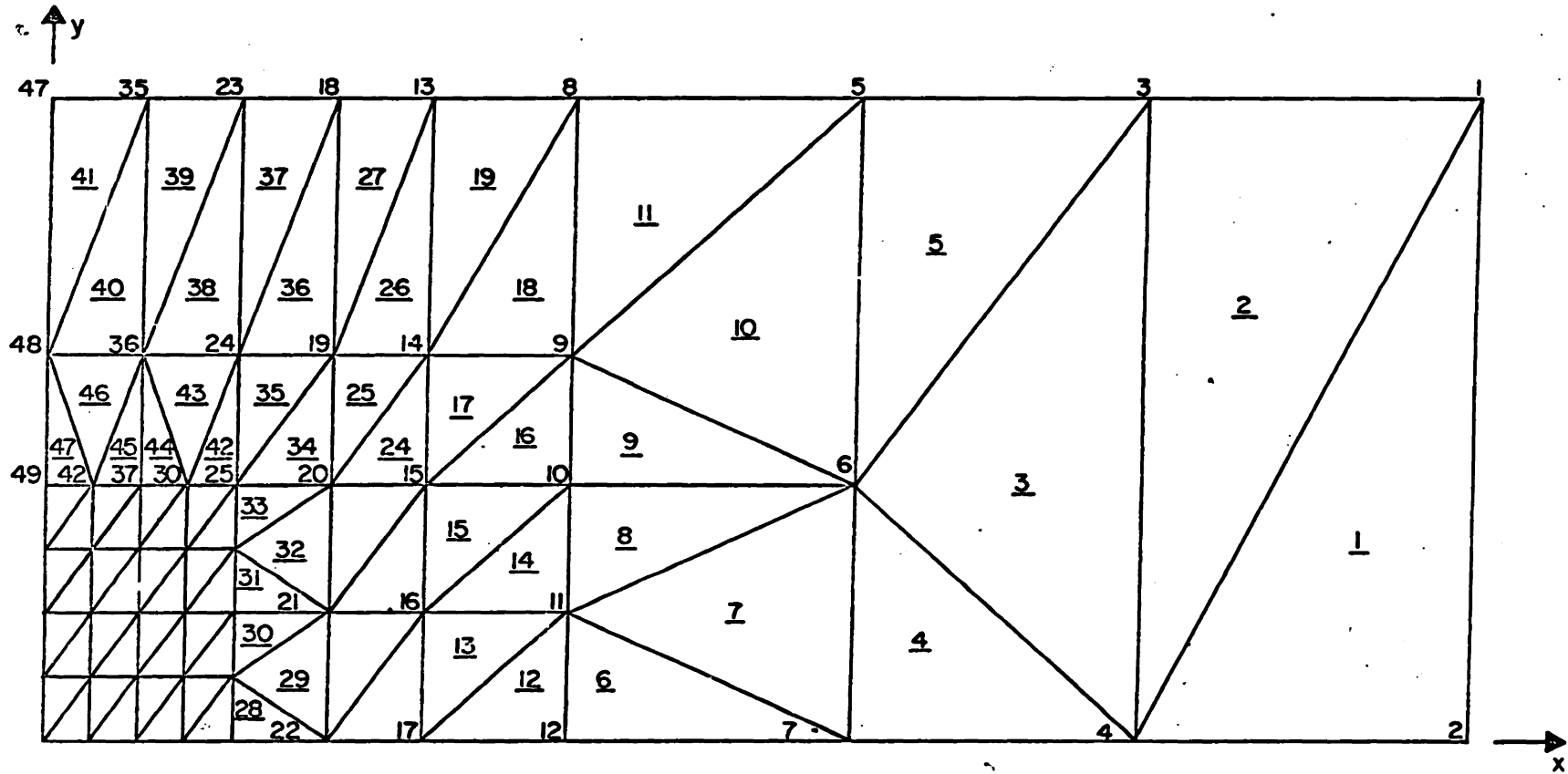
FIGURE 27: GRID FOR HEAT TRANSFER (SEE FIGURE 29 FOR FINE GRID)

132

The next group of input which is labeled "nodal data" is established in the following manner.

The first term is the radial coordinate in inches and the second is the coordinate in the vertical direction in inches. The third term is the initial temperature of the body at that node. For this example the body was estimated to be at 70°F initially. The fourth term is the net heat flow into the node in B.T.U. per second due to outside sources such as the laser. It is zero except for those nodes at the surface heated by the laser. This heat flow per node is equal to that heat which is incident on the surface which is closest to the node in question. The fifth term denotes if that node is a boundary node which must be held fixed at the specified boundary temperature. If this term is negative, the node is not held to the boundary temperature. It should be made positive if it is desired to fix the node at the given boundary temperature such as would be the approximate case for a water bath for example. For the laser heating example, this term should be negative for all the nodes.

The next group of input data is the information which tells the computer how to connect the nodes with elements.

Each element should have the three nodes associated with it listed in the same order as the coordinate system. That is, number the nodes counter-clockwise in a right-handed coordinate system and clockwise in a left-handed coordinate system.

This ends the required input. The rest of the output is data that the program generates and is printed to help in checking the input for error. The next group of print-out are the number of the elements which touch each node. A rapid comparison of this with the figure will indicate if an error has been made in the input of the element nodes.

The next group is the area of each element printed in numerical order. Again, a comparison of this data with the figure looking for elements with common areas is a quick way to check the accuracy of the input.

Following this is data on the total specific heat of each node. It has little value as a check of input data, but is included as a possible aid in debugging the program if changes to it are ever made.

All of the data printed out from this point is the temperatures of the nodes after a fixed integer number of time steps forward in time. The term KSTOP is the number of time increments which have posted before the temperatures are reached. This can be converted to the amount of heating

time by multiplying the KSTOP by the DTIME. The DTIME
is the size of the increment in seconds.

Following each print of the KSTOP is the temperature
of each node listed in numerical order.

Once the temperatures have been calculated over the
range of times of interest, it is necessary to calculate
the thermal stresses for specific times. For the thermal
stress analysis, the body is modeled by many finite
elements as it was for the heat transfer analysis. However,
there are two modifications required for the thermal stress
grid. One is that the size of the elements may have to be
of a different size for sufficient accuracy. Second, the
whole body must be modeled because the stresses in the
heated zone are influenced by the restraining action of the
material which remains at room temperature. With this in
mind the body is modeled by the grid shown in Figure 29.

The input for this problem is shown in listing
Following this is the information on the stress analysis
program called "Feast I" distributed by Professor John
Christian of the Soils Division of the Civil Engineering
Department at the Massachusetts Institute of Technology.
Professor Christian is in charge of the implementation

of this computer program at the Massachusetts Institute of
Technology's Computation Center. This information explains
in detail the input and output of the program for thermal
stresses.

For the example under consideration, the use of the
temperatures from the developed heat transfer computer
program in the stress analysis computer program requires
interpolation of the data because the grid size is smaller
in the stress analysis program. This interpolation can
be done in a linear manner because the heat transfer
analysis program is based on the assumption that the
temperature is a linear function across each element.

One apparent difference between the two computer
programs is the use of quadrilateral elements along with
triangular ones in the stress analysis. This presents
no problem whatsoever because the only information exchange
between the two programs is the nodal temperatures and no
information which requires an element correspondence. See
Figure 29 for the model used in this example.
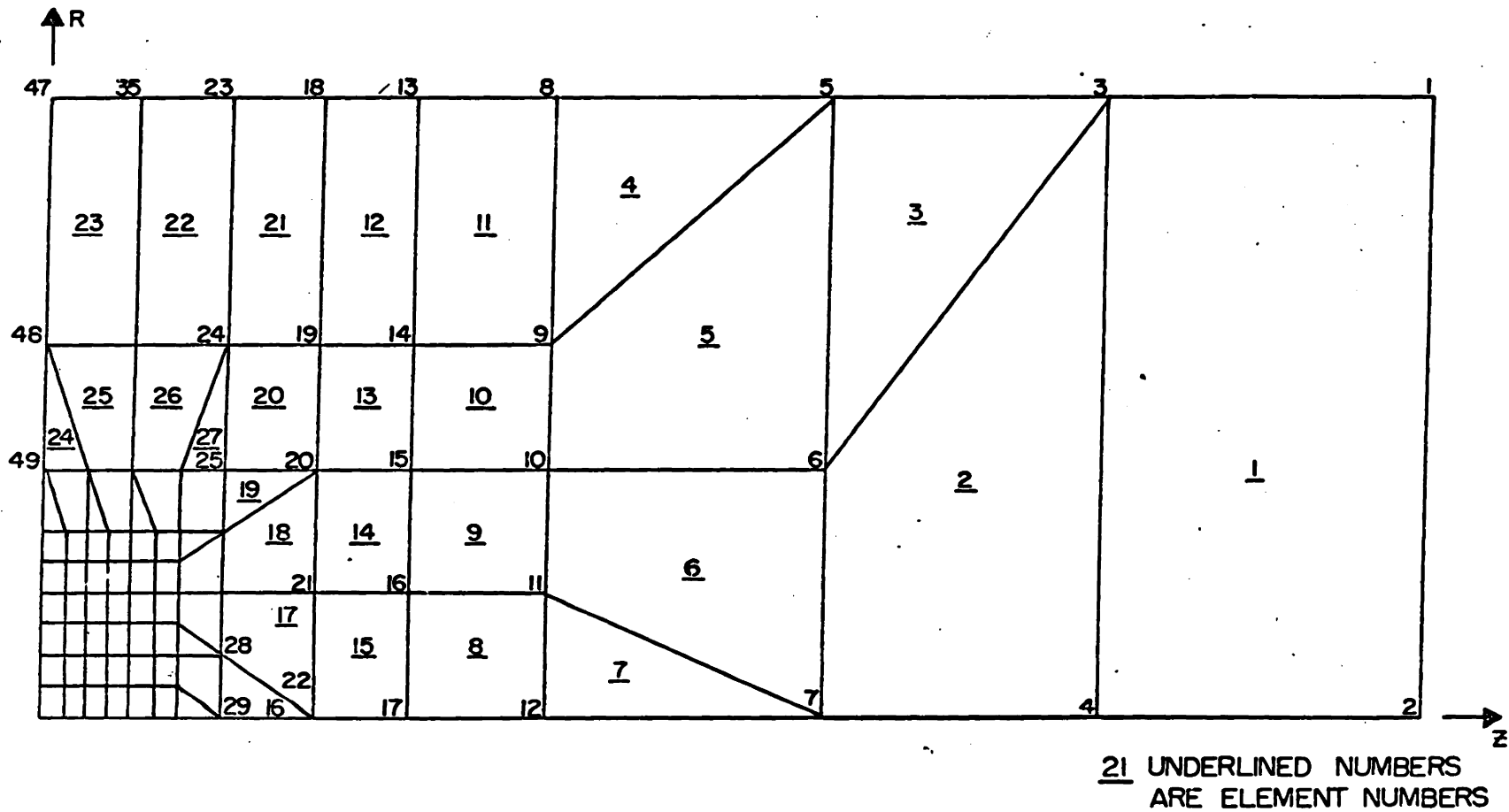
FIGURE 28: GRID FOR STRESS ANALYSIS (SEE FIGURE 29 FOR FINE GRID)
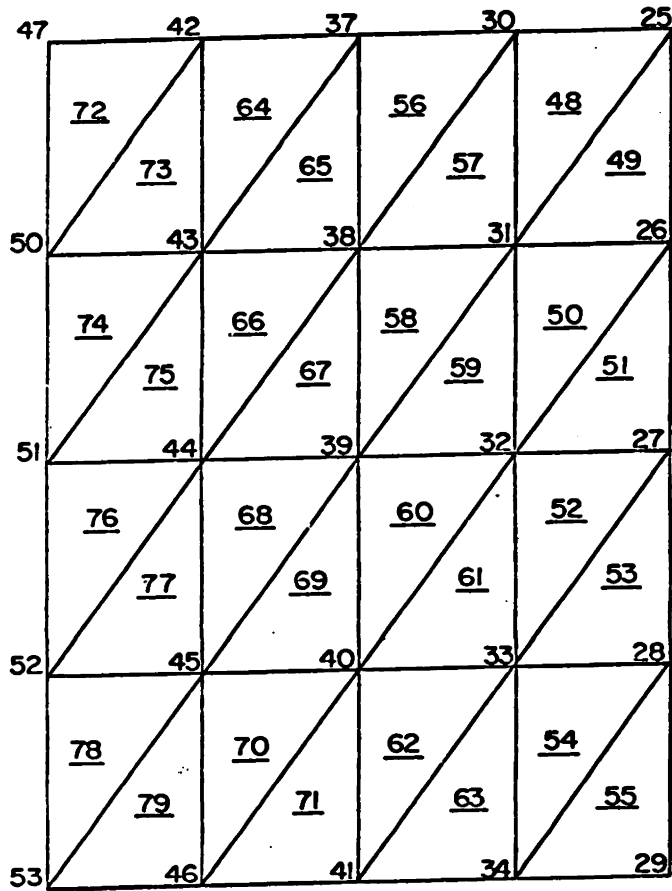
HEAT TRANSFER GRID
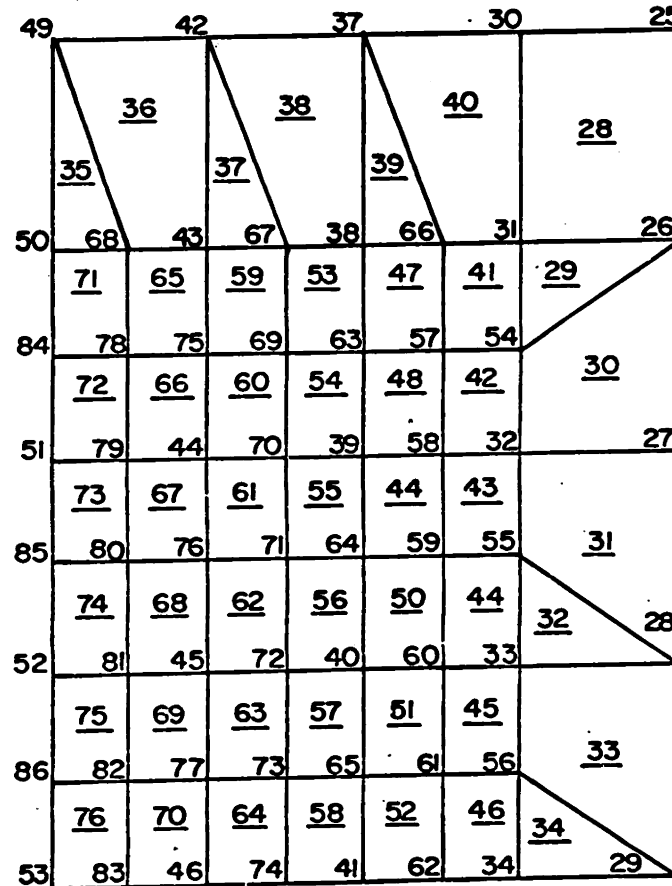
STRESS ANALYSIS GRID

FIGURE 29: FINE GRID FOR FINITE ELEMENT PROGRAMS

138

PROGRAM "FEAST 1 - 65"

USER'S MANUAL

DATE: MAY 1967

LANGUAGE   FORTRAN IV G LEVEL

PROGRAMMER: E. L. WILSON (UNIV. OF CALIF. 1966)

                     MODIFIED: JOHN T. CHRISTIAN, M.I.T.

DESCRIPTION: The purpose of this computer program is to determine the deformations and stresses within certain types of stressed bodies. The program will analyze problem situations in any of the following categories:

> Axial symmetry
>
> Plane stress
>
> Plane strain

Elastic, non-linear material properties are considered by a successive approximation technique. The effects of displacement or stress boundary condition, concentrated loads, gravity forces and temperature changes are included.

PROGRAM CAPABILITIES: The following restrictions are placed on the size of problems which can be handled by the program.

Item	Maximum Number
Nodal Points	900
Elements	800
Materials	12
Boundary Pressure Cards	200

The program incorporates a data-generating facility where-
by only a minimum amount of information need be inputted
to specify the problem topology and geometrics. Use of
this capability is described in the next section. The
program permits the use of quadrilateral and triangular
elements, as well as skew boundaries. If specified, a
data deck will be punched to provide the source data for
STRESSPLOT. This plots the vectors of major and minor
principal stress for each element.

Printed output includes:

1. Reprint of Input Data

2. Nodal Point Displacements

3. Stresses at the center of each element.

4. An approximate fundamental frequency. (The
    displacements for the given load condition
    are used as an approximate mode shape in the
    calculation of a frequency by Rayleigh's pro-
    cedure. A considerable amount of engineering
    judgement must be used in the interpretation
    of this frequency.)

Running time for typical problems is about 10 mins.

INPUT DATA FORMAT:

A. IDENTIFICATION CARD -(20A4)

Columns 1 to 80 of this card contain information to be printed with results.

B. CONTROL CARD - (4I5, 3F10.2, 3I5)

Columns	1 - 5	Number of nodal points
	6 - 10	Number of elements
	11 - 15	Number of different materials
	16 - 20	Number of boundary pressure cards
	21 - 30	Axial acceleration in the Z-direction
	31 - 40	Angular velocity
	41 - 50	Reference temperature (stress free temperature)
	51 - 55	Number of approximations
	56 - 60	= 0 Axisymmetric analysis
		= 1 Plane stress analysis
		= -1 Plane strain
	65	= 1 A deck of stresses and displacements will be punched.

C. MATERIAL PROPERTY INFORMATION

The following group of cards must be supplied for each different material:

First Card - (2I5, 2F10.0)

Columns   1 - 5   Materials identification - any number 1 to 12.

           6 - 10   Number of different temperatures for which properties are given = 8 maximum.

          11 - 20   Mass density of material

          21 - 30   Ratio of plastic modulus to elastic modulus

Following Cards - (8F10.0) One card for each temperature

Columns   1 - 10   Temperature

          11 - 20   Modulus of elasticity - E_r and E_z

          21 - 30   Poisson's ratio - ν_{rz}

          31 - 40   Modulus of elasticity - E_θ

          41 - 50   Poisson's ratio $\nu_{\theta r}$ and $\nu_{\theta z}$

          51 - 60   Coefficient of thermal expansion - α_r and α_z

          61 - 70   Coefficient of thermal expansion α_θ

          71 - 80   Yield stress σ_y
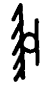
Material properties vs. temperature are input for each material in tabular form. The properties for each element in the system are then evaluated by interpolation. The mass density of the material is required only if acceleration loads are specified or if the approximate frequency is desired. Listing of the coefficients of thermal expansion are necessary only for thermal stress analysis. The plastic modulus ratio and the yield stress are specified only if nonlinear materials are used.

D. NODAL POINT CARDS - (2I5, 5F10.0)

One card for each nodal point with the following information:

Columns   1 - 5   Nodal point number

                10   Number which indicates if displacements or forces are to be specified

       11 - 20   R - ordinate

       21 - 30   z - ordinate

       31 - 40   XR

       41 - 50   XR

       51 - 60   Temperature

If the number in column 10 is

0   XR is the specified R-load and

     XZ is the specified Z-load.   free

1   XR is the specified R-displacement and

     XZ is the specified Z-load.

2   XR is the specified R-load and

     XZ is the specified Z-displacement.

3   XR is the specified R-displacement and

     XZ is the specified Z-displacement.   fixed

All loads are considered to be total forces acting
on a one radian segment (or unit thickness in the case
of plane stress analysis). Nodal point cards must be in
numerical sequence. If cards are omitted, the omitted
nodal points are generated at equal intervals along a
straight line between the defined nodal points. The neces-
sary temperatures are determined by linear interpolation.
The boundary code (column 10), XR and XZ are set equal to
zero.

    SKEW BOUNDARIES

    If the number in columns 6-10 of the nodal point
cards is other than 0, 1, 2 or 3, it is interpreted as
the magnitude of an angle in degrees. This angle is
shown on the following page.
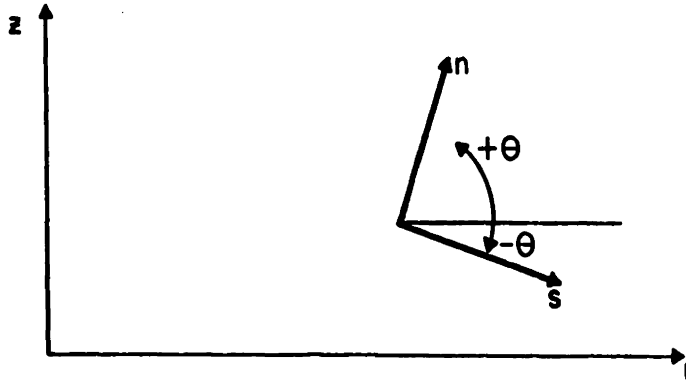
The terms in columns 31 - 50 of the nodal point card
are then interpreted as follows:

>   XR is the specified load in the s-direction
>
>   XZ is the specified displacement in the n-
>   direction

The angle must always be input as a negative angle and
may range from -.001 to -180 degrees. Hence, +1.0 degree
is the same as -179.0 degrees. The displacements of these
nodal points which are printed by the program are

> u_r = the displacement in the s-direction
>
> u_z = the displacement in the n-direction

E. ELEMENT CARDS - (6I5)

>   One card for each element.

>   Columns   1 - 5   Element number
>
>   6 - 10   Nodal Point I
>
>   11 - 15   Nodal Point J
>
>   16 - 20   Nodal Point K
>
>   21 - 25   Nodal Point L

26 - 30   Material Identification

1.   Order nodal points counter-clockwise around element.

2.   Maximum difference between nodal point I.D. must be less than 50.

Element cards must be in element number sequence. If element cards are omitted, the program automatically generates the omitted information by incrementing by one the preceding I, J, K and L. The material identification code for the generated cards is set equal to the value given on the last card. The last element card must always be supplied.

Triangular elements are also permissible; they are identified by repeating the last nodal point number (i.e., I, J, K, L).·

F.   PRESSURE CARDS - (2I5, 1F10.0)

One card for each boundary element which is subjected to a normal pressure.

Columns   1 - 5   Nodal Point I

6 - 10   Nodal Point J

11 - 20   Normal Pressure

Normal Pressure
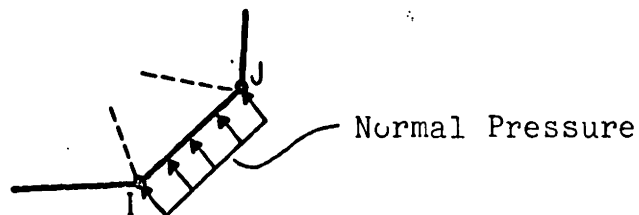
As shown previously, the boundary element must be on the left as one progresses from I. to J. Surface tensile force is input as a negative pressure.

PROGRAM USE:

a). USE OF THE PLANE STRESS OPTION

A one punch in column 60 of the control card indicates the body is a plane stress structure of unit thickness. In the case of plane stress analysis, the material property cards are interpreted as follows:

Column 11 - 20 Modulus of elasticity E_r

21 - 30 Poisson's ratio

31 - 40 Modulus of elasticity E_z

The corresponding stress-strain relationship used in the analysis is

$$\begin{Bmatrix} \sigma_r \\ \sigma_z \\ \tau_{rz} \end{Bmatrix} = \frac{E_r}{\mu - \nu^2} \times \begin{bmatrix} \mu & \nu & 0 \\ \nu & 1 & 0 \\ 0 & \frac{\mu - \nu^2}{2(\mu + \nu)} \end{bmatrix} \begin{Bmatrix} \varepsilon_r \\ \varepsilon_z \\ \gamma_{rx} \end{Bmatrix}$$

where

$$\mu = \frac{E_r}{E_z}$$

b). USE OF THE PLANE STRAIN OPTION

A punch of -1 in column 60 of the central card indicates that the body is a plane strain structure. The material property cards are interpreted as follows:

Column 11 - 20 Modulus of Elasticity E_V

21 - 30 Poisson's Ratio ν_{vH}

31 - 40 Modulus of Elasticity E_H

41 - 50 Poisson's Ratio ν_{HH}

The program must be run on the IBM 360/65 with the OS control cards. Two scratch tapes must be mounted on logical units 8 and 9. The source program has been punched on the 026 key punch (BCD).

```
0001              DIMENSION X(80), Y(80), T(80), F(80), NFIX(80), LNOD(80,3),
                 1AREA(80), THICK(80), HCAP(80), L(80), NODL(80,9), THCAP(80),
                 29(80), C(80), D(80), TNOEL(80) , TC(80)
0002              DIMENSION SE(80)
0003              READ (5,1) KTMAX,KTPRT,NODES,NOEL,DENS,SPHET,DTIME,COND,TEMP
0004              WRITE (6,1) KTMAX,KTPRT,NODES,NOEL,DENS,SPHET,DTIME,COND,TEMP
0005              DO 10 I=1,NODES
0006              READ (5,2) X(I),Y(I),T(I),F(I),NFIX(I)
0007              WRITE (6,2) X(I),Y(I),T(I),F(I),NFIX(I)
0008        10    CONTINUE
0009              DO 11 I=1,NCEL
0010              READ (5,3) LNOD(I,1),LNOD(I,2),LNOD(I,3)
0011              WRITE (6,3) LNOD(I,1),LNOD(I,2),LNOD(I,3)
0012        11    CONTINUE
0013        1     FORMAT (4I5, 5F10.3)
0014        2     FORMAT (4F12.5,I9)
0015        3     FORMAT (3I3)
0016        5     FORMAT (4F18.5)
0017              CONDX=COND
0018              CONDY=COND
0019              DO 20 I=1,NOEL
0020              L1=LNOD(I,1)
0021              L2=LNOD(I,2)
0022              L3=LNOD(I,3)
0023              AREA(I)=X(L2)*Y(L3)+X(L3)*Y(L1)+X(L1)*Y(L2)-X(L2)*Y(L1)-X(L3)*
                 1Y(L2)-X(L1)*Y(L3)
0024              AREA(I)=AREA(I)/2.
0025              THICK(I)=(X(L1)+X(L2)+X(L3))/3.
0026        20    HCAP(I)=DENS*SPHET*AREA(I)*THICK(I)
0027              WRITE (6,200) (AREA(I), I=1,NCEL)
0028       200    FORMAT (7E17.5)
0029              DO 22 I=1,NODES
0030              L(I)=0
0031              DO 22 J=1,NOEL
0032              DO 25 K=1,3
0033              IF (I-LNOD(J,K)) 25,21,25
0034        25    CONTINUE
0035              GO TO 22
0036        21    L(I)=L(I)+1
0037              LI=L(I)
0038              NODL(I,LI)=J
0039        22    CONTINUE
0040              DO 501 I=1,NODES
0041              WRITE (6,104) I
0042              LI=L(I)
0043              M=LI
0044              WRITE (6,400) (NODL(I,J),J=1,M)
0045       400    FORMAT (20I5)
```

```
0046        501     CONTINUE
0047                DO 23 I=1,NODES
0048                THCAP(I) = .0
0049                LI = L(I)
0050                DO 23 J=1,LI
0051                N=NODL(I,J)
0052        23      THCAP(I)=THCAP(I)+HCAP(N)/3.
0053                M=NODES
0054                WRITE (6,200) (THCAP(I), I=1,M)
0055                KSTOP=0
0056                KTIME=0
0057        32      KSTOP=KSTOP+1
0058                TSF = 0.0
0059                DO 32 I=1,NODES
0060                N=NFIX(I)
0061                IF(N) 32,137,137
0062        137     IF(KSTOP-1) 31,33,31
0063        33      T(I)=(T(I)+RTEMP)/2.
0064                GO TO 32
0065        31      T(I)=RTEMP
0066        32      CONTINUE
0067                DO 34 I=1,NOEL
0068                L1=LNOD(I,1)
0069                L2=LNOD(I,2)
0070                L3=LNOD(I,3)
0071                TNOEL(I)=(T(L1)+T(L2)+T(L3))/3.
0072                B(I)=((Y(L3)-Y(L2))*T(L1)+(Y(L1)-Y(L3))*T(L2)+(Y(L2)-Y(L1))*
                    1T(L3))/2./AREA(I)
0073        34      C(I)=((X(L3)-X(L2))*T(L1)+(X(L1)-X(L3))*T(L2)+(X(L2)-X(L1))*
                    1T(L3))/2./AREA(I)
0074                DO 40 I=1,NODES
0075                Q(I)=F(I)
0076                LI=L(I)
0077                DO 40 J=1,LI
0078                NODIJ=NODL(I,J)
0079                CONDX = 1. / ( 31500. + 21.5 * TNOEL(NODIJ))
0080                CONDY = CONDX
0081                QX = -B(NODIJ)*CONDX*THICK(NODIJ)
0082                QY=-C(NODIJ)*CONDY*THICK(NODIJ)
0083                K=0
0084        35      K=K+1
0085                IF (K-3)42,42,41
0086        41      CONTINUE
0087                WRITE (6,102)
0088                WRITE (6,104) I
0089                WRITE (6,105) J
0090        104     FORMAT (3H I=I3)
0091        105     FORMAT (3H J=I3)
```

```
0092              GO TO 57
0093        102   FORMAT (5H KRIG)
0094        42    CONTINUE
9095              IF (I-LNCD(NOIJ,K)) 35,36,35
0096        36    IF(K-2) 37,38,39
0097        37    LA=LNCD(NCIJ,2)
0098              LB=LNOD(NOIJ,3)
0099              GO TO 401
0100        38     LA=LNOD(NCIJ,3)
0101              LB=LNCD(NOIJ,1)
0102              GO TO 401
0103        39    LA=LNCD(NCIJ,1)
0104              LB=LNOD(NCIJ,2)
0105        401   Q(I)=(Y(LB)-Y(LA))*)X/2.+(X(LB)-X(LA))*GY/2.+)(I)
0106        40    CONTINUE
0107              KTIME=KTIME+1
0108              DO 50 I=1,NODES
0109        50    T(I)=T(I)+Q(I)*DTIME/THCAP(I)
            C     THE THREE CARDS FOR FAHRENHEIT TO CENTIGRADE CONVERSION COME HERE
0110              DO 979 I = 1, NODES
0111              TC(I) = ( T(I) - 32. ) * ( 5. / 9. )
0112        979 CONTINUE
0113              IF (KTIME-KIPRT) 54,51,51
0114        51    KTIME =0
0115              WRITE (6,120) KSTOP
0116        120   FORMAT (7H KSTOP=I4)
0117        52    WRITE (6,5) (TC(I), I=1,NODES)
0118        54    IF (KSTOP - KTMAX) 30,57,57
0119        57     CONTINUE
0120              CALL EXIT
0121              END
```

151

200	10	53	79	0.094	0.210	0.020	0.000	0.0

1.50000	0.75000	70.00000	0.0	-1
1.50000	0.0	70.00000	0.0	-1
1.15000	0.75000	70.00000	0.0	-1
1.15000	0.0	70.00000	0.0	-1
0.85000	0.75000	70.00000	0.0	-1
0.85000	0.30000	70.00000	0.0	-1
0.85000	0.0	70.00000	0.0	-1
0.55000	0.75000	70.00000	0.0	-1
0.55000	0.45000	70.00000	0.0	-1
0.55000	0.30000	70.00000	0.0	-1
0.55000	0.15000	70.00000	0.0	-1
0.55000	0.0	70.00000	0.0	-1
0.40000	0.75000	70.00000	0.0	-1
0.40000	0.45000	70.00000	0.0	-1
0.40000	0.30000	70.00000	0.0	-1
0.40000	0.15000	70.00000	0.0	-1
0.40000	0.0	70.00000	0.0	-1
0.30000	0.75000	70.00000	0.0	-1
0.30000	0.45000	70.00000	0.0	-1
0.30000	0.30000	70.00000	0.0	-1
0.30000	0.15000	70.00000	0.0	-1
0.30000	0.0	70.00000	0.0	-1
0.20000	0.75000	70.00000	0.0	-1
0.20000	0.45000	70.00000	0.0	-1
0.20000	0.30000	70.00000	0.0	-1
0.20000	0.22500	70.00000	0.0	-1
0.20000	0.15000	70.00000	0.0	-1
0.20000	0.07500	70.00000	0.0	-1
0.20000	0.0	70.00000	0.0	-1
0.15000	0.30000	70.00000	0.0	-1
0.15000	0.22500	70.00000	0.0	-1
0.15000	0.15000	70.00000	0.0	-1
0.15000	0.07500	70.00000	0.0	-1
0.15000	0.0	70.00000	0.0	-1
0.10000	0.75000	70.00000	0.0	-1
0.10000	0.45000	70.00000	0.0	-1
0.10000	0.30000	70.00000	0.0	-1
0.10000	0.22500	70.00000	0.0	-1
0.10000	0.15000	70.00000	0.0	-1
0.10000	0.07500	70.00000	0.0	-1
0.10000	0.0	70.00000	0.0	-1
0.05000	0.30000	70.00000	0.0	-1
0.05000	0.22500	70.00000	0.0	-1
0.05000	0.15000	70.00000	0.0	-1
0.05000	0.07500	70.00000	0.0	-1
0.05000	0.0	70.00000	0.0	-1
0.0	0.75000	70.00000	0.0	-1
0.0	0.45000	70.00000	0.0	-1
0.0	0.30000	70.00000	0.0	-1
0.0	0.22500	70.00000	0.0	-1
0.0	0.15000	70.00000	0.00225	-1
0.0	0.07500	70.00000	0.00300	-1
0.0	0.0	70.00000	0.00225	-1

1	4	2
1	3	4
3	6	4
4	6	7
3	5	6
7	11	12
6	11	7
6	10	11
6	9	13
5	9	6
5	8	9
11	17	12
11	16	17
10	16	11
10	15	16
9	15	10
9	14	15
8	14	9
8	13	14
16	22	17
16	21	22
15	21	16
15	20	21
14	20	15
14	19	20
13	19	14
13	18	19
22	28	23
21	28	22
21	27	23
21	26	27
20	26	21
20	25	26
19	25	20
19	24	25
18	24	13
18	23	24
23	36	24
23	35	35
35	48	36
35	47	44
24	36	25
24	36	36
36	36	37
36	42	37
36	48	42
42	49	43
25	36	31
25	31	26
26	31	32
26	32	27
27	32	33
27	33	33
28	33	34
28	34	29
30	37	33
30	38	31
31	39	39
31	39	32
32	39	42
32	40	33
33	40	41
33	41	34
37	42	43
37	43	38
38	43	44
38	44	39
39	44	45
39	45	40
40	45	46
40	46	41
42	49	50
42	50	43
43	50	51
43	51	44
44	51	52
44	52	45
45	52	53
45	53	46

0.13125E-00 0.13125E-0? 0.11250E-00 0.45000E-01 0.67639E-01 0.22503E-01 0.45000E-01
0.27530E-01 0.67500E-01 0.67500E-01 0.45003E-01 0.11250E-01 0.11253E-01 0.11250E-01
0.11250E-01 0.11253E-01 0.11250E-01 0.22503E-01 0.22530E-01 0.22530E-01 0.11250E-01
0.75000E-02 0.75000E-02 0.75000E-02 0.75000E-02 0.15032E-01 0.15033E-01 0.17500E-02
0.15000E-01 0.15000E-01 0.15000E-01 0.74999E-02 0.37503E-02 0.75000E-02 0.75000E-02
0.15000E-01 0.15000E-01 0.15000E-01 0.15000E-01 0.15000E-01 0.15003E-01 0.17500E-02
0.75000E-02 0.37500E-02 0.37500E-02 0.37500E-02 0.37530E-02 0.37500E-02 0.37500E-02
0.18750E-02 0.18753E-02 0.18750E-02 0.18753E-02 0.18753E-02 0.18753E-02 0.18750E-02
0.18750E-02 0.18753E-02 0.18750E-02 0.18753E-02 0.18750E-02 0.18753E-02 0.18750E-02
0.18750E-02 0.18753E-02 0.18750E-02 0.18753E-02 0.18750E-02 0.18753E-02 0.18750E-02

I=					
I= 1	2				
I= 2					
I= 1					
I= 2	3	4			
I= 1	2	3	4		
I= 5	10	11			
I= 6	4	4	7	8	9	10
I= 7	6	7			
I= 11	18	19			
I= 9	10	11	16	17	18
I= 10	9	14	15	16	
I= 11	7	8	12	13	14
I= 12	17				
I= 13	26	27			
I= 14	18	19	24	25	26
I= 15	16	17	22	23	24
I= 16	14	15	20	21	22
I= 17	19	20			
I= 18	26	27			
I= 19	25	26	27	34	35	36
I= 20	24	25	32	33	34
I= 21	22	23	30	31	32
I= 22	21	29	30		
I= 23	34	35			
I= 24	36	37	46	47	48
I= 25	34	35	44	45	46
I= 26	32	33	42	43	44
I= 27	31	32	52	53	
I= 28	36	37	53	54	55
I= 29	55				
I= 30	63	64	65	66	67
I= 31	60	60	67	68	69
I= 32	51	52	54	63	64
I= 33	53	54	61	62	64
I= 34	55	63			
I= 35	60	61			
I= 36	53	62	63	64	65	66
I= 37	65	56	64	65	
I= 38	57	58	65	66	67
I= 39	59	60	67	68	69
I= 40	61	62	63	70	71
I= 41	63	71			
I= 42	66	67	68	77	73
I= 43	65	66	74	74	75
I= 44	67	63	75	76	77
I= 45	63	70	77	74	78
I= 46	71	70			
I= 47					
I= 48	63	64	67		
I= 49	77				
I= 50	73	74			
I= 51	74	75	76		
I= 52	77	74			
I= 53	79				

0.27844E-03 0.23947E-03 0.22941E-03 0.33447E-03 0.34975E-03 0.27241E-03 0.59465E-03
0.33111E-03 0.45016E-03 0.57324E-03 0.21147E-03 0.11124E-03 0.13571E-03 0.26609E-03
0.15921E-03 0.45024E-03 0.39414E-04 0.42250E-05 0.16653E-03 0.11372E-04 0.44430E-04
0.53462E-04 0.42645E-04 0.43734E-04 0.19275E-04 0.11255E-04 0.13725E-04 0.31255E-04
0.41134E-04 0.42734E-04 0.11114E-04 0.11114E-04 0.11114E-04 0.59431E-05 0.21010E-04
0.53145E-04 0.43794E-05 0.76226E-05 0.74073E-05 0.76473E-05 0.41125E-05 0.41495E-05
0.37013E-05 0.37213E-05 0.37213E-05 0.72413E-05 0.43900E-05 0.12743E-04 0.61641E-06
0.42250E-06 0.42250E-06 0.43250E-06 0.61641E-05 0.61641E-06 0.12743E-04 0.61641E-06

154

KSTOP= 10

21.11110	21.11110	21.11110	21.11110
21.11110	21.11110	21.11110	21.11110
21.11110	21.11110	21.11110	21.11110
21.11110	21.11110	21.11110	21.11110
21.11110	21.11110	21.11110	21.11110
21.11110	21.11110	21.11110	21.11110
21.11110	21.11110	21.11111	21.11111
21.11113	21.11110	21.11116	21.11412
21.11514	21.11557	21.11110	21.11110
21.11113	21.11543	21.27647	21.33098
21.35767	21.11243	21.27707	27.69820
29.81937	30.95134	21.11110	21.11110
21.17506	25.53850	290.29248	383.60327
388.44678			

KSTOP= 20

21.11110	21.11110	21.11110	21.11110
21.11110	21.11110	21.11110	21.11110
21.11110	21.11110	21.11110	21.11110
21.11110	21.11110	21.11110	21.11110
21.11110	21.11110	21.11110	21.11110
21.11110	21.11110	21.11110	21.11110
21.11110	21.11113	21.11259	21.11232
21.11378	21.11113	21.11444	21.16449
21.18282	21.19206	21.11110	21.11110
21.11317	21.18497	22.31474	22.71992
22.95303	21.13466	22.29378	42.99069
50.01877	54.48178	21.11110	21.11136
21.56172	35.82095	504.39208	680.37793
694.85718			

KSTOP= 30

21.11110	21.11110	21.11110	21.11110
21.11110	21.11110	21.11110	21.11110
21.11110	21.11110	21.11110	21.11110
21.11110	21.11110	21.11110	21.11110
21.11110	21.11110	21.11110	21.11110
21.11113	21.11118	21.11110	21.11110
21.11110	21.11177	21.12210	21.12042
21.13083	21.11185	21.13423	21.34518
21.42772	21.47328	21.11110	21.11115
21.12555	21.42545	24.48441	25.63307
26.35677	21.21304	24.31093	61.82958
75.02322	84.14186	21.11110	21.11249
22.33400	48.45874	683.93970	937.30200
962.89038			

KSTOP= 40

21.11110	21.11110	21.11110	21.11110
21.11110	21.11110	21.11110	21.11110
21.11110	21.11110	21.11110	21.11110
21.11110	21.11110	21.11110	21.11110
21.11110	21.11110	21.11110	21.11110
21.11150	21.11174	21.11110	21.11110
21.11122	21.11465	21.15115	21.14636
21.18343	21.11494	21.19193	21.72533
21.94688	22.07637	21.11110	21.11142
21.16144	21.91394	27.68617	29.96638
31.47314	21.37599	27.22102	81.91830
101.90567	116.34813	21.11110	21.11517
23.43288	61.89645	939.64771	1167.07520
1204.48657			

KSTOP=   50

21.11110	21.11110	21.11110	21.11110
21.11110	21.11110	21.11110	21.11110
21.11110	21.11110	21.11110	21.11110
21.11110	21.11110	21.11110	21.11110
21.11110	21.11110	21.11110	21.11111
21.11261	21.11346	21.11110	21.11110
21.11180	21.12273	21.21359	21.20444
21.29709	21.12346	21.31029	22.34540
22.79912	23.07460	21.11110	21.11215
21.23473	22.68544	31.73201	35.47940
38.02259	21.63992	30.81241	102.17836
129.27733	149.33171	21.11111	21.12006
24.77913	75.40688	977.80225	1376.91968
1426.63281			

KSTOP=   60

21.11110	21.11110	21.11110	21.11110
21.11110	21.11110	21.11110	21.11110
21.11110	21.11110	21.11110	21.11110
21.11110	21.11110	21.11110	21.11110
21.11113	21.11110	21.11110	21.11110
21.11522	21.11742	21.11110	21.11127
21.11337	21.14006	21.11110	21.11113
21.49684	21.14124	21.32306	21.31018
24.00754	24.49864	21.50851	23.22034
21.35722	23.74249	21.11110	21.11363
45.65884	22.01143	36.42712	41.91728
156.45656	182.20552	34.89859	122.09210
26.30396	98.64597	21.11119	21.12770
1633.74292		1102.43579	1571.35400

KSTOP=   70

21.11110	21.11110	21.11110	21.11110
21.11110	21.11110	21.11110	21.11110
21.11110	21.11160	21.11110	21.11110
21.11110	21.11110	21.11110	21.11119
21.11125	21.11110	21.11110	21.11165
21.12025	21.12497	21.11110	21.11127
21.11684	21.17139	21.49136	21.47844
21.80386	21.17255	21.80014	24.34682
25.56880	26.34686	21.11110	21.11618
21.53741	25.06754	41.60245	49.05373
54.22368	22.49026	39.32823	141.41994
183.11061	214.52771	21.11136	21.13857
27.95483	101.45647	1216.23297	1753.40674
1828.78052			

KSTOP=   80

21.11110	21.11110	21.11110	21.11110
21.11110	21.11110	21.11110	21.11110
21.11110	21.11110	21.11110	21.11110
21.11110	21.11110	21.11110	21.11140
21.11156	21.11110	21.11110	21.11243
21.12488	21.13783	21.11110	21.11157
21.12329	21.22163	21.72777	21.72227
22.23407	21.22165	22.19286	25.71002
27.46259	29.59630	21.11110	21.12018
21.78038	26.63259	47.12115	56.70190
63.36774	23.07209	43.98524	160.06468
209.08405	245.08749	21.11163	21.15303
29.69389	113.77518	1321.33057	1925.21753
2013.83594			

KSTOP=   90

21.11110	21.11110	21.11110	21.11110
21.11110	21.11110	21.11110	21.11110
21.11110	21.11110	21.11110	21.11110
21.11110	21.11110	21.11110	21.11182
21.11215	21.11110	21.11110	21.11385
21.14236	21.15782	21.11110	21.11211
21.13414	21.29555	22.03889	22.05219
22.79779	21.29231	22.68912	27.28894
29.65915	31.21179	21.11119	21.12598
22.08830	28.40578	52.87621	64.71300
72.94823	23.75012	48.79291	178.00034
234.31395	276.79663	21.11203	21.17143
31.49449	125.58687	1418.99658	2089.36108
2190.44482			

KSTOP= 100

21.11110	21.11110	21.11110	21.11110
21.11110	21.11110	21.11110	21.11110
21.11110	21.11110	21.11110	21.11110
21.11110	21.11110	21.11116	21.11253
21.11314	21.11110	21.11111	21.11618
21.16206	21.18686	21.11110	21.11301
21.15091	21.39746	22.42873	22.47603
23.50023	21.38779	23.28752	29.05989
32.12454	34.15257	21.11131	21.13394
22.46103	30.35518	58.78543	72.97079
87.82310	24.51657	53.65742	195.23747
258.79760	306.63184	21.11259	21.19405
33.33795	136.90076	1510.39453	2244.03540
2359.76538			

KSTOP= 110

21.11110	21.11110	21.11110	21.11110
21.11110	21.11110	21.11110	21.11110
21.11110	21.11110	21.11110	21.11110
21.11110	21.11110	21.11127	21.11368
21.11473	21.11110	21.11119	21.11978
21.18935	21.22684	21.11110	21.11435
21.17519	21.53104	22.84912	22.99895
24.34225	21.51057	23.98378	30.99889
34.92425	37.37656	21.11151	21.14442
22.89679	32.45094	64.78642	81.38559
92.88330	25.36320	58.56230	211.80499
282.51758	335.60352	21.11336	21.22107
35.21115	147.73969	1596.38721	2393.17041
2522.70801			

KSTOP= 120

21.11110	21.11110	21.11110	21.11110
21.11110	21.11110	21.11110	21.11110
21.11110	21.11110	21.11110	21.11110
21.11110	21.11110	21.11147	21.11540
21.11708	21.11110	21.11134	21.12500
21.22556	21.27962	21.11110	21.11630
21.20863	21.69923	23.45009	23.62363
25.32138	21.66254	24.77185	33.08296
37.72519	40.84315	21.11182	21.15771
23.39268	34.66629	70.33208	89.88855
103.04582	26.23138	63.46391	227.73964
305.52881	363.73975	21.11436	21.25270
37.10472	158.12770	1677.66211	2536.51660
2679.99976			

KSTOP= 130

21.11110	21.11110	21.11110.	21.11110
21.11110	21.11110	21.11110	21.11110
21.11110	21.11110	21.11110	21.11115
21.11110	21.11110	21.11180	21.11783
21.12045	21.11110	21.11159	21.13226
21.27197	21.34688	21.11110	21.11897
21.25279	21.90425	24.08028	24.35072
26.43253	21.84482	25.64465	35.29089
40.79691	44.51468	21.11223	21.17412
23.94511	36.97774	76.88699	98.42715
113.24776	27.76483	68.33809	243.08035
327.85425	391.07739	21.11562	21.28905
39.01187	168.09636	1754.77783	2674.70020
2832.23486			

KSTOP= 140

21.11110	21.11110	21.11110	21.11110
21.11110	21.11110	21.11110	21.11110
21.11110	21.11110	21.11110	21.11124
21.11110	21.11110	21.11234	21.12170
21.12506	21.11110	21.11195	21.14201
21.32982	21.43024	21.11119	21.12256
21.30914	22.14766	24.78725	25.17909
27.66390	22.05804	26.59473	37.60358
44.01202	48.35713	21.11278	21.19386
24.55013	39.36510	82.92477	106.96155
123.44164	28.30472	73.16760	257.86597
349.52783	417.65576	21.11719	21.33025
40.92746	177.67305	1828.19482	2308.21143
2979.90210			

KSTOP= 150

21.11110	21.11110	21.11110	21.11110
21.11110	21.11110	21.11110	21.11110
21.11110	21.11110	21.11110	21.11136
21.11110	21.11110	21.11308	21.12570
21.13116	21.11110	21.11249	21.15468
21.40013	21.53105	21.11127	21.12720
21.37901	22.43033	25.56779	26.10616
29.02258	22.30234	27.61455	40.00398
47.34637	52.34033	21.11349	21.21718
25.20361	41.81122	88.92572	115.46153
133.59143	29.39481	77.94035	272.13403
370.58374	443.51465	21.11906	21.37637
42.84750	186.88499	1898.29761	2937.48657
3123.40674			

KSTOP= 160

21.11110	21.11110	21.11110	21.11110
21.11110	21.11110	21.11110	21.11110
21.11110	21.11110	21.11118	21.11157
21.11110	21.11110	21.11414	21.13150
21.13902	21.11110	21.11325	21.17070
21.48393	21.65053	21.11143	21.13307
21.46359	22.75259	26.41817	27.12833
30.48505	22.57741	28.69693	42.47726
50.77884	56.43784	21.11441	21.24425
25.90152	44.30168	94.87537	123.90437
143.67078	39.52888	82.64806	285.91895
391.05519	468.69263	21.12131	21.42749
44.76888	195.75749	1965.41089	3062.87939
3263.09424			

KSTOP= 170

21.11110	21.11110	21.11110	21.11110
21.11110	21.11110	21.11110	21.11110
21.11110	21.11110	21.11127	21.11186
21.11110	21.11113	21.11555	21.13889
21.14894	21.11110	21.11424	21.19054
21.58205	21.78969	21.11165	21.14034
21.56389	23.11430	27.33434	28.24113
32.04749	22.88274	29.83505	45.01045
54.29112	60.62680	21.11554	21.27525
26.63986	46.82436	100.76315	132.27252
153.66006	31.70134	87.28519	299.25293
410.97339	493.22632	21.12393	21.48360
46.68898	204.31476	2029.81152	3184.70679
3399.26392			

KSTOP= 180

21.11110	21.11110	21.11110	21.11110
21.11110	21.11110	21.11110	21.11110
21.11110	21.11110	21.11140	21.11226
21.11110	21.11122	21.11743	21.14801
21.16121	21.11110	21.11557	21.21461
21.69519	21.94934	21.11192	21.14915
21.68071	23.51494	28.31210	29.43961
33.70117	23.21753	31.02258	47.59235
57.86746	64.88751	21.11691	21.31032
27.41486	49.36919	106.58151	140.55432
163.54477	32.90703	91.84831	312.16553
430.36816	517.15015	21.12698	21.54482
48.60570	212.57825	2091.73828	3303.23535
3532.17407			

KSTOP= 190

21.11110	21.11110	21.11110	21.11110
21.11110	21.11110	21.11110	21.11110
21.11110	21.11111	21.11159	21.11281
21.11110	21.11133	21.11983	21.15912
21.17609	21.11110	21.11726	21.24333
21.82393	22.13014	21.11229	21.15967
21.81474	23.95363	29.34717	30.71843
35.43755	23.58081	32.25378	50.21323
61.49435	69.20313	21.11858	21.34953
28.22299	51.92783	112.32520	148.74089
173.31447	34.14137	96.33546	324.68384
449.26733	540.49561	21.13051	21.61105
50.51718	220.56801	2151.39795	3418.69751
3662.05249			

KSTOP= 200

21.11110	21.11110	21.11110	21.11110
21.11110	21.11110	21.11110	21.11110
21.11110	21.11121	21.11185	21.11110
21.11110	21.11150	21.12285	21.17247
21.19388	21.11116	21.11940	21.27711
21.96873	22.33252	21.11276	21.17204
21.96645	24.42926	30.43532	32.07211
37.24860	23.97151	33.52344	52.86479
65.16023	73.55920	21.12051	21.39305
29.06096	54.49339	117.99071	156.82588
182.96181	35.40022	100.74590	336.83252
467.69653	563.29370	21.13451	21.68234
52.42186	228.30238	2208.97119	3531.30835
3789.10132			

159

CYLINCER 1.5 * 1.5   CHARLES AELSCA   THFRMAL STRESS

 NUMBER CF ACDAL PCINTS------ 86

 NUMBER OF ELEMENTS---------- 76

 NUMBER CF DIFF. MATERIALS--- 1

 NUMBER CF PRESSURF CARCS---- 0

 AXIAL ACCELERATICN---------- C.C

 ANGULAR VELCCITY------------ 0.0

 REFERENCE TEMPERATURE------- C.21110 C2

 NUMBER CF APPRC:IMATICNS---- 1

MATERIAL NUMBER= 1. NUMBER CF TEMPERATURE CARCS= 1. MASS CENSITY= C.1CCCO C1.MCDLLLS RATIO= C.10CCC C1

TEMPERATURE	E(RZ)	NU(RZ)	E(T)	NU(T)	ALPHA(RZ)	ALPHA(T)	YIELC STRESS
21.11	C.24CCCD C7	C.1CCCCC CC	C.2400CD C7	C.1CCCCC CC	C.72CCCC-05	C.72CCCC-C5	C.24CCCC C7

160

NODAL POINT	TYPE	R-ORDINATE	Z-ORDINATE	R LOAD OR DISPLACEMENT	Z LOAD OR DISPLACEMENT	TEMPERATURE
1	0.0	0.750	1.500	0.0	0.0	21.110
2	0.00	0.0	1.500	0.0	0.0	21.110
3	0.0	0.750	1.150	0.0	0.0	21.110
4	0.0	0.0	1.150	0.0	0.0	21.110
5	0.0	0.750	0.850	0.0	0.0	21.110
6	0.0	0.300	0.850	0.0	0.0	21.110
7	0.0	0.0	0.850	0.0	0.0	21.110
8	0.0	0.750	0.550	0.0	0.0	21.110
9	0.0	0.450	0.550	0.0	0.0	21.110
10	0.0	0.300	0.550	0.0	0.0	21.110
11	0.0	0.150	0.550	0.0	0.0	21.110
12	0.0	0.0	0.550	0.0	0.0	21.110
13	0.0	0.750	0.400	0.0	0.0	21.110
14	0.0	0.450	0.400	0.0	0.0	21.110
15	0.0	0.300	0.400	0.0	0.0	21.110
16	0.0	0.150	0.400	0.0	0.0	21.110
17	0.0	0.0	0.400	0.0	0.0	21.110
18	0.0	0.750	0.300	0.0	0.0	21.110
19	0.0	0.450	0.300	0.0	0.0	21.110
20	0.0	0.300	0.300	0.0	0.0	21.110
21	0.0	0.150	0.300	0.0	0.0	21.110
22	0.0	0.0	0.300	0.0	0.0	21.110
23	0.0	0.750	0.200	0.0	0.0	21.110
24	0.0	0.450	0.200	0.0	0.0	21.110
25	0.0	0.300	0.200	0.0	0.0	21.110
26	0.0	0.225	0.200	0.0	0.0	21.120
27	0.0	0.150	0.200	0.0	0.0	21.210
28	0.0	0.075	0.200	0.0	0.0	21.210
29	0.0	0.0	0.200	0.0	0.0	21.200
30	0.0	0.300	0.150	0.0	0.0	21.200
31	0.0	0.225	0.150	0.0	0.0	21.120
32	0.0	0.150	0.150	0.0	0.0	21.310
33	0.0	0.075	0.150	0.0	0.0	22.340
34	0.0	0.0	0.150	0.0	0.0	22.450
35	0.0	0.750	0.100	0.0	0.0	23.075
36	0.0	0.450	0.100	0.0	0.0	21.110
37	0.0	0.300	0.100	0.0	0.0	21.130
38	0.0	0.225	0.100	0.0	0.0	21.230
39	0.0	0.150	0.100	0.0	0.0	22.460
40	0.0	0.075	0.100	0.0	0.0	31.730
41	0.0	0.0	0.100	0.0	0.0	35.460
42	0.0	0.300	0.050	0.0	0.0	35.030
43	0.0	0.225	0.050	0.0	0.0	31.840
44	0.0	0.150	0.050	0.0	0.0	70.410
45	0.0	0.075	0.050	0.0	0.0	102.200
46	0.0	0.0	0.050	0.0	0.0	125.300
47	0.0	0.750	0.0	0.0	0.0	145.300
48	0.0	0.450	0.0	0.0	0.0	21.110
49	0.0	0.300	0.0	0.0	0.0	21.120
50	0.0	0.225	0.0	0.0	0.0	24.760
51	0.0	0.150	0.0	0.0	0.0	35.400
52	0.0	0.075	0.0	0.0	0.0	571.500
53	1.00	0.0	0.0	0.0	0.0	1333.000
54	0.0	0.100	0.100	0.0	0.0	1423.000
55	0.0	0.112	0.150	0.0	0.0	21.500
56	0.0	0.037	0.150	0.0	0.0	22.600
57	0.0	0.100	0.125	0.0	0.0	23.075
58	0.0	0.150	0.125	0.0	0.0	26.600
59	0.0	0.112	0.125	0.0	0.0	23.000
60	1.0	0.075	0.125	0.0	0.0	25.000
61	0.0	0.037	0.125	0.0	0.0	25.000
62	0.0	0.0	0.125	0.0	0.0	30.500
63	0.0	0.150	0.100	0.0	0.0	35.500
64	0.0	0.112	0.100	0.0	0.0	31.500
65	0.0	0.037	0.100	0.0	0.0	33.500
66	0.0	0.225	0.125	0.0	0.0	36.500
67	0.0	0.225	0.075	0.0	0.0	32.000
68	0.0	0.225	0.075	0.0	0.0	27.000
69	0.0	0.188	0.075	0.0	0.0	53.000
70	0.0	0.150	0.075	0.0	0.0	62.000
71	0.0	0.112	0.075	0.0	0.0	61.000
72	0.0	0.075	0.075	0.0	0.0	82.000
73	0.0	0.037	0.075	0.0	0.0	82.000
74	0.0	0.0	0.075	0.0	0.0	53.000
75	0.0	0.188	0.050	0.0	0.0	76.000
76	0.0	0.112	0.050	0.0	0.0	115.000
77	0.0	0.037	0.050	0.0	0.0	135.000
78	0.0	0.188	0.025	0.0	0.0	450.000
79	0.0	0.150	0.025	0.0	0.0	540.000
80	0.0	0.112	0.025	0.0	0.0	740.000
81	0.0	0.075	0.025	0.0	0.0	753.000
82	0.0	0.037	0.025	0.0	0.0	775.000
83	0.0	0.0	0.025	0.0	0.0	765.000
84	0.0	0.188	0.0	0.0	0.0	525.000
85	0.0	0.112	0.0	0.0	0.0	1175.000
86	0.0	0.037	0.0	0.0	0.0	1465.000

ELEMENT NO.	I	J	K	L	MATERIAL
1	1	2	4	3	1
2	3	4	7	6	1
3	3	6	5	5	1
4	5	6	8	6	1
5	6	6	10	9	1
6	6	7	11	10	1
7	7	12	11	11	1
8	11	12	17	16	1
9	10	11	16	15	1
10	9	10	15	14	1
11	8	9	14	13	1
12	13	14	19	18	1
13	14	15	20	19	1
14	15	16	21	20	1
15	16	17	22	21	1
16	22	25	26	26	1
17	21	22	28	27	1
18	20	21	27	26	1
19	20	26	25	25	1
20	19	20	25	24	1
21	18	19	24	23	1
22	23	24	36	35	1
23	35	36	48	47	1
24	42	45	46	46	1
25	36	37	42	46	1
26	24	30	37	36	1
27	24	25	30	30	1
28	25	26	31	30	1
29	26	32	31	31	1
30	26	27	32	54	1
31	27	28	55	32	1
32	28	33	56	55	1
33	28	29	56	33	1
34	29	34	56	56	1
35	49	68	50	50	1
36	42	43	66	49	1
37	43	67	43	43	1
38	37	38	67	42	1
39	37	66	38	38	1
40	30	31	66	37	1
41	31	54	57	66	1
42	32	55	57	54	1
43	32	55	56	56	1
44	33	60	55	58	1
45	33	56	61	60	1
46	34	62	61	56	1
47	35	66	57	63	1
48	35	63	57	56	1
49	36	56	50	64	1
50	49	64	59	60	1
51	40	60	61	65	1
52	41	65	61	62	1
53	35	62	65	63	1
54	35	70	66	63	1
55	35	64	71	70	1
56	40	72	71	64	1
57	40	65	73	72	1
58	41	74	73	65	1
59	43	67	69	75	1
60	44	75	69	70	1
61	44	70	71	76	1
62	45	76	71	72	1
63	45	72	73	77	1
64	46	77	73	74	1
65	43	75	78	66	1
66	44	70	78	75	1
67	44	76	80	70	1
68	45	81	80	70	1
69	45	77	53	81	1
70	46	83	83	77	1
71	50	48	75	54	1
72	51	84	78	75	1
73	51	79	80	85	1
74	52	85	80	81	1
75	52	81	83	94	1
76	53	86	93	83	1

N.F. NUMBER	UR	UZ
1	-0.2747707D-05	0.5461050D-05
2	-0.0	-0.0
3	-0.3161675D-05	0.6563220D-05
4	-0.0	-0.2457751D-05
5	-0.3065285D-05	0.5264224D-05
6	-0.2756267D-05	-0.1522655D-05
7	-0.0	-0.8661050D-05
8	0.7313572D-05	0.1835723D-04
9	0.2356345D-06	0.2424246D-05
10	-0.1611051D-05	-0.1051046D-04
11	-0.1566225D-05	-0.2376652D-04
12	-0.0	-0.2121155D-04
13	0.1267455D-04	0.2766717D-04
14	0.8864156D-05	0.2526255D-05
15	0.4126156D-05	-0.1761004D-04
16	0.1661632D-04	-0.4156755D-04
17	-0.0	-0.5606644D-04
18	0.2302222D-04	0.2231761D-04
19	0.2022004D-04	0.4465152D-05
20	0.1226606D-04	-0.2046402D-04
21	0.4646643D-05	-0.5534351D-04
22	-0.0	-0.5602641D-04
23	0.3516075D-04	0.2746465D-04
24	0.3745555D-04	0.6217651D-05
25	0.3537604D-04	-0.1504175D-04
26	0.2746765D-04	-0.4675600D-04
27	0.1606831D-04	-0.6111341D-04
28	0.6476601D-05	-0.1114215D-03
29	-0.0	-0.1265455D-03
30	0.5264246D-04	-0.1656764D-04
31	0.5000064D-04	-0.4616425D-04
32	0.4647642D-04	-0.6265526D-04
33	0.2266246D-04	-0.1226546D-03
34	-0.0	-0.1454766D-03
35	0.6656511D-04	0.2542655D-04
36	0.6666117D-04	-0.1167562D-04
37	0.6146601D-04	-0.1162611D-04
38	0.6172662D-04	-0.4247626D-04
39	0.7661564D-04	-0.1665265D-03
40	0.4663022D-04	-0.1664650D-03
41	-0.0	-0.1776646D-03
42	0.1102616D-03	-0.6225670D-05
43	0.1642044D-03	-0.5212155D-04
44	0.1603777D-03	-0.1225667D-03
45	0.5324266D-04	-0.1572262D-03
46	-0.0	-0.2167416D-03
47	0.6656663D-04	0.4226646D-04
48	0.7622655D-04	0.1256765D-04
49	0.1452626D-03	-0.1641266D-04
50	0.2676066D-03	-0.5666566D-04
51	0.2666671D-03	-0.2526671D-03
52	0.1577732D-03	-0.6561656D-03
53	-0.0	-0.6671166D-03
54	0.4366022D-04	-0.7116655D-04
55	0.3144461D-04	-0.1167216D-03
56	0.1136656D-04	-0.1446626D-03
57	0.6761767D-04	-0.2274656D-04
58	0.5656643D-04	-0.1602620D-03
59	0.4570614D-04	-0.1265246D-03
60	0.3241406D-04	-0.1456651D-03
61	0.1665346D-04	-0.1564664D-03
62	-0.0	-0.1622226D-03
63	0.6610716D-04	-0.7621476D-04
64	0.6666024D-04	-0.1256646D-03
65	0.2466725D-04	-0.1727526D-03
66	0.6664284D-04	-0.4564141D-04
67	0.1246727D-03	-0.4626721D-04
68	0.2212066D-03	-0.4726666D-04
69	0.1244066D-03	-0.6627626D-04
70	0.1134717D-03	-0.1164475D-03
71	0.6370156D-04	-0.1456762D-03
72	0.6766521D-04	-0.1746226D-03
73	0.3611264D-04	-0.1656246D-03
74	-0.0	-0.1664466D-03
75	0.1746516D-03	-0.6621152D-04
76	0.1326726D-03	-0.1664262D-03
77	0.4626664D-04	-0.2146656D-03
78	0.2412166D-03	-0.1266666D-03
79	0.2212664D-03	-0.1571656D-03
80	0.1621766D-03	-0.2516571D-03
81	0.1256644D-03	-0.2676214D-03
82	0.6671462D-04	-0.2616666D-03
83	-0.0	-0.2142665D-03
84	0.2222166D-03	-0.2227274D-03
85	0.2761462D-03	-0.4456746D-03
86	0.7736575D-04	-0.6226626D-03

163

FL.NO.	Φ Θ	Z	R-STRESS	Z-STRESS	T-STRESS	RZ-STRESS	MAX-STRESS	MIN-STRESS	ANGLE	IJ-STRESS	JK-STRESS	SHEAR
1	0.38	1.32	-1.2145D 01	3.5057D 00	-1.3636D 01	9.5543D 00	9.2427D 00	-1.6994D 01	44.35	-1.215D 01	3.510D 00	5.550D 00
2	0.26	1.04	-1.3741D 01	2.8295D 01	-1.6356D 01	2.2656D 01	3.4165D 01	-2.3626D 01	46.43	-1.370D 01	2.670D 01	2.270D 01
3	0.60	0.65	-5.2333D 00	-2.2621D 01	-1.4632D 01	2.5744D 02	1.2527D 01	-4.1762D 01	35.16	1.250D 01	-4.170D 01	1.420D 00
4	0.65	0.35	1.6162D 01	-7.1669D 01	-4.8116D 00	2.4775D 01	2.8250D 01	-3.3716D 01	15.20	7.070D 00	-4.250D 01	-4.350D 01
5	0.45	0.73	1.1345D 01	1.4545D 01	-3.7657D 00	4.1131D 01	5.4160D 01	-3.8215D 01	44.13	1.130D 01	1.450D 01	4.110D 01
6	0.15	0.70	-2.6753D 00	1.2432D 02	-1.7900D 01	5.3256D 01	1.4760D 02	-2.2062D 01	73.00	-2.680D 00	1.240D 02	5.330D 01
7	0.05	0.65	-6.6764D 00	1.7637D 02	-9.0454D 00	5.4655D 01	1.7147D 02	-2.7793D 01	74.64	1.770D 02	-9.360D 00	-5.360D 01
8	0.08	0.47	2.5618D 01	3.4345D 02	7.8446D 00	7.6347D 01	3.8154D 02	7.6347D 00	77.32	2.540D 01	3.630D 02	-7.550D 01
9	0.22	0.47	5.4156D 01	2.5642D 02	1.5036D 01	1.7832D 01	2.6265D 02	-2.3360D 00	62.56	5.420D 01	2.660D 02	1.050D 02
10	0.37	0.47	6.2493D 01	6.1786D 01	2.7722D 01	6.5725D 01	1.3162D 02	-5.6640D 00	44.65	6.290D 01	6.180D 01	6.570D 01
11	0.62	0.47	2.1644D 01	-7.1891D 01	1.6726D 01	9.2975D 00	2.2465D 01	-7.1747D 01	5.75	2.110D 01	-7.060D 01	9.440D 00
12	0.60	0.35	2.3660D 01	-8.4274D 01	5.7167D 01	-2.3373D 01	2.7356D 01	-8.7650D 01	-13.31	2.370D 01	-8.470D 01	-2.030D 01
13	0.37	0.35	1.6437D 02	2.5524D 01	9.5114D 01	5.1360D 01	1.2565D 02	2.6331D 01	27.00	1.640D 02	2.550D 01	5.150D 01
14	0.22	0.35	1.3731D 02	2.6466D 01	4.5263D 01	1.5542D 02	2.6531D 02	3.2672D 01	56.11	1.370D 02	2.650D 02	1.560D 02
15	0.08	0.35	1.2347D 02	5.9521D 02	7.2673D 01	1.2672D 02	6.2261D 02	6.0660D 01	74.24	1.240D 02	5.850D 02	1.400D 02
16	0.03	0.23	4.5368D 02	5.0466D 02	4.4936D 02	2.1363D 02	1.1432D 02	3.2161D 02	71.64	5.560D 02	4.520D 02	-2.650D 02
17	0.06	0.35	2.7747D 02	8.2023D 02	2.6036D 02	1.6145D 02	5.6664D 02	3.1656D 02	73.53	2.760D 02	8.200D 02	1.630D 02
18	0.21	0.35	2.7252D 02	3.2216D 01	2.8366D 02	1.7763D 02	4.7470D 02	1.1644D 02	51.27	2.530D 02	2.220D 02	1.760D 02
19	0.27	0.23	2.7252D 02	2.7643D 01	2.6531D 02	1.6213D 02	1.6732D 02	-1.6673D 01	36.16	2.680D 02	4.200D 01	-1.550D 02
20	0.37	0.35	5.6771D 01	-2.6146D 01	1.7725D 02	-2.1511D 01	5.6651D 01	-2.6616D 01	-1.20	5.660D 01	-2.610D 01	-2.110D 01
21	0.60	0.35	4.3232D 00	-8.3756D 01	1.0543D 02	-5.4653D 01	2.1437D 01	-1.1565D 02	-26.65	4.330D 00	-5.360D 01	-5.440D 01
22	0.62	0.15	-5.6556D 01	-5.7846D 01	1.6434D 02	-7.3737D 01	2.2665D 01	-1.1566D 02	-43.67	-5.660D 01	-5.750D 01	-7.660D 01
23	0.60	0.65	-1.1347D 02	-2.7743D 01	2.2234D 02	-4.3534D 01	-1.4735D 00	-1.3663D 02	-46.41	-1.130D 02	-2.270D 01	-4.450D 01
24	0.35	0.62	-1.6566D 02	-4.2126D 00	4.5632D 02	-3.6147D 02	1.2366D 02	-1.1946D 02	-71.66	-4.310D 00	-1.660D 02	2.620D 02
25	0.37	0.66	-6.4766D 02	-3.4213D 01	4.4366D 02	-2.6114D 02	3.2541D 01	-1.4544D 02	-47.27	-6.490D 02	-5.420D 01	-2.510D 02
26	0.37	0.14	-1.3562D 02	-1.3132D 02	3.2303D 02	-1.1732D 02	7.6256D 01	-1.4662D 02	-45.66	-2.660D 02	-5.720D 02	-1.660D 02
27	0.35	0.10	4.6864D 01	-1.2426D 02	2.7643D 02	-1.7056D 02	1.6167D 02	-3.3621D 02	-33.62	4.550D 01	-1.240D 02	-1.750D 02
28	0.26	0.17	1.3734D 02	1.3453D 01	4.2466D 02	-1.9652D 01	1.6463D 02	5.1564D 01	-5.66	1.630D 02	1.350D 01	-1.550D 01
29	0.21	0.17	2.6433D 02	1.5712D 02	4.2363D 02	1.4332D 02	4.6147D 02	3.6143D 01	36.1	4.390D 02	5.461D 01	-5.660D 01
30	0.10	0.17	4.3564D 02	4.6567D 02	5.6756D 02	1.6172D 02	5.4647D 02	3.9721D 02	44.41	3.740D 02	5.070D 02	1.520D 02
31	0.12	0.17	5.6545D 02	5.2944D 02	4.1436D 02	1.2533D 02	6.4666D 02	5.1736D 02	33.36	5.560D 02	5.650D 02	1.250D 02
32	0.06	0.13	7.3736D 02	1.1566D 02	7.5366D 02	3.1636D 02	1.2636D 03	6.4675D 02	47.13	1.140D 03	7.770D 02	-2.140D 02
33	0.05	0.17	4.6156D 02	1.2946D 02	4.6156D 02	7.4746D 01	1.2674D 03	6.6736D 02	44.12	6.620D 02	1.250D 03	7.670D 01
34	0.01	0.17	5.2616D 02	1.2616D 02	5.1365D 02	1.1452D 02	1.1347D 03	3.1756D 02	31.51	1.250D 03	6.250D 02	2.640D 02
35	0.25	0.01	-4.3663D 01	1.1136D 02	1.3891D 03	-6.744D 02	1.3466D 03	-4.4654D 04	-31.67	-3.260D 02	7.290D 01	-2.330D 03
36	0.26	0.03	-2.5066D 02	2.6366D 02	1.7537D 03	-6.7663D 02	4.6663D 02	-7.6515D 03	-76.76	-2.610D 02	2.610D 03	-5.660D 02
37	0.25	0.06	-1.4316D 02	1.2357D 02	1.6647D 03	-1.1664D 02	6.6466D 02	-1.6331D 03	-43.75	-6.220D 02	-6.560D 02	-1.360D 02
38	0.26	0.08	-6.2473D 02	-4.2046D 01	4.5266D 02	-6.7466D 02	2.6576D 03	-6.2746D 02	-65.56	-6.650D 02	-4.290D 01	-4.470D 02
39	0.25	0.11	-2.5637D 02	1.3436D 02	7.2466D 02	-4.6736D 02	1.647D 03	-6.6456D 02	-63.27	4.330D 01	-4.560D 02	-4.470D 02
40	0.26	0.13	2.6471D 01	-6.5627D 01	5.4636D 02	-1.6176D 01	1.7663D 03	-2.5637D 02	-33.10	2.660D 01	-6.660D 01	-1.520D 02
41	0.21	0.14	4.5367D 02	2.2222D 02	4.6636D 02	-1.2136D 02	4.7646D 02	1.7671D 02	-23.62	4.390D 02	2.250D 02	-1.210D 02
42	0.17	0.14	4.1566D 02	5.3773D 02	7.5452D 02	-7.6376D 01	6.2676D 02	3.2166D 02	-44.47	4.380D 02	4.160D 02	7.540D 01
43	0.13	0.14	7.2946D 02	6.1437D 02	6.6376D 02	4.6546D 01	8.2671D 02	7.1737D 02	36.62	7.140D 02	6.160D 02	4.660D 01
44	0.06	0.14	6.4366D 02	1.1615D 03	6.5641D 02	1.6176D 01	1.1637D 03	6.4726D 02	67.37	1.160D 03	6.430D 02	-1.620D 01
45	0.06	0.14	1.3346D 03	1.3763D 03	1.3334D 03	2.4746D 01	1.3656D 03	1.3124D 03	66.74	1.360D 03	1.360D 03	2.440D 01
46	0.07	0.14	1.3656D 03	1.4523D 03	1.3545D 03	-1.3456D 01	1.4567D 03	1.3346D 03	-56.75	1.450D 03	1.671D 03	-2.210D 01
47	0.21	0.11	2.6646D 02	1.6432D 02	6.5526D 02	-2.4417D 02	6.3431D 02	-7.3333D 01	-26.01	2.660D 02	2.660D 02	-2.640D 02
48	0.17	0.11	5.4613D 02	4.7346D 02	6.3036D 02	-2.4145D 01	7.4731D 02	2.7136D 02	-36.16	5.660D 02	4.330D 02	-2.430D 02
49	0.13	0.11	6.2653D 02	4.5566D 02	1.1326D 03	-1.4455D 02	1.3646D 03	6.7716D 02	-47.61	5.660D 02	6.240D 02	1.640D 02
50	0.06	0.11	1.0836D 03	1.1716D 03	1.2556D 03	-1.3136D 02	1.3466D 03	6.6672D 02	-64.23	1.660D 03	1.170D 03	-1.310D 02

EL.NO.	P	Z	R-STRESS	Z-STRESS	T-STRESS	RZ-STRESS	MAX-STRESS	MIN-STRESS	ANGLE	IJ-STRESS	JK-STRESS	SHEAR
51	0.06	0.11	1.2714D 03	1.2443D 03	1.2413D 03	-6.4132D 01	1.4566D 03	1.2962D 03	-55.56	1.36D 03	1.27D 03	9.41D 01
52	0.02	0.11	1.3976D 03	1.3571D 03	1.3651D 03	-1.2067D 01	1.4103D 03	1.3944D 03	-44.17	1.40D 03	1.40D 03	-1.39D 01
53	0.21	0.09	-4.2216D 01	5.2235D 01	1.0569D 03	-6.6273D 02	6.8565D 02	-6.2176D 02	-47.54	-4.32D 01	5.22D 01	-6.62D 02
54	0.17	0.09	3.3512D 03	3.3655D 02	1.0517D 03	-5.3311D 02	6.4645D 02	-1.6776D 02	-45.01	3.36D 02	3.35D 02	5.33D 02
55	0.13	0.09	7.2603D 02	7.5554D 02	1.1944D 03	-4.3592D 02	1.1522D 03	7.0262D 02	-46.07	7.26D 02	7.55D 02	-4.35D 02
56	0.09	0.09	1.0551D 03	1.0630D 03	1.1154D 03	-2.4156D 02	1.4264D 03	6.9742D 02	-45.31	1.06D 03	1.06D 03	3.62D 02
57	0.06	0.09	1.2976D 03	1.2959D 03	1.1672D 03	-2.4723D 02	1.5213D 03	1.0732D 03	-35.75	1.39D 03	1.21D 03	-2.47D 02
58	0.02	0.09	1.4266D 03	1.2146D 03	1.4145D 03	-7.1251D 01	1.4465D 03	1.1925D 03	-16.54	1.21D 03	1.43D 03	7.19D 01
59	0.21	0.06	-4.3492D 02	3.4751D 01	1.1056D 03	-1.3559D 03	7.6712D 02	-1.3612D 03	-64.20	3.46D 01	-6.35D 02	1.01D 03
60	0.17	0.06	7.5259D 00	1.3344D 02	1.1115D 03	-5.5471D 02	1.2562D 03	-5.5525D 02	-46.66	1.63D 00	1.33D 02	-6.57D 02
61	0.13	0.06	4.6171D 02	5.4637D 02	1.1657D 03	-8.2091D 02	1.3271D 03	-3.1762D 02	-46.51	5.46D 02	4.63D 02	6.21D 02
62	0.09	0.06	9.4291D 02	9.3162D 02	1.2449D 03	-4.6521D 02	1.5465D 03	2.2572D 02	-43.56	9.42D 02	6.32D 02	-6.55D 02
63	0.06	0.06	1.1275D 03	5.1615D 02	1.2456D 03	-2.5973D 02	1.4452D 03	6.1736D 02	-37.62	5.16D 02	1.13D 03	3.55D 02
64	0.02	0.06	1.2121D 03	5.9562D 02	1.1522D 03	-1.2649D 02	1.2565D 03	4.4571D 02	-15.19	1.21D 03	6.55D 02	-1.27D 02
65	0.21	0.04	-2.6162D 03	-1.3962D 02	-5.4136D 02	-1.7151D 03	3.1517D 02	-3.6649D 01	-37.55	-3.51D 03	-1.36D 02	-1.32D 03
66	0.17	0.04	-4.1291D 03	-3.1905D 02	-2.5251D 03	-1.1811D 03	1.7371D 03	-4.4665D 03	-74.16	-3.15D 03	-4.13D 03	1.18D 03
67	0.13	0.04	-4.2572D 03	3.5932D 02	-1.3371D 03	-1.1050D 03	5.5565D 02	-4.5565D 03	-77.35	-4.25D 03	2.55D 02	-1.10D 03
68	0.09	0.04	-4.3962D 03	3.6507D 02	-4.1575D 03	-5.5343D 02	4.3356D 02	-4.5462D 03	-73.57	3.66D 02	-4.44D 03	8.55D 02
69	0.06	0.04	-4.3723D 03	5.2513D 02	-4.3174D 03	-4.3294D 03	5.7621D 02	-4.4314D 03	-64.31	-4.37D 03	5.25D 02	-4.53D 02
70	0.02	0.04	-4.4562D 03	4.6666D 02	-4.4527D 03	-1.3546D 02	4.6434D 03	-4.4556D 03	-66.42	4.61D 02	-4.44D 03	1.36D 02
71	0.21	0.01	-7.3331D 03	-1.3670D 03	-2.4273D 03	3.3470D 02	-1.3547D 02	-7.3311D 03	-55.52	-1.31D 02	-7.33D 03	-2.30D 00
72	0.17	0.01	-1.60074D 04	-5.4254D 02	-7.5545D 03	-4.7903D 02	-5.4935D 02	-1.6556D 04	-57.12	-1.01D 04	-5.43D 02	-4.80D 02
73	0.13	0.01	-1.3414D 04	-1.1644D 03	-1.1515D 04	-5.174D 02	-5.4532D 01	-1.2444D 04	-57.15	-1.16D 02	-1.34D 04	6.75D 02
74	0.09	0.01	-1.4175D 04	-1.5114D 03	-1.4131D 04	-4.7141D 02	-1.7526D 02	-1.4151D 04	-65.07	-1.42D 04	-1.51D 03	-4.72D 02
75	0.06	0.01	-1.5249D 04	6.3513D 00	-1.5374D 04	-3.1473D 02	1.2564D 01	-1.5256D 04	-63.61	6.35D 00	-1.52D 04	3.16D 02
76	0.02	0.01	-1.5665D 04	5.7664D 01	-1.5707D 04	-6.1346D 01	5.7644D 01	-1.5665D 04	-65.77	-1.57D 04	5.76D 01	-6.16D 01

APPENDIX D

LIST OF FIGURES

APPENDIX D

LIST OF FIGURES
(Continued)

APPENDIX D

LIST OF FIGURES
(Continued)

APPENDIX E

LIST OF TABLES